FINAL REPORT

The Molecular Biology of Nitroamine Degradation in Soils

SERDP Project ER-1608

JULY 2015

Stuart E. Strand
University of Washington

Neil C. Bruce
University of York

David A. Stahl
University of Washington

Jalal Hawari
National Research Council of Canada

SERDP
DOD ▪ EPA ▪ DOE

REPORT DOCUMENTATION PAGE

Form Approved
OMB No. 0704-0188

1. REPORT DATE *(DD-MM-YYYY)*	2. REPORT TYPE	3. DATES COVERED *(From - To)*
07/26/2015	Final Report	2008-2012

4. TITLE AND SUBTITLE
The Molecular Biology of Nitroamine Degradation in Soils

5a. CONTRACT NUMBER
W912HQ-08-C-0050

5b. GRANT NUMBER

5c. PROGRAM ELEMENT NUMBER

6. AUTHOR(S)
Stuart E. Strand
Neil C. Bruce
David A. Stahl
Jalal Hawari

5d. PROJECT NUMBER
ER-1608

5e. TASK NUMBER

5f. WORK UNIT NUMBER

7. PERFORMING ORGANIZATION NAME(S) AND ADDRESS(ES)
College of Engineering, University of Washington, Seattle, WA
Biotechnology Research Institute, National Research Council of Canada, Montréal, Québec, Canada
CNAP, Department of Biology, University of York, York, UK

8. PERFORMING ORGANIZATION REPORT NUMBER

9. SPONSORING/MONITORING AGENCY NAME(S) AND ADDRESS(ES)
Strategic Environmental Research and Development Program

10. SPONSOR/MONITOR'S ACRONYM(S)
SERDP

11. SPONSOR/MONITOR'S REPORT NUMBER(S)

12. DISTRIBUTION/AVAILABILITY STATEMENT
Distribution A

13. SUPPLEMENTARY NOTES

14. ABSTRACT
Molecular characterization of microbial communities in soils with RDX degradation, determination of RDX metabolites and metabolic pathways, determine the diversity of xplA in the environment and possible evolutionary origin, determine the mechanism of horizontal gene transfer of xplA, investigate the regulation and transcription of xplA/B, and discover new bacteria capable of degrading RDX and determine the enzymes involved.

15. SUBJECT TERMS

16. SECURITY CLASSIFICATION OF:			17. LIMITATION OF ABSTRACT	18. NUMBER OF PAGES	19a. NAME OF RESPONSIBLE PERSON
a. REPORT	b. ABSTRACT	c. THIS PAGE			19b. TELEPHONE NUMBER *(Include area code)*
A	A	A	UU	111	

INSTRUCTIONS FOR COMPLETING SF 298

1. REPORT DATE. Full publication date, including day, month, if available. Must cite at least the year and be Year 2000 compliant, e.g. 30-06-1998; xx-06-1998; xx-xx-1998.

2. REPORT TYPE. State the type of report, such as final, technical, interim, memorandum, master's thesis, progress, quarterly, research, special, group study, etc.

3. DATE COVERED. Indicate the time during which the work was performed and the report was written, e.g., Jun 1997 - Jun 1998; 1-10 Jun 1996; May - Nov 1998; Nov 1998.

4. TITLE. Enter title and subtitle with volume number and part number, if applicable. On classified documents, enter the title classification in parentheses.

5a. CONTRACT NUMBER. Enter all contract numbers as they appear in the report, e.g. F33315-86-C-5169.

5b. GRANT NUMBER. Enter all grant numbers as they appear in the report. e.g. AFOSR-82-1234.

5c. PROGRAM ELEMENT NUMBER. Enter all program element numbers as they appear in the report, e.g. 61101A.

5e. TASK NUMBER. Enter all task numbers as they appear in the report, e.g. 05; RF0330201; T4112.

5f. WORK UNIT NUMBER. Enter all work unit numbers as they appear in the report, e.g. 001; AFAPL30480105.

6. AUTHOR(S). Enter name(s) of person(s) responsible for writing the report, performing the research, or credited with the content of the report. The form of entry is the last name, first name, middle initial, and additional qualifiers separated by commas, e.g. Smith, Richard, J, Jr.

7. PERFORMING ORGANIZATION NAME(S) AND ADDRESS(ES). Self-explanatory.

8. PERFORMING ORGANIZATION REPORT NUMBER. Enter all unique alphanumeric report numbers assigned by the performing organization, e.g. BRL-1234; AFWL-TR-85-4017-Vol-21-PT-2.

9. SPONSORING/MONITORING AGENCY NAME(S) AND ADDRESS(ES). Enter the name and address of the organization(s) financially responsible for and monitoring the work.

10. SPONSOR/MONITOR'S ACRONYM(S). Enter, if available, e.g. BRL, ARDEC, NADC.

11. SPONSOR/MONITOR'S REPORT NUMBER(S). Enter report number as assigned by the sponsoring/ monitoring agency, if available, e.g. BRL-TR-829; -215.

12. DISTRIBUTION/AVAILABILITY STATEMENT. Use agency-mandated availability statements to indicate the public availability or distribution limitations of the report. If additional limitations/ restrictions or special markings are indicated, follow agency authorization procedures, e.g. RD/FRD, PROPIN, ITAR, etc. Include copyright information.

13. SUPPLEMENTARY NOTES. Enter information not included elsewhere such as: prepared in cooperation with; translation of; report supersedes; old edition number, etc.

14. ABSTRACT. A brief (approximately 200 words) factual summary of the most significant information.

15. SUBJECT TERMS. Key words or phrases identifying major concepts in the report.

16. SECURITY CLASSIFICATION. Enter security classification in accordance with security classification regulations, e.g. U, C, S, etc. If this form contains classified information, stamp classification level on the top and bottom of this page.

17. LIMITATION OF ABSTRACT. This block must be completed to assign a distribution limitation to the abstract. Enter UU (Unclassified Unlimited) or SAR (Same as Report). An entry in this block is necessary if the abstract is to be limited.

Table of Contents

List of Tables

List of Figures

List of Acronyms

cDNA	Complimentary DNA
DHP	dihydroxy-picolinicacid
FAD	Flavin adenine dinucleotide
HMX	High metling explosive (octahydro-1,3,5,7-tetranitro-1,3,5,7-tetrazocine)
HPLC	High performance liquid chromatography
MEDINA	Methylendinitramine
MS	Mass Spectrometry
NDAB	4-nitro-2,4-diazabutanal
NAD	Nicotinamide adenine dinucleotide
NADP	Nicotinamide adenine dinucleotide phosphate
PCR	Polymerase chain reaction
RGB	*E. coli* Rosetta-gami B

RDX	Royal demolition explosive (hexahydro-1, 3, 5-trinitro-1,3,5-triazine hexahydro- 1,3,5-trinitro-1,3,5-triazine
TNT	2,4,6-Trinitrotoluene
UY	University of York
UW	University of Washington
XplA	RDX-degrading enzyme from *Rhodococcus rhodochrous* 11Y
xplA	Gene encoding RDX-degrading enzyme from *Rhodococcus rhodochrous* 11Y
XplB	Reductase encoded adjacently to *xplA* in *Rhodococcus rhodochrous* 11Y genome
xplB	Gene for reductase encoded adjacently to xplA in *Rhodococcus rhodochrous* 11Y genome

Keywords

RDX, *Rhodococcus rhodochrous*, XplA, XplB, MarR, Permease, Functional Screening

Acknowledgements

Chun Shiong Chong acknowledges funding from the Ministry of Higher Education, Malaysia. Dana Khdr Sabir recognizes the HCDP program-Kurdistan Regional Government/Iraq for funding.

We thank Prof Zeev Ronen from Israel for providing Rhodococcus sp. YH1 and the National Institute of Technology and Evaluation (NITE) NITE Biological Resource Centre (NBRC), Japan for supplying Gordonia terrae strain NBRC 100016.

Abstract

Objectives

Molecular characterization of microbial communities in soils with RDX degradation, determination of RDX metabolites and metabolic pathways, determine the diversity of *xplA* in the environment and possible evolutionary origin, determine the mechanism of horizontal gene transfer of *xplA*, investigate the regulation and transcription of *xplA/B*, and discover new bacteria capable of degrading RDX and determine the enzymes involved.

Technical Approach

We used a two-pronged approach to characterize RDX degradation in soils: based on known RDX-degrading isolates and a culture independent molecular approach to characterize the microbial communities of soils polluted to varying degrees with RDX. Sequenced clone libraries combined with stable isotope probing were used to characterize *in situ* microbial populations of munitions polluted soils. The occurrence of *Rhodococcus* and the diversity of *xplA/B* genes for RDX degradation in the environment were studied. The relative importance of anaerobic and aerobic RDX degrading pathways was determined. The evolutionary origin of known RDX degradation pathways was investigated and the significance of horizontal gene transfer of *xplA* was studied. Genetic control of RDX degradation was studied and we attempted to discover new RDX degrading bacteria and enzymes.

Results

Military range soils were screened for RDX degradation activity. Our efforts to develop a functional screen for genes from the soil metagenome were unsuccessful. We developed efficient methods of packaging large fragments of partially digested DNA in vectors. However, we were unable to enrich clones from the partially digested DNA of any of the known RDX degraders; *Rhodococcus* 11Y, *Microbacterium* MA1, or *Mycobacterium* MA2 in either competent *E. coli* Rosetta-gami B or *P. putida* KT2440 as hosts. There may be a toxic effect of the expression of the DHP reductase or that expression of *xpl*BA in the vector was inhibited by the upstream DNA.

We investigated degradation of MNX (hexahydro-1-nitroso-3,5-dinitro-1,3,5-triazine), a key RDX initial product and frequently found as contaminant with RDX. In the presence of $^{18}O_2$, *Rhodococcus* DN22 degraded RDX and produced NO_2^- that subsequently oxidized to NO_3^- containing one ^{18}O atom, but in the presence of $H_2{}^{18}O$ we detected NO_3^- without ^{18}O. A control containing NO_2^-, DN22, and $^{18}O_2$ gave NO_3^- with one ^{18}O, confirming biotic oxidation of NO_2^- to NO_3^-. Treatment of MNX with DN22 and $^{18}O_2$ produced NO_3^- incorporating two ^{18}O atoms and another incorporating only one ^{18}O. In the presence of $H_2{}^{18}O$, we detected NO_2^- with two different masses, one representing NO_2^- and another representing NO_2^- with the inclusion of one ^{18}O, suggesting auto-oxidation of NO to NO_2^-.

We were unable to demonstrate horizontal gene transfer of the plasmid containing *xplBA* using transconjugants that expressed *xplAB* in the recipient. Nevertheless, the 454 genome draft sequencing showed the presence in *Rhodococcus sp*. type strain 11Y of genes potentially involved in plasmid transfer. Overexpression and deletion of the permease *aroP* showed no change in RDX removal. In resting cells assays, the rate of RDX removal by the *marR* knock-out was decreased, suggesting that MarR may be involved in the detection of high nitrogen. Activity towards RDX was present in resting cell incubations of *R. rhodochrous* 11Y , although in the absence of RDX, activity increased when cells were grown with RDX or low concentrations of

NH_4Cl as the N source, suggesting that *xplA* expression is a response to low N levels rather than RDX.

The regulation of RDX degrading genes in *Rhodococcus* strain 11Y has parallels with the regulation of genes encoding atrazine degradation in *Pseudomonas* sp. strain ADP. Transcription of *atzR*, a regulator that activates the atrazine gene cluster, is switched on by a metabolite of atrazine degradation, cyanuric acid, and by nitrogen limitation, and this control is thought to link to central nitrogen metabolism in *Pseudomonas* sp.

Analysis of the *R. rhodochrous* 11Y sequence identified two putative promoter regions, one upstream of *aroP* and one upstream of *xplB*. For the putative promoter region upstream of *xplB*, primer extension analysis and RACE PCR did not amplify any products. Furthermore, the sequence is only eleven bases from the ATG start codon of *xplB*, a distance that does not leave much space for RNA polymerase binding prior to translation. Primer extension analysis and RACE PCR did confirm the BPROM-predicted transcription start site upstream of *aroP*.

The construction of a Tn5 insertion library of 11Y was successful but while initial screenings for mutants with decreased RDX removal were promising, subsequent analysis failed to confirm inhibition in RDX removal.

2D-Gel electrophoresis of 11Y grown on either RDX or NH_4Cl as sole N sources identified some proteins upregulated after RDX treatment involved in nitrogen metabolism; however, no RDX-specific proteins as XplA were found, suggesting that the chosen treatment, as shown for the resting cell assays, results in a similar response and expression of xplA and related proteins arguing that XplA expression is linked to the central nitrogen metabolism and not a specific response to RDX.

Enrichment studies identified number of RDX degrading bacteria isolated from contaminated soil from England. Belgium and Ukraine. All isolates were gram positive bacteria and belong to the *Rhodococcus* clade with the exception of Microbacterium isolated from Belgium soil. The different enrichment conditions have not allowed the isolation of gram negative bacteria, or bacteria degrading RDX with an enzyme other than xplA. Our isolates of RDX degrading bacteria are identical in 16S rDNA, which suggests that they form a monoclonal population. They constitute a closely related but different genotype in comparison to the other RDX degrader *Rhodococcus* isolated in the UK. These results indicated that *Rhodococcus* so far remains the main genus found to biodegrade RDX.

The evolutionary origin of XplA is still unclear. So far XplA is the only enzyme which actively degrades RDX. Both *xplA* and *xplB* are part of a high GC content gene cluster which is nearly identical among *Rhodococcus* spp, isolated from United Kingdom, Ukraine, United States, Belgium and Israel. The region is also highly conserved in two known genera of actinomycetes: *Microbacterium* sp. MA1 and *Williamsia* sp. EG1. The machinery mechanism of transferring the gene cluster around the world is not yet understood yet, however the finding that the XplA genomics island is limited to actinomycetes suggests that there is a specific transfer system, possibly via phages.

Benefits

This project contributed to our understanding of the biodegradation of RDX *in situ* at DoD field sites. Our study helped identify the microbial communities, pathways and enzymes responsible for the dissimilation of RDX in soils.

Objectives

Task 1: Molecular characterization of microbial communities in soils with RDX degradation (UW).

The goal of this task was to develop and apply functional assays for RDX degradation to screen for novel functional genes from RDX contaminated environments.

Our research was focused on the development of an enrichment protocol for the selection of transformed *E. coli* clones carrying RDX degradation genes extracted from RDX degrading soil samples. We developed an anaerobic enrichment protocol that was applied to a clone library generated from metagenomic DNA that had been extracted from RDX-degrading soil microcosms and separated using density gradient centrifugation. A large number of clones were positive for RDX-degradation in these experiment.

Task 2: Determination of RDX metabolites and metabolic pathways (NRC)

Our objectives was to understand how RDX reacts under aerobic and anaerobic conditions with particular emphasis on the initial steps involved in RDX decomposition. Three important initial redox reactions were studied 1) 1e–transfer to –N–$\underline{NO_2}$ leading to denitration and ring cleavage, 2) 2e–transfer to –$\underline{NO_2}$ leading to the formation of the corresponding nitroso derivatives (MNX, DNX and TNX), and 3) $H^{\bullet}$-abstraction from one of the –CH_2– groups in RDX by a free radical, $OH^{\bullet}$ and $O_2^{\bullet -}$ followed by ring cleavage and decomposition.

Task 3: Determine the diversity of *xplA* in the environment and possible evolutionary origin *(UY)*

This project aimed to address the problem of the recalcitrance of RDX on training ranges by gaining insights into the metabolic diversity among microorganisms that can utilize RDX to support growth, either as a nitrogen or carbon source. We approached this objective by selective enrichment studies and a combination of conventional and innovative molecular fingerprinting techniques.

Task 4: Determine the mechanism of horizontal gene transfer of *xplA (UY)*

The project also focused on the horizontal gene transfer of the only known microbial gene encoding an RDX degrading enzyme XplA. This novel RDX degrading cytochrome P450 has been found with near sequence identity at geographically distinct RDX contaminated sites around the world and confers on bacteria the ability to utilize RDX as a nitrogen source for growth.

Task 5: Investigate the regulation and transcription of *xplA/B*. *(UY)*

Our approach was to determine the order and genetic environment of the xplA and xplB genes of known RDX degrading isolates.

Task 6: Discover new bacteria capable of degrading RDX and determine the enzymes involved *(UW & UY)*

A major objective of this project was to identify and isolate strains of bacteria other than *Rhodococcus* that can metabolize RDX and determine if RDX degradation is catalyzed by enzymes other than XplA. Two approaches will be taken in elucidating the enzymes mediating the degradation of RDX. The culture independent approach is described in Task 1. In addition,

we will screen for RDX utilizing microorganisms from samples from a variety of habitats contaminated with RDX from soil environments in the UK, US, Canada, and elsewhere.

Background

Hexahydro-1,3,5-trinitro-1,3,5-triazine (RDX) is a widely used military explosive; however, its recalcitrance in soil and groundwater is causing serious concern. RDX is extensively used by the military and in the construction industry (Jenkins et al. 2006). Large scale manufacturing and extensive global usage of RDX has led to the contamination of vast areas of soil, sediment, and water. Environmental contamination by RDX raises serious concerns because the chemical is toxic, and is considered as a possible carcinogen and a potent convulsant (Lachance et al. 1999). RDX is highly mobile in surface run off water and soil leachates, rapidly migrating through soils to underlying groundwater. The mobility of RDX has resulted in plumes of groundwater contamination at training ranges, as observed at the Massachusetts Military Reservation, ultimately threatening the long-term sustainability of bases.

The development of *in situ* biotic processes to contain these materials would greatly improve DoD's ability to sustain their training range activities without endangering groundwater resources, and to improve and restore contaminated sites in a cost effective manner. Current technologies used to contain or remediate energetic materials on training ranges are expensive and inefficient, leading to a pressing need for novel technologies. The development of in situ bioremediation processes and methods of containment has been limited by the resistance of RDX to microbial degradation. Over recent years bacteria have been isolated that have the metabolic capabilities to mineralize RDX. But since RDX persists on training ranges and other military sites, it is apparent that the microorganisms present in contaminated soils do not possess enough biomass or metabolic activity to degrade munition compounds before they migrate into groundwater.

Extensive research has been conducted recently to understand biodegradation pathways of RDX under both aerobic and anaerobic conditions. Thus far we know that RDX can be degraded by two distinctive pathways, 1) anaerobic reductive pathway involving sequential reduction of the –N–$\underline{NO_2}$ functional groups to give the corresponding nitroso derivatives MNX (hexahydro-1-nitroso-3,5-dinitro-1,3,5-triazine), DNX (hexahydro-1,3-dinitroso-5-nitro-1,3,5-triazine) and TNX (hexahydro-1,3,5-trinitroso-1,3,5-triazine) (McCormick et al. 1981; Gregory et al. 2004), and 2) a denitration route involving the cleavage of the –N–NO_2 bond(s) leading to decomposition of the energetic chemical and the formation of benign products such as nitrite, ammonia, HCHO and HCOOH (Fournier et al. 2002; Bhushan et al. 2003; Jackson et al. 2007; Kwon and Finneran 2010; Fuller et al. 2010). The denitration route also leads to the formation of the two characteristic intermediates 4-nitro-2,4-diazabutanal (NDAB, NO_2NHCH_2NHCHO) and methylenedinitramine (MEDINA, $NO_2NHCH_2NHNO_2$) whose formation depends on the stoichiometry of the denitration step (Figure 1).

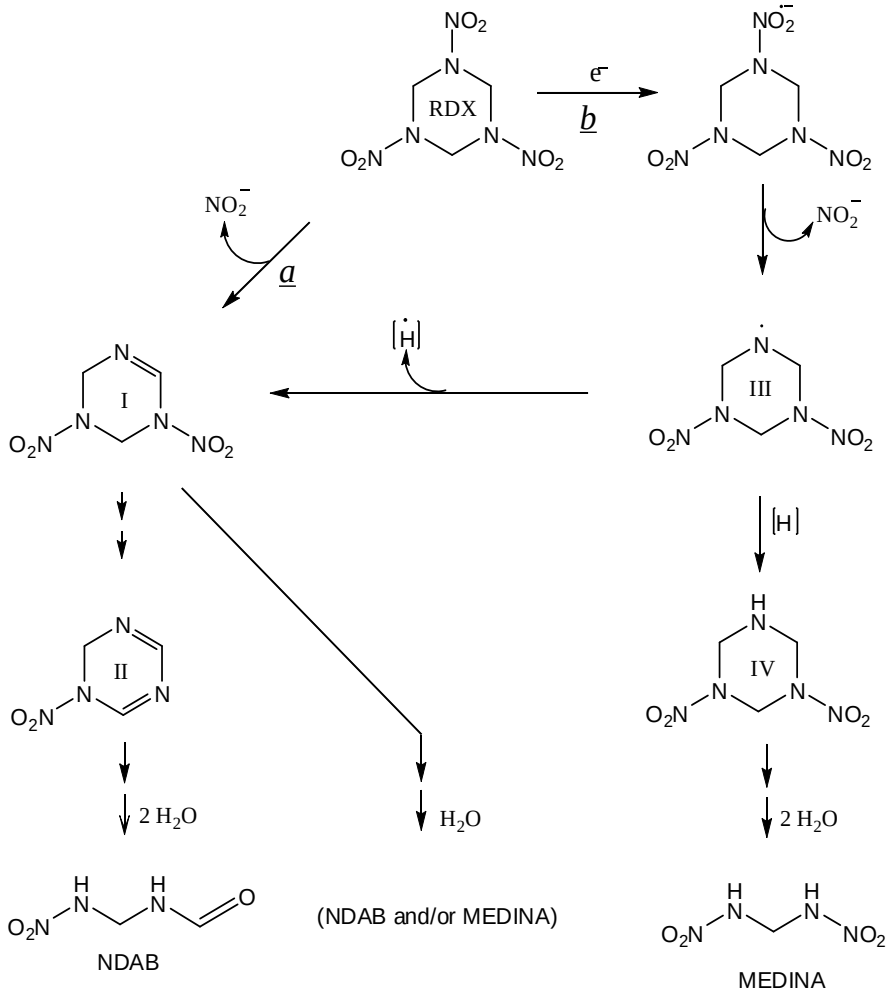

Figure 1. Summary of RDX denitration routes under aerobic (*a*) and anaerobic (*b*) conditions (Fournier et al. 2002; Jackson et al. 2007; Bhushan et al. 2002a; Strobel and Coon, 1971)**.**

Water on arrows does not represent the actual stoichiometric amounts needed to form the ring cleavage product NDAB. However, once intermediate **I** or **II** are formed one H_2O would be needed to transform each –C=N– bond into the unstable –CH(OH)–NH– bond which in turn reacts with another molecule of water leading to ring cleavage. After ring cleavage another molecule of water comes into play to split NDAB off. Water stoichiometry in MEDINA formation is much simpler, e.g. intermediate **IV** reacts with $2H_2O$ leading to the formation of MEDINA (and $OHCH_2NHCH_2OH$)

RDX produces NDAB following the loss of two nitrite anions prior to RDX ring cleavage as we observed during aerobic treatment of RDX with the cytochrome P450 XplA/B system from *Rhodococcus* sp. (Fournier et al. 2002; Jackson et al. 2007*;* Seth-Smith et al. 2007).

On the other hand, monodenitration of RDX often leads to the predominant formation of MEDINA as observed following RDX reduction with zero valent iron, ZVI (Oh et al. 2001), and nano iron particles (Naja et al. 2008) or during anaerobic treatment with diaphorase (Bhushan et al. 2002a), nitrate reductase (Bhushan et al. 2002b), *Shewanella halifaxensis* (Zhao et al. 2008) and *Geobacter metallireducens* (Kwon and Finneran, 2008). However, NDAB was produced

from monodenitrated RDX under mild alkaline hydrolysis (Balakrishnan et al. 2003). NDAB is stable in water under ambient conditions but MEDINA is unstable and decomposes to N_2O and HCHO (Halasz et al. 2002; Lamberton 1951). Both MEDINA and NDAB are extremely soluble in water and only recently have been successfully detected because of their rapid elution during HPLC analysis.

The above discussion clearly demonstrates that an RDX degradation pathway triggered by denitration would be the preferred choice for the development of remediation technologies. To gain more insight into the initial denitration step involved in RDX degradation and the subsequent abiotic and biotic reactions that follow the denitration step, we investigated biodegradation of RDX with *Rhodococcus* sp. strain DN22 in the presence of $^{18}O_2$ and $H_2{}^{18}O$ and searched for ^{18}O-containing products to determine their role in the degradation process. We also investigated biodegradation of MNX, the most common nitroso derivative of RDX (Cassada et al. 1999; Beller and Tiemeier, 2002), with DN22 to determine which of the two N–NO and N–NO_2 bonds is preferentially cleaved. We hope that new knowledge gained on each of the initial denitration step(s), subsequent secondary reactions and products distributions would provide new insights into the degradation pathway of RDX and thus help in the development of effective *in situ* remediation technologies.

RDX is a highly oxidized molecule whose degradation is governed by the electronic structure and redox chemistry of its $–CH_2–N(NO_2)–$ multifunctional group. A survey of RDX-degrading bacteria from different contaminated sites capable of utilizing RDX as a sole nitrogen source identified all bacteria as unique strains of *Rhodococcus*. A follow up work in the Bruce laboratory at the University of York (UY) on *R. rhodochrous* strain 11Y determined that an *unusual cytochrome P450 system, encoded by the genes xplA* and *xplB*, was responsible for the action on RDX. Further studies including Southern blot analysis using *xplA* to probe the DNA from new RDX-degrading rhodococci revealed the presence of *xplA* in all strains. Homologues of *xplA* have now been identified in rhodococci isolated from explosives-contaminated soil in the UK (strain 11Y), Australia (strain DN22) and Israel (strain YH1). The homologues analyzed so far have a high degree of similarity to one another (>99% amino acid identity covering 60% of *xplA*) and importantly, they appear to be absent in strains of rhodococci isolated from sites that are not contaminated with RDX. To date, *xplA* is the only microbial gene identified in the environment that encodes an RDX-degrading activity.

The UY group has achieved a high degree of purification for both XplA and XplB and initial characterization studies have confirmed that XplB is the reductase partner for XplA. Together XplA and XplB can very efficiently degrade RDX (264 turnovers per minute) and with high affinity (K_d~6010 µM). Interestingly, examination of the breakdown products of RDX by XplA anaerobically revealed a different picture to that observed in the presence of oxygen. Rather than 4-nitro-2,4-diazabutanal (NDAB), which is formed during aerobic metabolism of RDX, methylenedinitramine (MEDINA) is formed under anaerobic conditions. This is a clear demonstration of different breakdown pathways dependent on the presence of oxygen. The aerobic pathway may well follow a more classic hydroxylation route, but the anaerobic pathway generates different intermediates and endpoint metabolites.

Before the start of this work, the proposed mechanism for the aerobic biodegradation of RDX was cleavage of a NO_2 group from the RDX molecule. This step liberates nitrite and an unstable intermediate which probably autodecomposes to yield the breakdown product NDAB and formamide. Formamide degrades in culture, ultimately to yield ammonia, formaldehyde (HCHO)

and CO_2. In total, 2 moles nitrite and 1 mole ammonia are liberated per molecule of RDX. This is most likely explained by the thermodynamics of the molecule with degradation of RDX beginning with the breaking of the weakest bonds. As N-N bonds have the lowest bond dissociation energy (48 kcal mol^{-1}), these are likely to be cleaved first. In contrast, the other bonds have much higher dissociation energies of 85 kcal mol^{-1} (C-N) and 94 kcal mol^{-1} (C-H) respectively. Once the $N\text{-}NO_2$ bond is broken, the dissociation energy for the inner C-N becomes 2 kcal mol^{-1} which can readily lead to ring cleavage and the formation of the same breakdown products. Since cleavage of a single bond is enough for microorganisms to liberate sufficient quantities of nitrogen for growth it is highly likely that strains of bacteria other than known strains exist that utilize a different catalytic activity to XplA for growth on RDX.

Rhodococcus rhodochrous strain 11Y was first isolated from explosives-contaminated soil using selective enrichments with RDX supplied as a sole source of nitrogen for growth (Seth-Smith et al., 2002a, Jackson et al., 2007, Rylott et al., 2006b, Sabbadin et al., 2009). The genes encoding the ability to metabolize RDX were identified and the proteins, XplA and XplB characterized (Jackson et al., 2007, Rylott et al., 2006b, Sabbadin et al., 2009). While RDX-degrading microorganisms are found in contaminated training range soil, they appear to be present in insufficient numbers or are not active enough to contain or remediate RDX from training range soil.

Known microorganisms capable of RDX degradation are few in number. The only pathway for RDX degradation that has been worked out in detail is the xplBA cytochrome P450 attack. Stable isotope probing studies of training range soils suggest that other organisms are capable of degrading RDX and utilizing its nitrogen for growth (Roh et al. 2009; Andeer et al. 2013), including gram negatives. Thus we attempted to develop a selection and screening technique to examine a library of clones hosting random fragments of the soil metagenome for the function of RDX degradation, based on the use of nitrite produced by RDX degradation as the sole source of nitrogen.

The explosive RDX is a truly xenobiotic compound, new to the biosphere, that has been heavily used since the Second World War So far, XplA has just been identified in bacteria from RDX contaminated soil, and there are no natural substrates known to XplA, facts initiating speculations about the origin of XplA. We therefore performed selective enrichments to isolate more bacteria able to use RDX as a sole source of nitrogen from soils from different geographical regions, with the aim to identify new bacteria harboring similar or other enzymes with activity towards RDX allowing the construction of an evolutionary map for *xplA*.

The RDX degrading genes in *Rhodococcus sp.* strain 11Y were found to be located on an approximately 200 kb plasmid. Plasmid conjugation among different bacteria is a common method to horizontally transfer accessory functions to adapt to changes in environments. In order to investigate the functional barriers to successful *xplA* transfer by natural mechanisms, we tried to transfer the 11Y catabolic plasmid to other genomic backgrounds.

The gene *xplA* and its reductase partner *xplB* were found on a gene cluster highly identical to the gene cluster harboring these genes in *Microbacterium* MA1(Andeer et al., 2009). We identified this gene cluster in a variety of other *xplA*-containing bacteria and enquired the importance about this gene cluster and surrounding genes. Therefore we analyzed this genomic island in all available species and investigated the function of the surrounding genes by creating knock-out strains.

Materials and Methods

The Griess assay

The Griess assay is used as a functional assay of genes conferring RDX activity in genomic DNA libraries. Prior to applying this assay to a soil metagenomic library the Griess assay was tested using a Rhodococcus gene library, an organism which is known to contain genes for enzymes involved in the breakdown of RDX. The DNA from Rhodococcus 11Y was digested using Sau3A to create fragments approximately 5-20kb in size. These fragments were purified and ligated into the expression vector pet16B. The ligated vectors were then transformed into electrocompetent *E. coli* strains Rosetta-gami B cells and plated on LB agar plates containing the appropriate antibiotics. Clones were picked off and inoculated individually in wells of LB medium and the appropriate antibiotics on a 96 well plate and incubated at 30°C overnight. Once the cells had grown expression in the vectors was induced by the addition of IPTG, FeCl3 and α-amino levuleic acid. Induced cells were then diluted 1 in 4 into 100µM RDX and allowed to grow up overnight at 20°C. The Griess assay to detect the presence of nitrite was then carried out with the addition of suphanilamide (10mg/ml in 0.68M HCL) and 1-naphthyl ethylene diamine (NED) solution (5mg/ml), after which OD540 was measured.

The Griess assay detects the production of nitrite which is produced during the metabolism of nitrite, with nitrite producing a colorimetric reaction following the addition of sulphanilamide and 1-naphthyl-ethylenediamine (Scheideler and Ninnemann 1986). RDX was first dissolved in dimethyl sulfoxide (DMSO), before being diluted in H2O. This method of preparation greatly reduced the number of colonies giving false positives.

Soil Sampling

Soil was collected from six different of locations at Eglin Air Force base during November 2009. The top soil at each of these locations was sampled. Preliminary analysis of the soils ability of breakdown RDX was carried out with the use of soil slurries.

A number of Aberdeen soil samples were collected in May 2010 and used to set up enrichments with RDX media and agar, in order to isolate RDX degraders. Approximately 10 different species were isolated from an RDX agar plate whereby RDX is the only nitrogen source.

These species were tested to confirm growth on RDX media and determine if they are degraded and used the RDX. Subsequently DNA was extracted and the 16S genes were sequenced to establish an identity.

Soil slurry enrichments were set up containing 40ppm of RDX in a 40mM potassium phosphate buffer (pH 7.2) containing 10mM glycerol, 5mM succinate, 5mM glucose as well as trace elements. Each soil slurry contained 5g soil in 30ml of medium. Controls containing soil autoclaved for 1 hour were included. The slurries were incubated at 30 in the dark at 40 rpm. 1ml samples were removed at time point's day 0, 3 and 7. The samples were place in a 1.5ml Eppendorf tube and centrifuged at max speed for 10 minutes. This separated the liquid and soil fractions. The soil fractions were stored at -80°C to be analyzed at a later time using the EPA method 8330. Equal volumes of acetonitrile were added to the liquid samples, shaken and filter sterilized with a 0.45µm Teflon filter into a brown HPLC vial which was then sealed. RDX concentrations from enrichment cultures were analyzed using a modular waters HPLC system

consisting of Waters 717+ autosampler, two waters 515 HPLC pumps, and a Waters 9926 photodiode array detector.

DNA extraction

DNA was extracted from soils using a modification of the method of Dong et al. (2006) which incorporates the use of aluminum sulfate to reduce the amount of humic acid co-extracted with the DNA which could affect downstream applications. This method was optimized previously in the lab and found to extract high molecular weight DNA which is required for stable isotope probing and for the preparation of genome libraries.

Rosetta-gami B strain of *E. coli*

Initially the Rosetta-gami B strain of *E. coli* (Novagen, RGB) was used for the clone library due to the incorporation of novel transfer RNAs into the strain, which gives this strain the ability to properly produce protein from a wider range of environmental DNA. For example the RGB strain can express active forms of xplA/B enzymes produced from DNA extracted from Rhodococcus 11Y.

Solvent Screening

Solvents are required for the preparation of RDX. However some solvents such as DMSO many affect cell growth and protein expression. A number of solvents were examined, none of which were found to inhibit growth or protein folding, including DMSO, DMF and acetone. Acetone was subsequently chosen as optimal growth was obtained with RGB in M9 media and acetone was shown to not inhibit xplA activity.

Control experiments using xplA gene from Rhodococcus 11 Y

RGB containing the expression vector ligated with the xplA gene, was inoculated in M9 medium with RDX concentrations ranging from 10µM to 250µM RDX, whereby RDX was the sole nitrogen source. The media contained glycerol, sodium formate, required antibiotics, IPTB, alpha amino leuvic acid, cysteamine (formaldehyde trap), and trace elements. RDX was prepared in acetone. The RGB was grown under both microaerobic and anaerobic conditions. While higher levels of growth of Rosetta-gami B was observed for microaerobic conditions initially, RDX removal was similar for both conditions over most RDX concentrations. A concentration of 200µM RDX was chosen for subsequent studies as this level promoted the highest levels of growth for both conditions as well as producing high levels of nitrite.

Subsequently 200 µM of RDX medium was inoculated with varying dilutions of cells containing the xplA gene in relation to empty cells containing an empty vector ranging from ratios of 1:0 to 1:1000. Growth and nitrite concentrations were monitored. RDX levels were determined. DNA was extracted and qPCR was used to determine copy numbers of xplA gene per ng of DNA. Growth was observed at all dilution ranges containing the xplA gene, with highest growth in cultures containing the higher ratios of the xplA gene. QPCR analysis of the anaerobic cultures indicated that for all ratios the xplA gene was detected at increasing amounts relative to total DNA with approximately a 10 fold increase for media containing one xplA gene for every empty vector.

Stable Isotope Labeling Experiment Using Soils From Aberdeen MD Training Range and Milan TN

A stable isotope experiment using soil from Aberdeen, Maryland, which had been shown to degrade

RDX, was performed. Soil was exposed to ^{14}N-RDX and ^{15}N-RDX. RDX was completely degraded by day 11. Samples were taken on Day 0, 7 and 11 and DNA was extracted. The DNA was subjected to ultra-centrifugation to separate DNA containing heavy labeled nitrogen (^{15}N) from the lighter labeled (^{14}N). DNA was collected in fractions from each centrifuge run. Density of each fraction and the concentration of DNA of each fraction was determined and compared for ^{15}N eand ^{15}N samples from Day 7 to Day 11. Shifts in maximum DNA concentration relative to density were observed in samples containing heavy labeled DNA. qPCR of the xplA gene was carried out on each fraction and peaks were observed at points similar to the maximum DNA ratio for each range of samples.

Samples from the fractions D7 and D11, with the higher DNA concentrations at the higher densities were selected and amplified via multiple displacement amplification (MDA). This is a non PCR method that randomly amplifies whole genome DNA and can be optimized to reduce any bias. MDA increased the concentration of each fraction approximately 100 fold. DNA fractions from were pooled along with fractions from the same time point and concentrated. DNA was digested with Sau3aI to create fragments approximately 10kb in length which were ligated to the expression vector Pet16B.

Vectors were transformed and inoculated into LB medium containing the appropriate antibiotics.

A similar SIP set up was carried out with bacteria enriched from soil samples taken from Milan, Tennessee. Complete degradation occurred after 8 days. Again DNA was extracted and subject to centrifugation with fractions from ^{15}N labeled DNA on day 8 chosen to create a genomic library.

DNA Fractionation

In order to fractionate environmental DNA into usable sizes for insertion into the function screening vector partially digested DNA was fractionated using a 15% - 35% sucrose gradient (ca. 16 hrs at 40,000 rpm) (Figure 2).

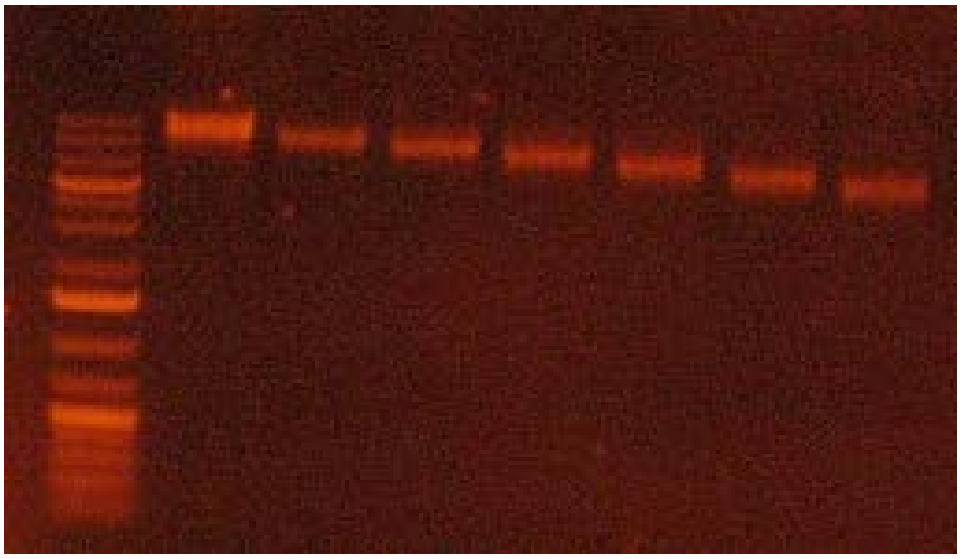

Figure 2. DNA fractionation in a sucrose gradient

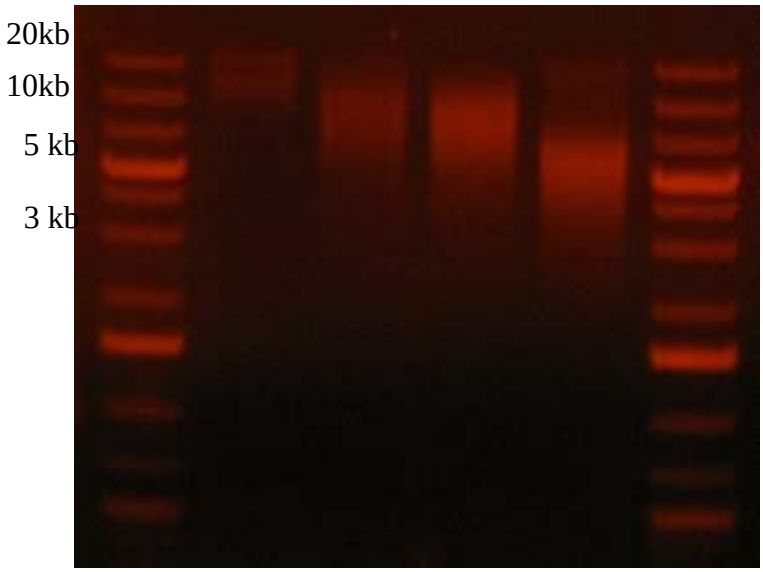

Figure 3. Library Construction.

Extracted DNA was partially digested, fractionated and size selected (e.g., 5 kb – 20 kb). Pooled fractions of *Mycobacterium* sp. MA2 were partially digested with PvuI.

Fosmid construction

We used fosmid 28A, a 50Kbp fosmid which contained xplBA and upstream operon elements from a RDX-degrading *Microbacterium* sp., as the source DNA to first determine if we could retrieve the functional genes in our metagenomic screen. We randomly sheared the fosmid through enzymatic digestion and used a sucrose gradient for size selection. Fragments were subsequently cloned into pJN104 for expression in *Pseudomonas putida* KT2440 and tested for RDX degradation in liquid and plate culture (Figure 2).

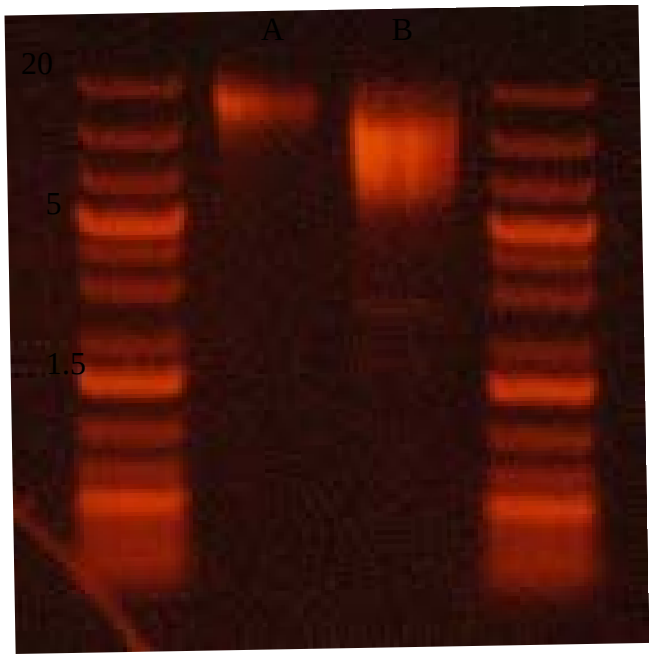

Figure 4. Method development: Ligations and transformations

We used two Fosmid clones (each with more than 30 kb of DNA from *Microbacterium* sp. MA1 with *xplB* and *xplA*). We pooled gradient fractions into two groups, A and B. Pool B included lower molecular weight DNA, but amplification of plasmids extracted from *E. coli* used DNA amplified from primers xplBF-xplAR (about 3 kb).

Library construction method development.

DNA extracted from *Mycobacterium* sp. MA2, an RDX degrader with the xplB/A gene cluster, was used to develop library construction methods and was used to evaluate the protocol outlined below and in Figure 5 and Figure 6:

A) DNA was partially digested and then fractionated on a sucrose gradient

B) DNA was ligated into the pJN105 vector PCR amplified with primers containing compatible digestion sites

C) *E. coli* (DH10B, NEB) was transformed with the ligation reactions via electroporation and plasmids extracted following brief growth on antibiotic selective plates

D) *P. putida* KT2440 cells were transformed with the extracted plasmids via electroporation and selected on minimal antibiotic selection plates

E) Dilutions of *P. putida* transformants were plated on RDX selection plates

1. Generate metagenomic library:

A) DNA was partially digested with a restriction enzyme

B) Digested DNA was size selected (> 5 kb) using sucrose gradients

C) DNA was ligated into the pJN105 expression vector

D) *E. coli* DH10B were transformed (e-poration) with ligation reactions and selected on LB agar w/ Gent 10

E) *E. coli* plates were swabbed into broth, washed twice and plasmids were extracted

2. Transform expression host cells with library:

F) *P. putida* KT2440 were transformed (e-poration) with extracted plasmids (100 ng) and selected on minimal media w/ Gent 15, NaI 10

3. Selection for RDX degradation enzymes:

G) *P. putida* KT2440 plates were swabbed into buffer and plated onto RDX plates and/or used to inoculate RDX liquid culture (RDX as sole N source)

Figure 5. Library construction – Method Overview

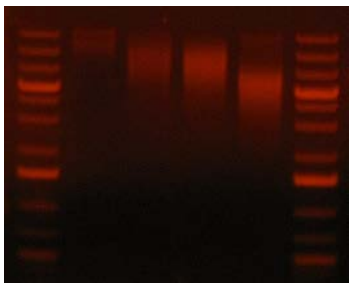

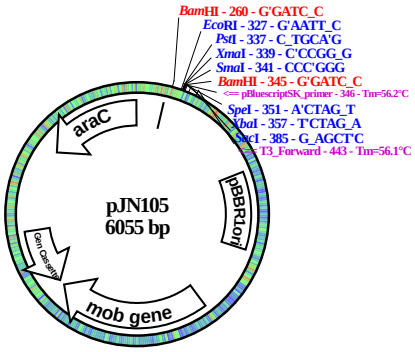

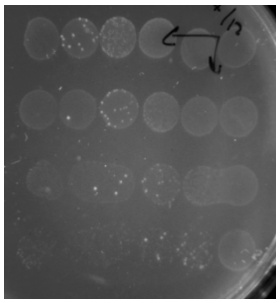

1. Generate metagenomic library

2. Transform expression host cells *P. putida* KT2440 with library

3. Select for RDX degradation enzymes

Figure 6. Functional Screen for RDX degradation enzymes in *Pseudomonas putida* KT2440

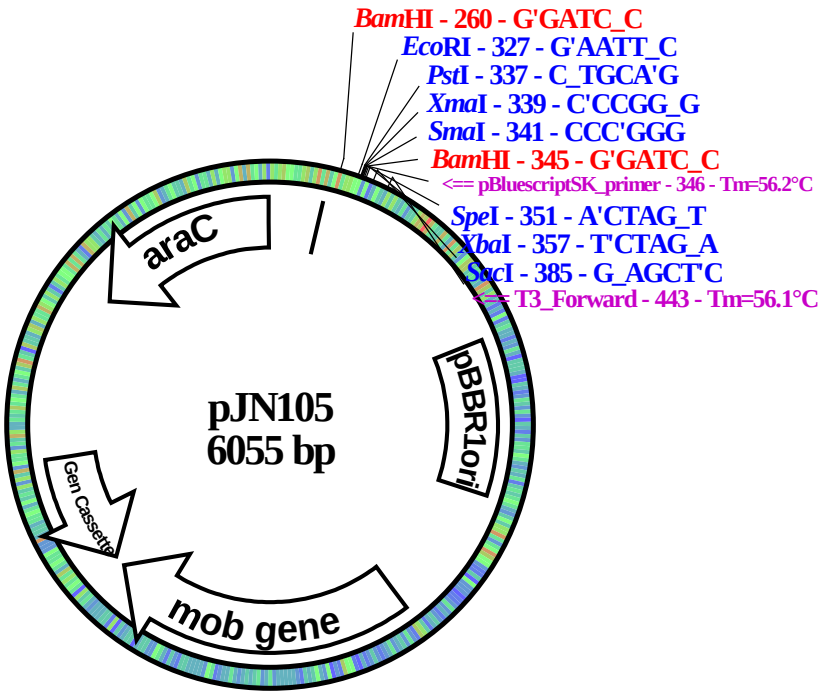

Figure 7. Library construction

Host vector construction. Size selected DNA was ligated into the broad expression vector, pJN105, which has the pBBR1 origin. Expression was induced by L-arabinose (Newman and Fuqua 1999).

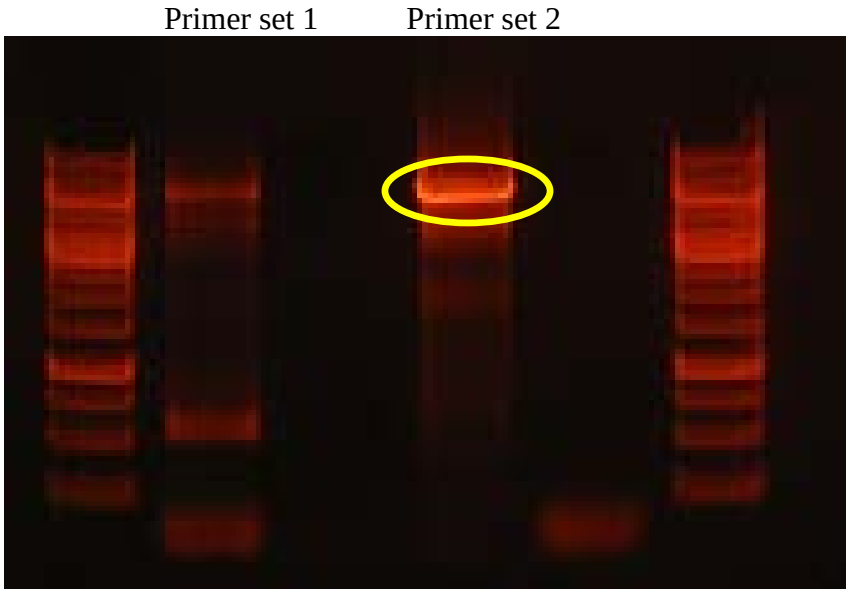

Figure 8. Vector preparation – PCR amplification

Inserts were amplified using amplification primers that included insertion sites. The band was gel purified, digested and dephosphorylated.

Development of high-efficiency clone library mating protocols

For the method to be successful, it was necessary to generate a sufficiently large metagenomic library (>10^4 clones) in *Pseudomonas putida* KT2440 containing fragmented DNA of size larger than 5 kb. Therefore, we tested several methods for transforming *P. putida* KT2440 (Figure 9). We determined that conjugative transfer from an *E. coli* donor is the best method for maximizing the size of the library. We tested two conjugative methods: a biparental mating protocol where a conjugative *E. coli* strain, S17-1, was transformed and then mated with *P. putida* KT2440 and a triparental method where *E. coli* DH10B was transformed and conjugation with *P. putida* KT2440 was facilitated by another *E. coli* strain carrying the helper plasmid pRK2013. The biparental method (Figure 10) was more direct and led to more exconjugant *P. putida* KT2440 cells, however the triparental method allows for the use of highly efficient competent cells (i.e., DH10B) in the initial library generation. We found that both mating protocols generated several orders of magnitude more *P. putida* KT2440 exconjugates than through direct transformation of *P. putida* KT2440 cells (Table 1).

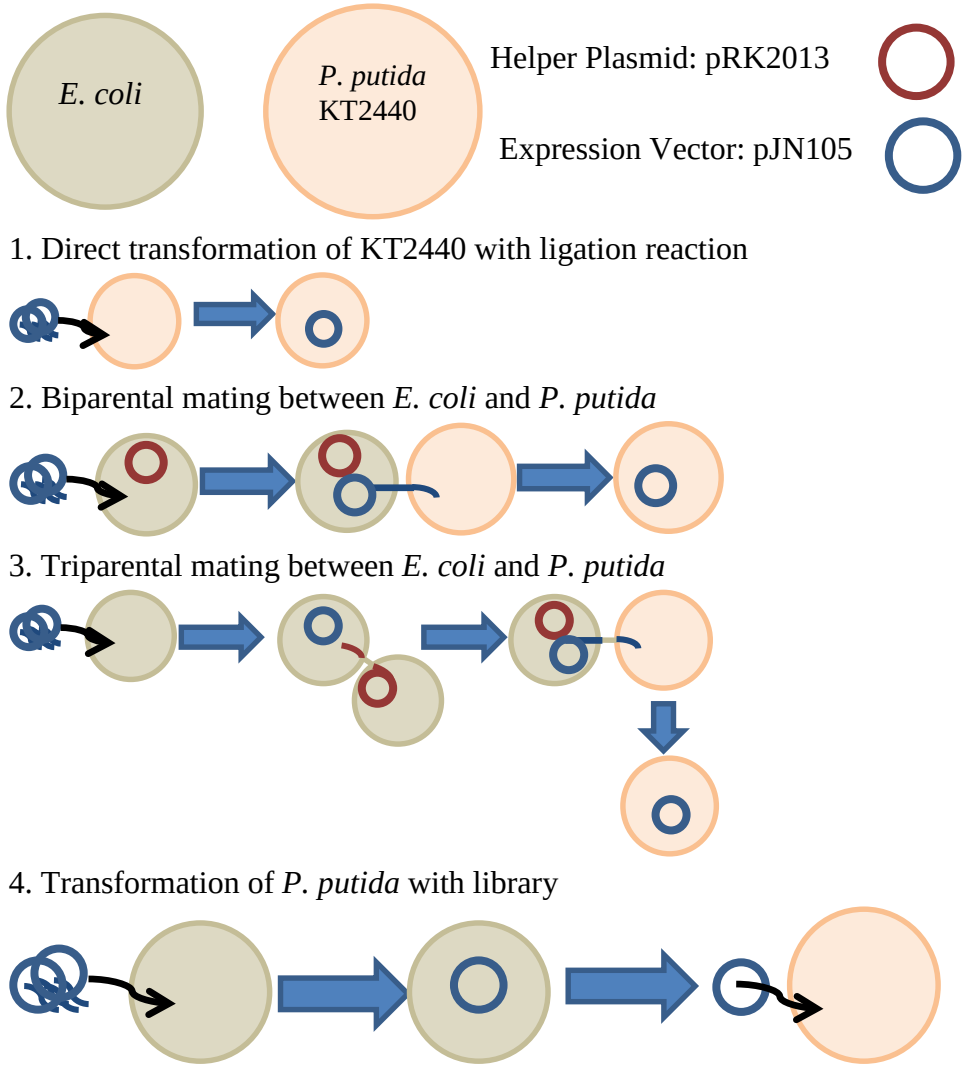

Figure 9. Methods for expression library creation in *Pseudomonas putida* KT2440

1. Mating mixtures plated:

Donor mix: 50 ml of DH10B ($3.0x10^7$ - based on OD), DH10B with pRK2013 or S17-1, and pJN105 plasmid mix ($3.3x10^4$ – based on OD). Negative controls consisted of about $1.5x10^7$ with pRK2013 only. Recipient: KT2440 (equivalent to *E. coli* or 2x based on OD).

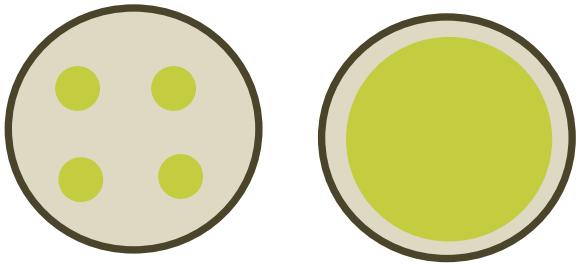

20 µl of mating mix

20 µl of mating mix

2. After ~20 hrs mating mixtures were scraped into buffer (N^-, C^-)

3. Cell suspensions were diluted as necessary and plated on minimal media with nitrite, glucose/glycerol/succinate and gentamicin and nalidixic acid

Figure 10. Evaluation of biparental -- mating protocols

Table 1. CFUs from biparental- mating test

Donor Mix	KT2440 Amount	Estimated CFUs from LB Spot	Estimated CFUs From R2A spot	Estimated CFUs from LB Smear
DH10B w/pRK2013 & pJN105 mix	1x	6,100	600	$7.3x10^4$
DH10B w/pRK2013 & pJN105 mix	2x	460	190	$5.6x10^4$
S17-1 pJN105 mix	1x	0	10	3,250
S17-1 pJN105 mix	2x	0	10	3,750
pRK2013 only	2x	0	0	<250

We also tested various methods of transforming host cells to optimize yields (Table 2).

Table 2. Transformation tests using pJN105 plasmids with mixed inserts

Cells	Preparation/ Transformation Method	DNA Conc	Colonies per transformation	Est CFU/ mg DNA
DH10B (NEB)	Chemical Comp	5 ng (est)	$1.9x10^5$	$3.8x10^7$
DH10B (NEB)	Electro-Comp	0.5 ng (est)	$5.08x10^5$	$1.02x10^9$
DH10B	Chem ($RbCl_2$)	5 ng (est)	$1.2x10^5$	$2.4x10^7$
DH10B+pRK2013	Chem ($RbCl_2$)	5 ng (est)	$1.36x10^5$	$2.5x10^7$
DH10B+pRK2013	E comp (GYT Buff)	10 ng	$8.70x10^5$	$8.70x10^7$
S17-1	E Comp (GYT)	10 ng	$5.5x10^4$	$5.5x10^6$
KT2440	E Comp (300 mM Sucrose)	10 ng	$2.5x10^3$	$2.5x10^5$

To maximize the size of the library, it was necessary to generate high quality insert DNA and vector. To generate high-quality, appropriately-sized DNA fragments, we tested several size selection methods. We determined that sucrose gradients work best for this purpose. We also developed a PCR based method for preparing the pJN105 vector suitable for our library generation. This method helped to reduce the number of empty vector clones and permitted the easy incorporation of restriction digest sites into the vector as desired.

Using these methods KT2440 transformations routinely generated more than 40,000 colonies/ transformation

Chemicals

RDX (99% pure) and ring-labeled [^{15}N]-RDX were provided by the Defence Research and Development Canada (DRDC), Valcartier, Canada. Hexahydro-1-nitroso-3,5-dinitro-1,3,5-triazine (MNX; 98% pure), ring-labeled [^{15}N]-MNX, 4-nitro-2,4-diazabutanal (NDAB; 99% pure), and methylenedinitramine (MEDINA) were purchased from SRI International. ^{18}O-labeled oxygen (minimum, 99 atom %) and ^{18}O-labeled water (97 atom %) were purchased from Isotec Inc., Miamisburg, Ohio. All other chemicals, including NH_2CHO, nicotinamide adenine dinucleotide phosphate (NADPH), and sodium nitrite, were reagent grade.

Enzymatic assays

XplA and XplB were produced as described by Jackson et al. (2007). Enzymatic assays using the XplA and XplB system were prepared to test the removal of MNX and to determine products distribution under aerobic and anaerobic conditions. Stock solutions of the substrates were prepared in 50 mM phosphate buffer (pH 6.9). Enzymes and NADPH were freshly prepared in water. In aerobic assays, the reaction mixtures contained 98 µM MNX, 700 µM NADPH, and 176 nM of XplA and XplB whereas in the anaerobic assays the reactions mixtures contained 99 µM MNX, 700 µM NADPH, and 220 nM XplA and XplB. The reactions were initiated by the addition of NADPH. The assays were conducted in 6 mL headspace vials, away from light, statically at 21 ^{o}C. Anaerobic reactions were prepared in an anaerobic chamber in the presence of nitrogen with up to 4% of hydrogen (Forma Anaerobic System, model 1025, Thermoscientific, Marietta, OH) using reagents that were made anaerobic by repetitive degassing (3 times) and introducing O_2-free Argon to the reagent vials. Controls with boiled XplA and XplB, in addition to NADPH and MNX, were also prepared.

Additional enzymatic assays with MNX were performed with XplA-heme and a substitute redox system composed of ferredoxin and ferredoxin reductase, under both aerobic and anaerobic conditions. The assays were performed in 50 mM phosphate buffer pH 7.0 and contained 175 nM of XplA-heme, 171-194 µM MNX, 500 µM NADPH, 20 µg spinach ferredoxin (Sigma Aldrich) and 0.02 units of spinach ferredoxin reductase (Sigma Aldrich). Controls without XplA-heme were prepared in parallel. The anaerobic conditions were made by degassing for 20 min and then performing 5 cycles of degassing and recharging with argon. The vials were incubated at room temperature (~20^{o}C). Aliquots were collected at different time intervals and assays were stopped by centrifugation through 30-kDa cut-off Millipore spin columns.

Other enzymatic assays were performed to determine the kinetics of the removal of RDX, MNX and TNX incubated separately, as binary mixtures of RDX/TNX, MNX/TNX and as a mixture of RDX, MNX, DNX and TNX (approximately 123 µM each) with XplA/XplB under the same conditions as described above. In the case of the different mixtures, the concentrations of XplA and XplB were 220 nM under both aerobic and anaerobic conditions, and 1.6 mM NADPH was used.

Growth of *Rhodococcus* sp. strain DN22 and resting cell assays

Rhodococcus sp. strain DN22, provided by N. V. Coleman, (University of Sydney, Sydney, Australia) was grown in mineral salt medium (MSM) supplemented with succinate (2.4 mM) as the carbon source (Fournier et al. 2002). RDX (220 µM) or MNX (220 µM) was added as the sole nitrogen source from an acetone stock solution. Acetone was evaporated followed by addition of the medium MSM (pH 7). Cultures were incubated at 25 ^{o}C with agitation (250 rpm) and growth was monitored at 530 nm as described by Fournier et al. (2002).

Resting cell assays were conducted using mid-log phase cultures (A_{530} = 0.60 to 0.65). Cells were harvested at 15000 x g, 4^{o}C, for 15 min using a Sorvall RC6 Plus centrifuge, then washed and resuspended in MSM to an absorbance of 1.0. No carbon or nitrogen sources were made available except for RDX or MNX (220 µM for both). In some cases, NH_4Cl (1.0 mM) was added to prevent the uptake of NO_2^-. The assay bottles were then incubated at 25^{o}C with agitation (250 rpm) under aerobic conditions (Fournier et al. 2002). Chemical controls containing either RDX or MNX or NO_2^- were prepared in MSM without DN22 cells. Products

analyses were conducted as described below. When LC–MS analysis was required, cells were washed and resuspended in deionized water (pH 5.5) to an absorbance of 4.0. For certain cell suspensions, ring-labeled [^{15}N]-RDX or [^{15}N]-MNX (220 μM for both) was used in order to identify metabolites with nitrogen atoms using LC/MS (see below).

To determine the role of oxygen in the denitration of RDX and MNX with DN22 the chemical(s) were incubated with the bacterium in the presence of either $H_2{}^{18}O$ or $^{18}O_2$. For tests that required $H_2{}^{18}O$, RDX or MNX grown cells were harvested as described above except they were resuspended in $H_2{}^{18}O$ in the presence of RDX, MNX, or NO_2^- (220 μM, 220 μM or 430 μM, respectively). For tests that required $^{18}O_2$, RDX or MNX grown cells were harvested as described above and resuspended in deionized water. Cell suspensions along with solutions of RDX, MNX, or NO_2^- (220 μM, 220 μM or 430 μM, respectively) in water were flushed with N_2 to remove air. Cell suspensions were then added to the substrate solutions in an anaerobic glove box. $^{18}O_2$ was then added as described by Fournier et *al*. (2002). Controls containing either RDX or MNX or nitrite were prepared in water in the presence of DN22 cells and air.

For experiments with NH_2CHO, RDX grown cells were harvested as described above and resuspended in deionized water to an absorbance of 1.28. No carbon or nitrogen sources were made available except for NH_2CHO (230 μM).

Chemical analysis

Aliquots from the liquid culture media described above were centrifuged at 16000 x g for 4 min using an Eppendorf Centrifuge 5415 D (Eppendorf AG, Hamburg) and the supernatant was used for chemical analysis. We determined RDX, MNX, and HCHO by HPLC (*22*) and NO_2^-, NO_3^-, and HCOOH by Ion Chromatography (Balakrishnan et al. 2004). Nitrous oxide was analyzed by GC/ECD (Bhatt et al. 2006). NH_2CHO was first derivatized by treatment with pentafluorobenzylhydroxylamine (Hawari et al. 2002) and analyzed by LC-MS as its deprotonated molecular mass ion $[M–H]^-$. NDAB and MEDINA were determined by HPLC and by comparison with authentic materials (Zhao et al. 2008). NDAB and NO-NDAB were analyzed by LC-MS (Halasz et al. 2010). Because MEDINA is unstable, the samples were analyzed shortly after sampling (Paquet et al. 2011).

NH_4^+ was determined colorimetrically using EPA method 350.1 (EPA 1993).

^{18}O-labeled NO_2^-, NO_3^-, NDAB coming from either MNX or RDX were analyzed using a mass spectrometer (MS) (Bruker MicroTOFQ mass analyzer) attached to an HPLC system (Hewlett Packard 1200 Series) equipped with a DAD detector. Aliquots (20 μL) from the previous assays were injected into a 3.5 micron-pore size Zorbax SB-CN column (2.1 mm ID by 100 mm; Agilent, Mississauga, Canada) at 25°C. The solvent system was composed of 10% to 80% (v/v) of CH_3CN/H_2O gradient at a flow rate of 0.15 mL min^{-1}. A negative electrospray ionization mode was employed to generate the deprotonated molecular mass ions $[M–H]^-$ using a mass range from 30 to 400 Da.

Growth media

Bacteria were grown in minimal medium (MM), Luria-Bertani (LB) broth and Luria-Bertani Peptone (LBP).

The MM (11.4 mM KH_2PO_4, 28.5 mM K_2HPO_4 , pH 7.2) was amended with 10 mM glycerol, 5 mM glucose, 5 mM succinate, trace elements and RDX or NH_4Cl at different concentrations. Trace element composition (250X) was done as follows : 50 ml concentrated

HCl, 10 g $MgSO_4$, 2 g $CaCO_3$, 5.6 g $FeSO_4.7H_2O$, 1.44 g $ZnSO_4.7H_2O$, 1.11 g $MnSO_4.7H_2O$, 0.25 g $CuSO_4.7H_2O$, 0.28 g $CoSO_4.7H_2O$, 0.062 g H_3BO_3 for 1 L final in water. Trace elements were added aseptically and RDX stock (1 M in DMSO) was diluted appropriately. When required, 1 % agarose (w/v) was added to solidify the medium.

LBP contained 1% (w/v) Bacto-peptone, 0.5% (w/v) yeast extract and 1% (w/v) NaCl.

LB contained 1% (w/v) Bacto-tryptone, 0.5% (w/v) yeast extract and 1% (w/v) NaCl. For the preparation of the agar, 15 g/l micro-agar (Duchefa Biochemie, Haarlem, Netherlands) was added to LB prior autoclaving.

Rhodococcus rhodochrous 11Y and the knock-out strains were grown at 30 °C under shaking (150 rpm).

E. coli were grown at 37 °C under shaking (180 rpm).

Mating experiments

Mating experiments were performed as in (Bröker et al., 2008). Briefly, cultures of recipient and donor strains were spun for 2 min at 5000 rpm and washed using LB. Cells were resuspended in LB and pelleted again for 2 min at 5000 rpm. The supernatant was removed and the mating pellet transferred onto LB plates at 28 °C for 24 h. The mating spot was then resuspended in 0.5-1ml LB and spread in serial dilutions on MM agar containing RDX and the appropriate antibiotic to select transconjugants able to grow on RDX as sole nitrogen source. Controls with single donor and single recipient strains were treated the same way. Different mating conditions were tested and described as follows ([volume, OD, strain]):

- [0.5ml, 1.8, 11Y]* [0.5ml, 0.92, CW25];
- [0.5ml, 1.8, 11Y]* [0.5ml, 0.4, NCIM9784] ;
- [0.5ml, 1.8, 11Y]* [0.5ml, 0.92, *P. fluorescens* F113];
- [1ml, 0.96, 11Y]*[1ml, 0.92, CW25] and
- [25ml, 0.8, 11Y]* [25ml, 1.6, CW25].

Degradation tests

Several compounds were tested to see whether they could be utilized as sole carbon or nitrogen sources by *Rhodococcus.* Therefore, bacteria were grown in MM as described above without the addition of any carbon sources, but with addition of NH_4Cl (1 mM) as nitrogen source. Taurine (15 mM final), benzoate (3 mM final), camphor (0.5 g/l final) and phenol (0.4 g/l and 0.8 g/l final) were aseptically added and 10 ml of medium were inoculated with 20 µl of a bacterial culture grown in LB to an OD_{600} of 0.3. Growth was scored visually and by OD_{600}. The following controls were set up:

- cultures without any carbon source,
- cultures without any nitrogen source,
- cultures without any carbon and nitrogen source and
- cultures with carbon and nitrogen sources.

Construction of knock-out strains

Using primers listed in Table 3, regions of ORF 27, ORF 29, ORF 31 and ORF 32 were amplified to produce PCR products with *Eco*RI and *Nde*I restriction sites for the upstream regions and *Nde*I and *Hind*III restriction sites for the downstream regions. Each pair of upstream and downstream regions were cloned together into *Eco*RI and *Hind*III-digested pK18mobsacB

(Figure 11) to produce the mutagenic plasmids: p11Y*orf27*, p11Y*orf29*, p11Y*xplB* and p11Y*xplA*.

The recipient strain, *R. rhodochorous* 11Y was spread onto LBP agar supplemented with nalidixic acid (30 µg/mL) and incubated at 30 °C for 5 days. Each mutagenic plasmid (pK18mobsacB-xplA, pK18mobsacB-xplB, pK18mobsacB-permease, and pK18mobsacB-MarR) was transformed by heat-shock (37°C for 5 min) into *E. coli* S17-1 (donor strain). Competent *E. coli* S17-1 were prepared by growing 0.5 ml of a pre-culture in 50 ml pre-warmed LB medium until OD_{600} 0.3-0.4. Cells were then pelleted and resuspended in 0.5 ml Transformation and Storage Solution medium (TSS). The TSS medium comprised 10 ml 2xLB ph 6.5, 5 ml PEG3350 40%, 1ml DMSO and 4 ml $MgCl_2$ (1M). 2xLB medium contained 2% tryptone, 1% NaCl and 1% yeast extract. The transformed *E. coli* S17-2 were grown on LBP agar supplemented with kanamycin (25 µg/mL) for 24h at 37°C and a further 24 h at room temperature. Recipient and donor strain were harvested from the agar by washing the agar with 2ml LBP. 750 µL of both strains were gently mixed together and centrifuged (8,000 x g) for one minute. Cells were resuspended in 1 mL of LBP and 200 µL aliquots were spread onto non-selective agar and incubated at 30 °C overnight. After the incubation, 2 mL LBP was added to the plates and cells were again harvested by rinsing the agar surface. Cells were diluted (2 and 4-fold) and aliquots (100 µL) were spread on LBP agar supplemented with nalidixic acid (30 µg/mL) and kanamycin (50 µg/mL). Transconjugants appeared after 3-4 days incubation and colonies that were kanamycin resistant and sucrose sensitive were selected by replica plating. Colony PCR using primers specific to *sacB* was performed to further confirm the presence of the mutagenic plasmid in the recipient strain.

Sucrose sensitive derivatives of strain 11Y (1^{st} mutant) were grown in 10 mL of non-selective LBP medium at 30 °C, 120 rpm overnight. Aliquots were spread on LBP agar supplemented with nalidixic acid (30 µg/mL) and sucrose (10 % w/v). Gene deletions in sucrose resistant, kanamycin sensitive mutants were confirmed by PCR using gene specific primers spanning each putatively deleted gene (Table 3).

Table 3: List of primers used for amplification of DNA fragments

Name	Sequence (5' to 3')	Target
Primers for mutagenic plasmids construction:		
ORF 29:		
UpF822(perm)+EcoRI	ACGTCGGAATTCAGTGTCGGGCGGACC	permease upstream
UpR30(perm)+NdeI	GAATTCCATATGGGACGTATAACCGAG	permease upstream
DwnF0(perm)+NdeI	ATTCCGCATATGAAGAAGACCGGGGAG	permease downstream
DwnR975(perm)+HindIII	GCGCAGAAGCTTCCTGGGCAGATCGAC	permease downstream
ORF 27:		
UpF861(rp)+EcoRI	GGGGAATTCCGAGGATCGCCGTGA	regulator upstream
UpR75(rp)+NdeI	TGGTCCCATATGGCCCGACACTCGACG	regulator upstream
DwnF116(rp)+NdeI	CTGGCGCATATGTCAAAAAACCCTAT	regulator downstream
DwnR852(rp) +HindIII	ACAGACAAGCTTCGATCAGTGCGGCGG	regulator downstream
ORF 32:		
UpF816(xplA)+EcoRI	CGATCTGAATTCGCACCCGGACACCCT	xplA upstream
UpR33(xplA)+NdeI	ATTCTCCATATGGGGTTCACTGCAGGC	xplA upstream
DwnF7(xplA)+NdeI	GTCCTGACATATGATCCGATCTCACCTGCC	xplA downstream
DwnR975(xplA)+HindIII	CCCAAGCTTGACGGTCCAGGGCGTTGT	xplA downstream
ORF 31:		
UpF1083(xplB)+EcoRI	ACCATGGAATTCACGAACATCAGAGCT	xplB upstream
UpR135(xplB)+NdeI	GTCGAGCATATGCACGTCGGGGATACG	xplB upstream
DwnF30(xplB)+NdeI	ACCCGACATATGACACCCGAGATGGAG	xplB downstream
DwnR849(xplB)+HindIII	CGTCCAAAGCTTCCAGTTTCGGCGTGA	xplB downstream
Primers for detection of sacB, permease, regulator and 16S:		
sacBf 488	GGTCAGGTTCAGCCACATTT	sacB
sacBr 1262	CCTTTCGCTTGAGGTACAGC	sacB
permF260	TGATCGCGCTGCTCGTCACCAT	permease
permR1086	CGAGGACGACCATCTGGAAGGCGAT	permease
permease-1F	ATGAGTCCGTGGGCGAACTTCG	permease
permease-1395R	CTACTCCCCGGTCTTCTTCGGAAT	permease
rpF1	GTGACGAACGACGATCTGGTGCAC	regulator
rpR543	ACAATGGTCATGTTCCGGTAACC	regulator

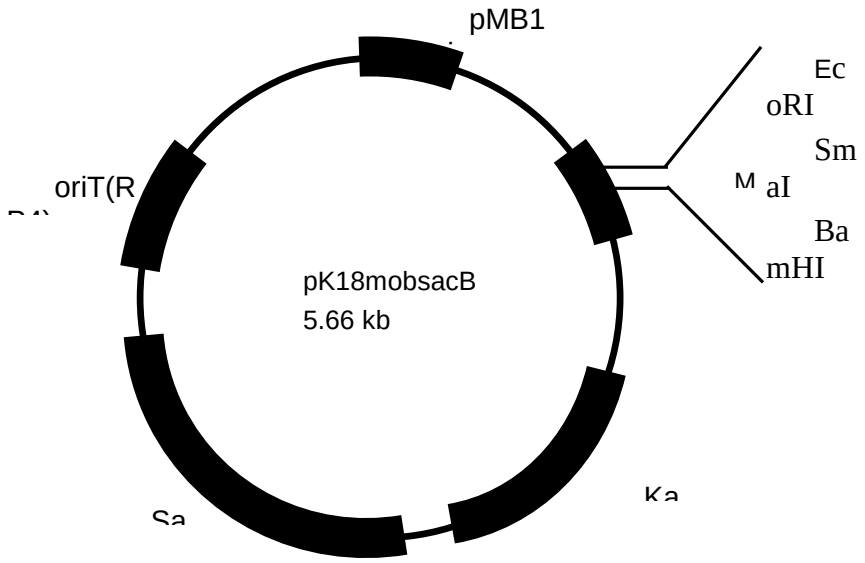

Figure 11: Plasmid map of pk18mobsacB

Cosmid and pGEM-T shotgun libraries construction

A cosmid library of the *Rhodococcus sp.* 11Y DNA was constructed using the pWEB vector from the pWEB cosmid vector kit (Epicentre) and phage T1 resistant EPI100-T^R *E. coli* following the instructions provided. The DNA was not mechanically sheared before the end-repaired step as it was already at the appropriate size (40 kb). Cells were selected on LB agar containing ampicillin (50 µg/ml) and 960 clones were inoculated in 50 µl LB in 96 well plates and incubated shaking for 40 h at 37 °C. Pools of eight different bacterial cultures were created by adding 1 µl of each culture to 42 µl sterile water. Cells were then lysed according to the PCR colony protocol as described above. Two µl of the lysates were used as PCR matrix using 531 *xpla*F and 1033 *xpla*R primers (total PCR volume of 25 µl) (Table 4) to identify pools with *xplA* clones. Positive clones from the pools containing *xplA* were identified by resuspending one µl of the original LB cultures in 45 µl of water and performing again a PCR using an internal *xplA* primer. Positive *xplA* clone cosmid DNA was extracted with a mini-prep kit (Qiagen) from two 10 ml LB cultures containing ampicillin. To elute the DNA from the column the elution buffer was pre heated to 70 °C.

Three independent partial digestions of 100 ng of cosmid DNA were performed using 1 µl of *Bser*I, *Hinc*II (New England Biolabs) or *Rsa*I (Promega) in a 10 µl reaction. Digestions were performed for 45 min at 37 °C. Partial digestions were stopped after 15 min incubation at 65 °C and loaded on a 1 % agarose gel. The smear of each digestion was cut from the gel in a range size of 800 to 3000 bp. All gel plugs were pooled together and purified with the Wizard SV gel and PCR purification system kit (Promega) according to the manufacture's recommendations.

DNA was concentrated under vacuum to 80 ng/µl and an A-tailing step (11.5 µl DNA, 4 µl buffer 5X, 2 µl 25 mM MgCl2, 0.5 µl 10 mM dATP and 2 µl GoTaq) was performed for 45 min at 70 °C. Inserts were ligated into pGEM-T and chemically transformed into competent Top10 (Invitrogen) cells. Cells were placed at 42 °C for 90 sec and then transferred back to ice for 5 min. Clones were selected and purified on selective agar containing X-gal for blue/white selection. Inserts were amplified and sequenced with the SP6 and T7 primers as described above (Table 4).

Table 4: Primer used for the cosmid library

531 *xpla*F	GAACAACCCCTATCCCTGGT	*xpla*
1033 *xpla*R	TCAGATAGCCGAAAGCGACT	*xpla*
sp6	AAGATATCACAGTGGATT TA	pGEM-T cloning site
T7	TAATACGACTCACTATAG GG	pGEM-T cloning site

Crude extracts and membrane proteins extraction.

Cultures were grown either in LB medium to an OD_{600} of 0.5 or in MM containing RDX to the stationary phase. Cells were then pelleted, washed in phosphate buffer and resuspended in 1 ml of phosphate buffer containing 15 µl fresh PMSF and 100 µl protease inhibitor cocktail. Cells were sonicated (Misonix) with a micro-probe for 6 min using a cycle of 3 sec on and 3 sec off and centrifuged for 15 min at 10000 x g at 4 °C. Protein concentrations were determined using Coomassie Dye Binding Reagent (Pierce, Rockford, IL, US, supplied by Perbio Science, Cramlington, UK) with the coomassie blue method (Spector, 1978). For quantification, a standard curve was prepared using bovine serum albumin (BSA) solutions of known concentrations and measured at 595 nm in a Spectrophotometer (UV-VIS Spectrophotometer UV-160A, Shimadzu Europe).

Total membrane proteins were isolated from crude protein extracts by ultracentrifugation at 160,000 x g according to(Drew et al., 2001). The formed pellet containing the membrane proteins were resuspended with SDS loading buffer (1 ml glycerol, 2 ml H_2O, 1 ml 0.5 M Tris-HCl, pH 6.8, 1.6 ml 10 % w/v SDS, 0.4 ml β-mercaptoethanol and 20 mg bromophenol blue).

Cloning

PCR products were cloned in pGEM-T (Promega) and pTOPO (Invitrogen) vectors according to the manufacturers' instructions. Cloning into the pET YSBLIC 3C expression vector was done with tagged primers as described in (Bonsor et al., 2006).

The *xplB*-glutamine synthetase (*xplB/glnA*) fusion gene was cloned into the pET-28a(+) expression vector and expressed, as a N-terminus his-tagged protein, in *E. coli* BL-21(DE3). Following the observation of high endogenous reductases activity when using the pET-28a(+) vector, the *xplB/glnA* fusion was subsequently also cloned into pGEX 4T-3 and also expressed in *E. coli* BL-21 (DE3).

Protein expression and His tag purification

A 1L culture of *E. coli* Rosetta 2 harboring the cloned gene of interest in the pETYSBLIC-3C expression vector was grown to an OD_{600} of 0.7-0.8 in LB containing kanamycin (100 µg/ml) and chloramphenicol (34 µg/ml) and induced with 1 mM IPTG for 3 h. The cells were then washed with 50 mM KPO_4, 0.3 M NaCl buffer (pH 7.5). 1g cell pellet was resuspended in 35 ml of 50 mM KPO_4, 0.3M NaCl buffer (pH 7.5) containing 100 µl of 0.1 M PMSF. Cells were sonicated for 8 min with a cycle of 4 sec on and 12 sec off and then centrifuged for 15 min at 1725 x g at 4 °C. The supernatant was added to 0.5 ml of HIS Nickel affinity resin (Sigma) previously washed with 10 column volumes of 50 mM KPO_4, 0.3M NaCl buffer (pH 7.5). The mix was incubated at room temperature for 2 h on a rocking table and then centrifuged 10 min at 500 x g. Prior to elution, the resin was washed (1 ml/min) with 5 ml of 0.05 M KPO_4, 0.3M NaCl containing 50 mM imidazole. The specific HIS-tag proteins were then released in a similar way, by increasing the imidazole concentration in the buffer to 250 mM. Imidazole was removed by two successive dialysis steps for 2 h and overnight in 4 l of 0.05 M KPO_4, 0.3 M NaCl without imidazole.The purified protein could be then concentrated with a microcon column (Millipore) according to the manufacturer instructions.

The XplB/GlnA fusion protein was expressed and purified as above, but with the following modifications:. *E. coli* BL-21 (ED3) wazs used, expression was induced with 1 mM IPTG and subsequently incubated for 14 hrs at 15 °C

Gel mobility shift assay: EMSA

The DNA probe was PCR amplified, cloned into the pTOPO vector (Invitrogen) and released by enzymatic digestion that leaves 5' overhangs. A fill-in reaction to generate ^{32}P radiolabelled blunt ends was performed using the fragments with the 5' overhangs, a Klenow fragment and ^{32}P alpha dCTP nucleotides (Amersham). The Klenow reaction (Fermentas) was done as follows: 10-15 µl (0.1-4 µg) of digested DNA, 2 µl of 10X reaction buffer, 0.5 µl of 2 mM d(ATG)TP, 0.1-0.5 µl (1-5 u) Klenow fragment and 2 µl ^{32}P-dCTP (740 kBq). The mix was incubated at 37 °C for 10-30 min and the reaction stopped by heating at 75 °C for 10 min. The probe was then cleaned from the unincorporated radiolablelled nucleotides with a G25 column (Amersham) and stored in an appropriate container at -20 °C.

For binding, 30µg of protein crude extract or 150 ng to 1.5 µg HIS-tag purified protein were incubated 10 min at room temperature in binding buffer (30 µl total volume). The EMSA binding buffer reaction consisted of 25 mM HEPES-KOH, pH 7.9, 20 mM KCl 10% glycerol, 1 mM DTT, 0.2 mM EDTA, pH 8.0, 0.5 mM PMSF, Protein cocktail (sigma) and 2 µg poly(dI-dC).(dI-dC) (sigma). The ^{32}P DNA probe was then added and incubated 30 min at room temperature. Loading blue (40 % glycerol, 1 % bromophenol in EMSA buffer) was added and the samples were separated on a 5 % native acrylamide gel for 1-1.5 h at 50 V. The gel was then dried and exposed on a phosphor screen for 4 h and bands containing the ^{32}P-dCTP visualized with a phosphoimager.

Nucleic acids extraction

For total genomic DNA isolation and purification, 5-20 ml of bacterial cultures in the exponential or stationary phase were pelleted and washed with TE (Tris 10 mM, EDTA 1mM, pH 8). The cells were then incubated at 37 °C in 500 µl of TE buffer containing 1 mg/ml of lysozyme. After 30 min 30 µl of 10 % SDS and 200 µg proteinase K were added and the mixture incubated shaking (60 rpm) at 37 °C. 20 h later 20 µl of 10 % SDS and 130 µl of NaCl (5 M)

were added. The cells were mixed by inversion and incubated for 30 min on ice. Cell debris was pelleted by centrifugation for 15 min at 500 x g and proteins in the supernatant were removed using phenol-chloroform. Nucleic acids were precipitated by adding $1/10^{th}$ of the total volume of 3 M sodium acetate, pH 5.2 and 1 part of isopropanol. If required, RNAs were removed by adding 3 µl of RNase (10 mg/ml) to the DNA extraction and the mixture was incubated for 3 h at 37 °C. DNA was suspended in water and concentration measured at A_{260} using the NanoDrop at the Technology Facility at the UoY.

RNAs were extracted using cultures grown either in LB or MM with the appropriate nitrogen source to an OD_{600} between 0.3 and 1.0 using the RNAeasy (Qiagen) and RNA protect bacteria (Qiagen) kits according to the manufacturer's instructions; however, a few changes to increase the efficiency of the cell lyses as follows: *Rhodococcus* cells were treated with lysozyme (80 mg/ml) and Protein kinase K (20 mg/ml) incubated shaking (150 rpm) for 2 h at 25 °C. Then RLT buffer and acid-washed glass beads were added and cells shaken in a fast prep machine (FastPrep FP120, Anachem) on power 6 with two cycles of 30 sec and one cycle on power 6.5 for 40 sec.

PCR and Reverse Transcriptase-PCR (RT-PCR)

PCRs were performed using the GoTaq kit (Promega), Taq polymerase and Phusion Taq according to the manufacturer's instructions. Colony PCRs were performed with single colonies suspended in 50 µl of sterile water. Cells were lysed either in a PCR machine with the following cycle: 5 min 95°C followed by 5 cycles of heating at 95°C for 30 sec and cooling at 15° for 30 sec, or by incubation for 10 min at 95°C. One or two µl of lysate were used as PCR matrix. RT-PCRs were done with the Power SYBR Green PCR Master Mix (Applied Biosystems) according to manufacturer's instructions. Relative expression values were calculated using *gyrB* as an internal reference.

HPLC measurement of RDX

Reverse phase HPLC was performed with a Waters HPLC system (2695 Separations Module and 2996 Photodiode Array Detector (PDA) using a Techsphere C18 column (250 x 4.6mm) or Sunfire C18 column (250 x 4.6mm) under isocratic conditions. Two methods were used. Method 1: 60 % water, 40 % acetonitrile at a flow rate of 1 ml/min over 10 min. Method 2: 40% water, 60% methanol at a flow rate of 1 ml/min over 10 min. The absorbance at 205 nm (when acetonitrile was used as a solvent) or 230 nm (when methanol was used as a solvent) was extracted from the PDA and the disappearance of the RDX peak measured by integration of the peak at approximately 7.5 and 4 min respectively using the Empower software.

Uptake assay permease deleted strain

The *R. rhodochrous* 11Y wild type and permease knockout cells were grown in LB medium, centrifuged and resuspended in phosphate buffer (0.05 g/ml). RDX (10 µM) was added and samples were incubated under shaking at 30 ^{o}C. Samples were taken at 0, 1, 3 and 5 min, centrifuged and the supernatant was analyzed for the RDX concentration using HPLC.

RDX degradation assay

The *R. rhodochrous* 11Y wild type and permease knockout mutant were grown in LB medium supplemented with nalidixic acid (30 µg/ml). After incubation over night at 30^{o}C under shaking (150 rpm), cells were harvested (16,000 x g centrifugation), washed and resuspended in

phosphate buffer (0.01 g/ml). Cells were incubated in MM containing 40 mM potassium phosphate buffer (pH 7.2), three carbon sources (10 mM glycerol, 5 mM glucose and 5 mM succinate), trace elements and RDX (90 μM) for 1 h. Samples were taken after 20 and 60 min and reaction stopped using 10 % of TCA (1.5 M). Samples were centrifuged at 4 ºC for 3 min and the supernatant used for RDX analysis measured by HPLC.

Resting cell assays

Resting cell assay 1

Liquid medium containing the appropriate nitrogen source was inoculated with bacteria grown on LB agar plates. At OD_{600} 0.7 the cells were harvested and washed with phosphate buffer to remove RDX. Cells were concentrated to 0.1 mg/ml. For each reaction, 50 μl of concentrated cells were complemented with 450 μl of RDX medium at 165 μM, bringing the final RDX concentration to 150 μM and the biomass to 0.01 mg/ml for the assay. Cells were incubated from 20 min to 2 h. Samples were centrifuged at 4ºC for 3 min and the supernatant used for RDX analysis measured by HPLC.

Resting cell assay 2

Strains were grown at 30 °C to an OD_{600} 0.3 in MM supplemented with one of the following nitrogen sources 5 mM KNO_3, 750 μM KNO_2, 750 μM KNO_3 or 250 μM RDX as described in Table 9 then the cells collected by centrifugation. The cells were subsequently resuspended in MM containing 5 mM KNO_3, 450 μM KNO_2, 450 μM KNO_3, no nitrogen or 150 μM RDX respectively, as described in Table 9 and grown for a further 3h, then again harvested by centrifugation. Cells were washed twice in 40 mM phosphate buffer, pH7.2 and resuspended at a concentration of 0.1 g (wet weight)/ml. Resting cell assays were performed at 30 ºC with shaking using 50 μl of cells in a total volume of 700 μl containing 40 mM phosphate buffer, pH7.2, 100 μM RDX and 100 μg/ml kanamycin. Time point samples of 100 μl were taken and each reaction stopped by the addition of 10 μl 1M trichloroacetic acid and RDX analyzed by HPLC.

Western analysis and activity assays

Cells were prepared as for resting cell assays then disrupted by sonication and centrifuged (10,000 g) at 4 °C for 30 min. For western blot analysis 25 μg of supernatant protein was loaded per lane. Antibodies to the XplA protein were as described in (Rylott et al., 2006a) the XplB antibody was prepared using purified XplB protein in rabbit.

The XplA activity in crude cell extracts was measured by monitoring absorbance change at 340 nm. Reactions performed in a total volume of 150 μl, contained 40 mM phosphate buffer pH7.2, 300 μM NADPH and 0.1 U/ml ferrodoxin reductase. Reactions were initialized by the addition of 100 μM RDX.

Determination of a putative transcription initiation site.

Rapid amplification of cDNA ends (RACE PCR) was performed using a SMARTer RACE kit (Clontech Laboratories, Inc.). Total RNA isolated from *R. rhodochrous* 11Y and first-strand cDNA synthesis was carried out according to the manufacturer's protocol. RACE PCR was performed using a Universal Primer Mix (Clonetech) in combination with the *rhodococcal*-specific primer 5'-GGCGACCATCACCACACCACACAG-3'. Nested PCR was then performed using Universal Primer A (Clonetech) and the nested *Rhodococcal*-specific primer 5'-

ATGGTGACGAGCAGCGCGATCAGATAC-3'. The PCR products were cloned into TOPO pCR2.1 (Invitrogen) and sequenced.

Primer extension analysis was performed as described in (Broadbent et al., 2010). Reverse transcription was carried out in a volume of 20 µl using 20 µg total RNA, 400 U Superscript III reverse transcriptase (Invitrogen), 5 nM primer (promoter region upsteam of permease 5'-FAM-CATAGGCGAAGACCGTGTAGATCCCGAC-3'or promoter region upstream of *xplB* 5'-FAM-CTTGCGGAGTTGCTGTGCGGTGAAAC-3'), 750 µM of dATP, dCTP, dTTP and dGTP, at 55 °C for 1.5 h. The reverse transcription reaction was repeated as described in (Lloyd et al., 2005). Primer extension products were mixed with 0.3 µl Genescan LIZ600 ladder and run on the AB3130XL instrument (Applied Biosystems) using default parameters. Results were analyzed using the Peak Scanner Software (Applied Biosystem).

Dynabead pull down assay

Streptavidin coupled M-280 Dynabeads were purchased from Invitrogen. Biotin-TEG modified primers were synthesized at Eurofins. promXbio5F 5'BITEG-TGCGTTCCGGCCTGGCGTCAAAAAACCCTATGTTTGTAGTATTTGGCGAAATC-3' and promXR 5'GGATTTCGCCAAATACTACAAACATAGGGTTTTTTGACGCCAGG CCGGAACGC-3'. Primers were diluted in TE buffer (10 mM Tris-HCl, pH 8.0, 0.1 mM EDTA). To anneal complementary strands nucleic acids samples were mixed in a 1:1 molar ratio at a final concentration of 1 pmol/ul in 10 mM Tris, 1 mM EDTA and 50 mM NaCl (pH 8.0). Annealing of the probes was performed in a Thermocycler using following program: 5 min at 95°C for, 15 min at 95°C (-1°C/min), 30 min at 80°C and 45 min at 80 °C (-1°C/min). Double stranded and biotin labeled DNA was also obtained by amplifying the region of interest using biotin labeled primer (flengthpromXbioF-5'biotin- TGAGTGTCC TGGGTCCGCA-3', flengthpromXR-CCAAACGGATTTCGCCAAATAC-3') in a Thermocycler. Prior further used samples were cleaned up using the Promega wizard clean up kit according to the manufacturer's instructions.

Immobilization of the DNA to the Dynabeads was done as described by the manufacturer. 40 µg Rhodococcus crude cell extract, prepared as described for the western blot analysis, in a total volume of 400 µl containing 100 µM NaCl, 20 µM Tris-HCl, pH 7.5, 1 µM DTE, protease inhibitors, and 1 U/ml poly-d(IC) were incubated on ice for 10 min and then 200 µg Dynabeads with immobilized DNA were added. The mixture was incubated for 15 min at room temperature in an orbital shaker at 20 rpm. Beads were fixed with the magnet and washed in 1 U/ml poly-d(IC), 80 µM NaCl, 20 µM Tris-HCl, pH 7.5, 1 mM DTE and protease inhibitors, and twice in 80 µM NaCl, 20 µM Tris-HCl, pH 7.5, 1 mM DTE and protease inhibitors. Beads were then washed in 20 mM Tris-HCl, pH 7.5, 1 mM DTE. Samples were analyzed by SDS-Gel electrophoresis and MALDI-TOF MS.

Tn5-mutagenisis

A random Tn5 insertion library of *R. rhodochrous* was created using the Tn5-Transposome kit from Epicentre Biotechnologies, Cambio, UK. Electrocompetent *R. rhodochrous* cells were prepared as described by (Fernandes et al., 2001)by inoculating 0.2 l LB medium supplemented with 2 % (w/v) glycine or 1% (w/v) glycine plus 0.5 % (w/v) glucose. Flasks were incubated shaking at 30 °C and grown to OD_{600}=0.22 respectively 0.45. Cells were pelleted and washed twice in 100 ml ice cold 10 % glycerol. Cells were centrifuged again and resuspended in 1ml ice cold glycerol (10 %) and until further use snap frozen in liquid nitrogen.

For the transformation 40 µl of electrocompetent cells were placed in a 0.1 cm gap electroporation cuvette and mixed with 20 ng EZ::TN(KAN-2)Tnp Transposome and electroporated at 1.6 kV, 25 µF at 200Ω. Cells were resuspended in 1 ml SMME (0.7 M sucrose, 50 mM maleic acid, 10 mM $MgCl_2$, 10 mM $CaCl_2$, pH 6.5) and plated onto LB agar containing 1 % glucose., incubated for 12 h at 30 °C and overlayed with soft agar (0.6%) containing 1 % glucose and 50 µM kanamycin.

Colonies were then transferred to fresh LB agar containing 1% Glucose and 50 µM kanamycin and replica plated on MM containing 1 mM RDX. Colonies showing slower growth on RDX were picked and further characterized.

Sampling sites

United Kingdom

Soil samples were collected in the UK from two MoD ordnance demolition sites (Longtown and Otterburn) and a munitions containment building (Farnborough). The sampling area in Longtown was grassy and explosives had not been used for at least six months at this site. Soils at the Otterburn site were sampled close to old explosion holes. The containment building in Farnborough had a sandy soil and was exposed to explosive storage for a few weeks.

Belgium

Soil samples were collected in Belgium, from an old TNT munitions manufacturing site close to Zwijndrecht (exact location not disclosed here).

Germany

Soil samples were collected from the training range at Senne in Germany. The soil at Senne was mainly sandy.

Ukraine

Soil collected from military site in Kharkiu district (exact location not disclosed here).

Moldova

Soil collected from military site in Kishinev district (exact location not disclosed here).

Russia

Soil collected from military site in Moskovsky district (exact location not disclosed here).

Enrichment cultures

For the isolation of RDX degrading bacteria enrichment cultures with several modifications were set up. Typically bacteria were enriched and selected in MM containing 1mM RDX and weekly sub-cultured; however, following alterations were made:

Enrichment method 1:

Bacteria were grown in 10 mM potassium phosphate buffer (pH 7.3)) containing 0.25 mM $MgSO_4$ supplemented with 5 mM glucose, 5 mM succinate and 10 mM glycerol as carbon sources. One litre was supplemented with 1 ml of a 12.5 g/l $CaCl_2$ solution and with 4 ml of 2 µm filtered 250X trace element solution. Nitrogen sources (1 mM of NH_4Cl, RDX or HMX) were aseptically added after autoclaving.

For inoculum preparation, 1 g of soil was suspended in 10 ml or 25 ml of buffered salt solution without nitrogen source, shaken at 30 °C for 1 h, and allowed to settle for 1 h. The supernatant was passed through a Whatman no. 1 filter, and the filtrate was used as an inoculum. A 1 ml aliquot of the filtrate was inoculated into 24 ml of 1 mM RDX or 1 mM HMX sterile

medium in 100-ml conical flasks and incubated at 30 °C on a rotary shaker at 220 rpm. Controls without nitrogen source or with NH_4Cl instead of RDX were run along with the experiments. The first enrichment cultures were incubated for around one week and 1 ml was sub-cultured into 25 ml fresh medium. Subcultures which gave more growth (scored visually) than the control without a nitrogen source were sub-cultured again one or two times. Serial dilutions of positive enrichments were spread onto RDX solidified MM (1.5 % (w/v) powdered agarose). Representatives of each colony type were picked from the agar plates and purified several times on similar or LB media.

Enrichment method 2:

Approximately one gram of soil was diluted into MM containing trace elements, carbon sources and 1 mM RDX. Cultures were grown under shaking at 30 ºC for one week and then sub-cultured by inoculating fresh MM containing RDX. This selection step was performed three times in total. Samples were then diluted and aliquots spread onto agar with and without RDX containing trace elements, sucrose and also onto rich medium. This was done to isolate RDX-degrading strains and to obtain pure cultures.

Enrichment method 3:

Enrichment cultures were set up as described under Enrichment cultures 2 but were grown at three different temperatures (30ºC, 20ºC, 37ºC). One enrichment culture was started by inoculating LB medium with the soil. This culture was grown for three days at 30ºC and then used to subsequently inoculate MM containing RDX and further grown at 30ºC. All cultures were then sub cultured three times into MM containing RDX and again incubated shaking at 20°C, 30 °C and 37 °C.

To isolate bacteria able to grow and degrade RDX, a range of dilutions were spread onto rich agar and also MM with and without RDX.

Enrichment method 4:

Further modifications were made by using MacConkey selective medium and agar. Therefore, 45 ml MacConkey medium was inoculated with 5 ml soil slurry (1g soil / 5 ml) and shaken at 30 °C overnight. 1 ml was then transferred to MM containing RDX and sub-cultured. Again, bacteria were isolated by spreading them onto rich agar. MacConkey agar was used after bacteria were grown and sub cultured in the liquid enrichment medium.

Enrichment method 5:

Enrichments were performed using either 2 or 6 mM leucine as a carbon source as described in (Wawrik et al., 2005).

Enrichment method 6:

TNT was used in enrichment studies. Bacteria were grown in RDX MM supplemented with 25 μM TNT.

Molecular characterization of bacterial isolates and phylogenetic analyses

Taxonomic characterization of isolates was performed by amplifying and sequencing a nearly full length (1500 nucleotides) 16S rDNA gene. PCR amplifications were performed with the GoTaq kit (Promega) or Taq Polymerase according to the manufacturer's recommendations using primer fD1 AGAGTTTGATCCTGGCTCAG and rD2 AAGGAGGTGATCCAGCC. Sequences were compared with reference strains in phylogenetic analyses.

Nucleotide alignments were constructed with Clustalx 1.83 and manually corrected in Bioedit 4.8.4. Phylogenetic trees were constructed with sequence alignments of 1250 nucleotides for the 16S rRNA gene. The Phylowin software was used to build neighbor-joining trees with the Kimura's two-parameter correction method and the robustness of the tree branches was estimated with 1000 bootstrap replications.

Results and Discussion

Task 1: Molecular characterization of microbial communities in soils with RDX degradation.

Griess assay

The Griess assay was successful in detecting the xplA gene from a *Rhodococcus* 11Y genome library. A clone containing an insert was found to produce a positive colorimetric reaction, which was reproducible. The presence of the xplA gene was confirmed by PCR. Approximately 5,000 clones were screened to detect the xplA genome from two different genome libraries. The first library contained digested *Rhodococcus* fragments that were gel purified. Approximately 4,000 clones from this library were analyzed, but the xplA gene was not detected. The ligation carried out following this type of fragment clean-up was shown to be an efficient, with approximately 10% of clones containing an insert. A new library was prepared, except this time the genome was purified using a Qiagen spin column. The efficiency of this was higher (about 40-50%) and the xplA gene was detected after screening 1000 clones. This positive result indicated that the assay would have a strong possibility of detecting functional genes involved in the breakdown of RDX

Analysis of soils from Eglin AFB.

Two soils were initially tested. Soil type one was from a crater used to detonate waste explosives at Eglin AFB, while soil type 2 was from a location used as a target at the AFB.

Soil type 1 was found to remove approximately 25 % of the added RDX over the week long period while no removal was observed in soil type 2. No degradation was observed in the autoclaved controls. No RDX was detected in the soils prior to the addition of the RDX medium.

Growth of Rosetta-gami B

Conditions for the optimum growth of RGB were examined in minimal media under anaerobic and microaerobic conditions. Various carbon sources were studied. Optimum growth of RGB was observed in media containing sodium formate, mannitol or glycerol as carbon sources. Concentration of nitrite and presence of oxygen were also shown to have different effects on growth. Microaerobic conditions can utilize low concentrations of nitrite better. Anaerobic conditions can utilize high concentrations of nitrite better, however results indicate that concentration of nitrite released by the xplA cleavage may be low to match early growth demonstrated by the microaerobic conditions.

Use of *Pseudomonas* as Host for Clone Library

We developed an alternative technique for screening metagenomic libraries for RDX-degrading enzymes, using *Pseudomonas putida* KT2440 (Nelson et al. 2002) as an expression host instead of the *E. coli* strain, Rosetta-gami B, which presented too many challenges to make an effective host. *P. putida* KT2440 was selected over several other Pseudomonas spp. tested because it is able to grow aerobically on the RDX metabolite, NO_2^-, it has already been sequenced, and it had been used in a previous study as an expression host for metagenomic libraries.

The functional screen consisted of the following steps that needed to be developed or refined. First, the metagenomic DNA from the sample was partially digested using the restriction enzyme

BsaWI. The DNA was then size selected (fragments > 5 kb), gel purified and ligated into the broad host range expression vector pJN105 (Newman and Fuqua 1999). Vector pJN105 contained the pBBR1 origin of replication that could be maintained by both *E. coli* and Pseudomonas sp. and expression of the inserted DNA is downstream of the PBAD promoter which can be induced by L-arabinose. Metagenomic DNA ligated into pJN105 were then electroporated into the conjugative *E. coli* strain, S17-1 (Simon et al. 1983). The library was transferred conjugatively from S17-1 into KT2440 and exconjugants were then plated on both rich media and RDX minimal media with the appropriate antibiotics. KT2440 exconjugates that grew on RDX were selected for further analyses.

Positive controls for method development were created by amplifying the xplA- and xplB-xplA genes from *Microbacterium* sp. MA1 (Andeer et al. 2009) and inserting them into vector pJN105. The design of these constructs and their induction were tested in the *E. coli* strain Rosetta-gami B by using the Griess assay (Green et al. 1982) to confirm nitrite was liberated from RDX. These two positive control plasmids along with an empty vector negative control were then inserted into KT2440 to verify its degradation of RDX and its ability to grow on it as a sole nitrogen source. In minimal RDX enrichment media (Andeer et al. 2009) supplemented with ammonium chloride (2 mM), KT2440 expressing xplA or xplA and xplB demonstrated complete RDX degradation within two days (empty vector controls showed no RDX degradation) as measured by HPLC. However when RDX was the sole nitrogen source, KT2440 was only able to degrade and grow on RDX when both genes, xplB and xplA, were inserted in pJN105. These tests indicate that while KT2440 appears to have an enzyme to fulfill the role of xplB in RDX degradation, it is not sufficient for its growth on RDX as a sole nitrogen source. For this reason, we subsequently used the CTX phage integration system (Hoang et al. 2000) to create a variant strain of KT2440 that contained xplB in its chromosome for the expression of the metagenomic libraries.

We designed the KT2440 strain with xplB and optimized the steps in the functional screen outlined above. We developed protocols for the metagenomic library generation and conjugative transfer from S17-1 to KT2440. To optimize and validate the protocol, we used a library generated from an RDX-degrading organism, *Mycobacterium* sp. MA2, as well as plasmid mixtures (i.e., empty pJN105, pJN105 with xplB and xplA) of known compositions. An additional 500 - 2000 ‘colonies’ of each transformation type were used directly to inoculate RDX medium. Plasmid preps from cultures made from each KT2440 transformation were positive for the xplB-xplA gene fragment (3 kb amplicon) (Figure 12), however, no growth was observed on RDX. Therefore the enrichment functional screen failed to elicit XplBA activity.

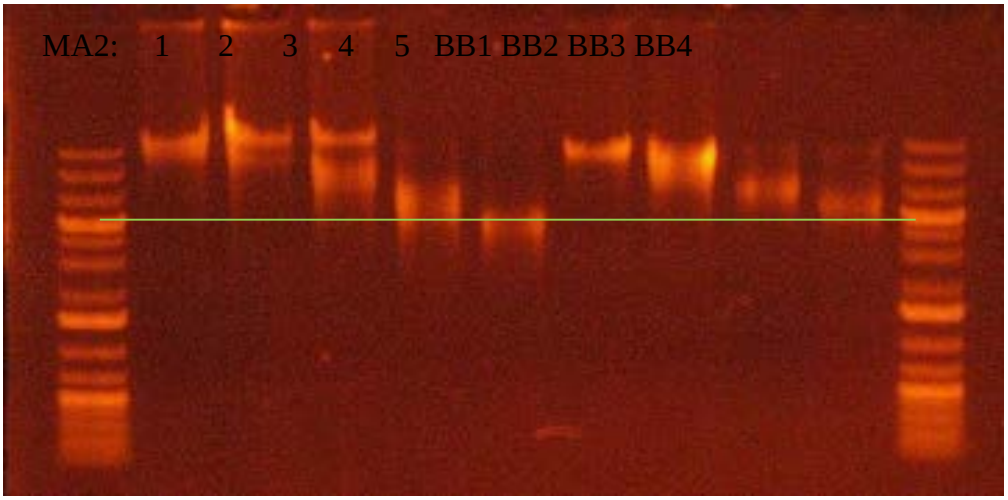

Left: High molecular weight DNA extraction. Right: Bead beating extraction used for soils.

Ligations	Insert	Transformants/ rxn	Colonies harvested	# of KT2440 colonies/ 100 ng plasmid	Colonies for RDX selection plates and/or broth
1	MA2 1	34,500	27,600	18,400	6,400
2	MA2 2	50,000	45,000	~15,000 - 20,000	26,000
3	MA2 BB1	2,800	2,240	12,000	4,200
4	MA2 BB2	10,000	6,100	95000	33,000
5	none	none			

Figure 12. Initial positive control library construction – *Mycobacterium* sp. MA2: PvuI

We considered two reasons that might have accounted for the failure of initial tests: perhaps PvuI did not digest the DNA frequently enough, or the pJN105 vector contained a promoter but lacked a ribosome binding site (RBS). To test the first hypothesis we changed to the Psp1406I vector and insert MspI. To address the second concern we created a version of the vector with an RBS upstream of the insert, either xplBA with the RBS in the vector (-) RBS or with xplBA in a vector in vector containing (+) RBS. Both positive controls with just the xplBA genes grew on RDX as sole source of nitrogen (Figure 13), but none of the library clones grew on RDX as sole source of nitrogen.

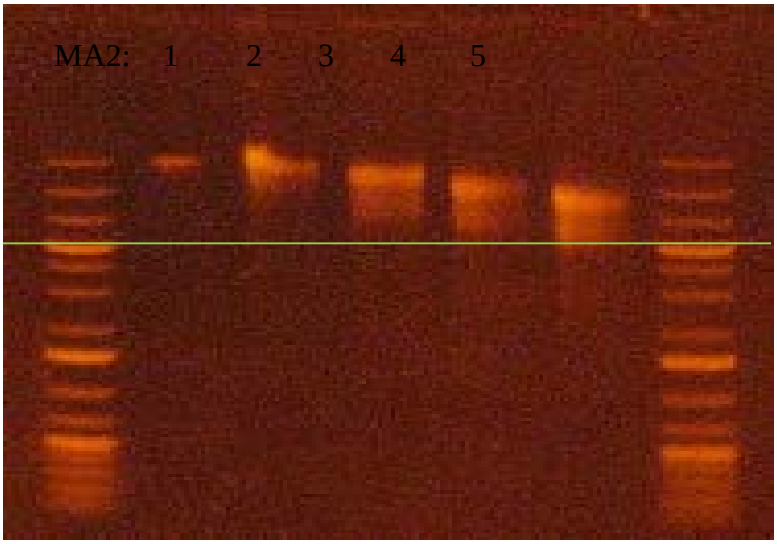

# of Trans	RBS	Insert	E. coli Library Construction Dates	Total colonies harvested	% w/insert	% Tested for xplBA	xplBA detected?	KT2440 cells transformed?	xplB/A detected in KT2440 Clones?
5	yes	MA2 #3	7/21, 8/16, 9/1	36,000	96%	88%	1/2 of preps	All but 9/1	Yes
4	no	MA2 #3	7/21, 7/25, 9/1	13,765	93%	70%	Several	All but 9/1	Yes
4	yes	MA2 #2	7/31, 8/6, 8/16, 9/4	16,750	89%	90%	Several	All but 9/4	Yes
4	no	MA2 #2	7/31, 8/6, 9/4	13,580	86%	60%	Several	All but 9/4	Yes
1	yes	MA2 #1	9/4	1,180	81%	NT		No	NT
1	no	MA2 #1	9/1, 9/4	6,681	62%	NT		No	NT

Figure 13. Enhanced library construction – *Mycobacterium* sp. MA2: Psp1406I/MspI. Improved yields.

Development of Screening Technique Using the *Microbacterium* MA1 Genome as a Positive Control

To identify positive clones (i.e., clones that contain DNA encoding RDX-degrading enzymes) we intended to exploit the growth of the targeted clones on RDX as a sole nitrogen source. Validation of this approach was conducted using *Pseudomonas putida* KT2440 containing the expression vector pJN105, with or without the xplB and xplA genes. By spotting dense cultures (OD600 ~1) of *P. putida* KT2440 on agar plates supplied with RDX as a sole nitrogen source, we were able to identify individual positive clones on the plates among over 10^7 negative clones (Figure 14).

Tests Using Genomic DNA from Rhodococcus 11Y as Positive Control

Protocols for processing metagenomic DNA for insertion and expression within a surrogate host were developed. The *Pseudomonas putida* KT2440 host strain containing pJN105xplBA, a vector constructed to express only xplBA under an arabinose-inducible promoter, successfully degraded RDX in liquid culture when the xplA gene was introduced to the vector. To determine the functionality of the screen, genomic DNA from *Rhodococcus rhodochrous* 11Y containing xplBA was used as source DNA for insertion. An alternative smaller source of DNA, a 30Kb fosmid containing the xplBA from *Microbacterium* sp. MA1, was also used to increase the chances of picking up xplBA in the screen. However, neither source of DNA provided a positive RDX-degrading clone in the screen.

To investigate the lack of any RDX-degrading clones in the screen from our selected DNA sources, we built plasmid constructs containing inserts of variable sizes containing xplBA. The plasmids, pJN105rbsF1.3 and pJN105rbsF3.1, contained increasing amounts of DNA sequence upstream of xplBA amplified from a fosmid containing the *Microbacterium* sp. MA1 xplBA. pJN105rbsF1.3 contained xplBA plus 2.4kbps of upstream DNA sequence encoding a putative amino acid permease and dihydroxy-picolinicacid (DHP) reductase while pJN105rbsF3.1 contained xplBA and the 1Kbps of upstream sequence encoding for the putative DHP reductase. In *P. putida* KT2440 grown in nutrient-rich media, both pJN105rbsF1.3 and pJN105rbsF3.1 still enabled RDX-degradation but at a significantly slower rate than the positive control pJN105xplBA. In liquid culture, a significant lower growth rate and maximum optical density was observed in the *P. putida* strains containing the larger inserts, which suggested some toxic effect associated with expression of the DHP reductase. This was further supported by the inability of the *P. putida* pJN105rbsF1.3 and pJN105rbsF3.2 to grow single colonies on minimal media plates with RDX as a sole N-source unlike the positive control *P. putida* KT2440 pJN105xplBA, which contained only the xplBA gene cassette.

Selection of *P. putida* KT2440 clones capable of degrading RDX.

P. putida KT2440 cells with xplB and xplA in pJN105 (positive control) were mixed with KT2440 cells with empty pJN105 vector (negative control) in 6 ratios from 100% positive control to 100% negative control. Serial dilutions of each mixture were spotted onto minimal media containing arabinose (0.5%), gentamicin (15 mg/L) and either: 200 mg/L RDX, 4 mM nitrite, or nitrogen free, as sole nitrogen sources. Even at high cell densities (OD600 =1), individual colonies growing on RDX were distinguishable (Figure 14). This result validated the enrichment strategy.

(+) control: pJN105 w/ *xplB/A*

(-) control: empty pJN105

% (+) control: 10^{-4} 10^{-3} 0.1 1 100

OD600=1

(1x)

10x Dilution

100x Dilution

1,000x Dilution

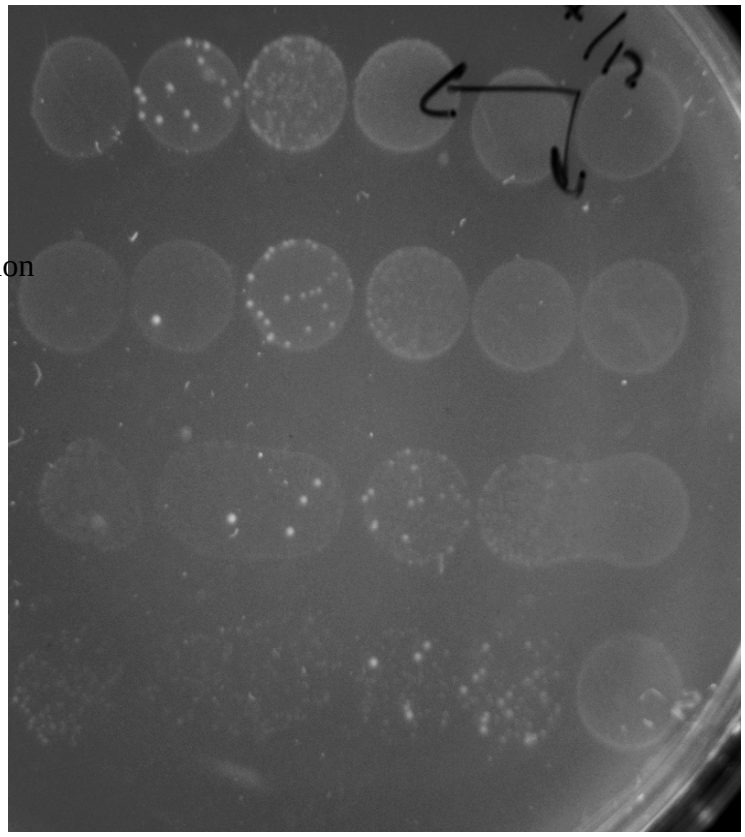

Figure 14. Selection of RDX degradation enzymes in *Pseudomonas putida* KT2440 – Positive control.

RDX degrading clones were selected for growth on minimal media with 500 mM RDX as sole source of nitrogen and 0.2% L-arabinose for induction. Mixtures of *P. putida* KT2440 transformed with xplBA and with empty vector were incubated on media with RDX as sole source of nitrogen at various dilutions. Growth of xplBA clones is evident at higher dilutions.

Three types of conditions were used to screen the functional library in liquid culture:

- Large inoculant (~ 1/5 – 1/3 of cell suspension, initial OD 600 > 0.5). This culture was tested for RDX degradation by HPLC analysis.
- Small inoculant (1/50 – 1/25). This culture was tested for growth on RDX
- Small/medium inoculant (1/50 – 1/10) including 50 mM of NO_2^-. This culture was tested for growth and RDX degradation

However no clones from the KT2440 library tested positive for growth on RDX as sole source of nitrogen.

Tests Using Genomic DNA from Rhodococcus 11Y as Positive Control

Protocols for processing metagenomic DNA for insertion and expression within a surrogate host were developed. The *Pseudomonas putida* KT2440 host strain containing pJN105xplBA, a vector constructed to express only xplBA under an arabinose-inducible promoter, successfully degraded RDX in liquid culture when the xplA gene was introduced into the vector. To determine the functionality of the screen, genomic DNA from *Rhodococcus rhodochrous* 11Y containing xplBA was used as source DNA for insertion. An alternative smaller source of DNA, a 30Kb fosmid containing the xplBA from *Microbacterium* sp. MA1, was also used to increase the chances of picking up xplBA in the screen. However, neither source of DNA provided a positive RDX-degrading clone in the screen.

Why did clone fragments containing xplBA not degrade RDX, while the positive control containing only the xplBA genes was successful and grew on RDX as sole source of nitrogen?

To investigate the lack of RDX-degrading clones in the screen from any of our selected DNA sources, including RDX degrading lines of *Microbacterium* sp. MA1, *Mycobacterium* sp. MA2, and *Rhodococcus rhodochrous* 11Y, we built plasmid constructs containing inserts of variable sizes containing xplBA. The plasmids, pJN105rbsF1.3 and pJN105rbsF3.1, contained increasing amounts of DNA sequence upstream of xplBA amplified from a fosmid containing the *Microbacterium* sp. MA1 xplBA. pJN105rbsF1.3 contained xplBA plus 2.4kbps of upstream DNA sequence encoding a putative amino acid permease and dihydroxy-picolinicacid (DHP) reductase while pJN105rbsF3.1 contained xplBA and the 1Kbps of upstream sequence encoding for the putative DHP reductase. In *P. putida* KT2440 grown in nutrient-rich media, both pJN105rbsF1.3 and pJN105rbsF3.1 still enabled RDX-degradation but at a significantly slower rate than the positive control pJN105xplBA. In liquid culture, a significant lower growth rate and maximum optical density was observed in the *P. putida* strains containing the larger inserts, which suggested some toxic effect associated with expression of the DHP reductase. This was further supported by the inability of the *P. putida* pJN105rbsF1.3 and pJN105rbsF3.2 to grow single colonies on minimal media plates with RDX as a sole N-source unlike the positive control *P. putida* KT2440 pJN105xplBA, which contained only the xplBA gene cassette.

Task 2. Determination of RDX metabolites and metabolic pathways

RDX decomposition by *Rhodococcus* sp. strain DN22: initial denitration and subsequent secondary reactions

Previously we found that RDX degradation with *Rhodococcus* sp strain DN22 produced the key ring cleavage product NDAB, representing 60% of C-content in RDX, carbon dioxide (30% detected as $^{14}CO_2$), nitrous oxide (N_2O) together with nitrite, and ammonia. The C mass balance was approximately 90% (Fournier et al. 2002). In the present study we incubated RDX with DN22 under aerobic conditions and found that the missing 10% C was due to the formation of MEDINA, which decomposed to HCHO and $2N_2O$ (Figure 15).

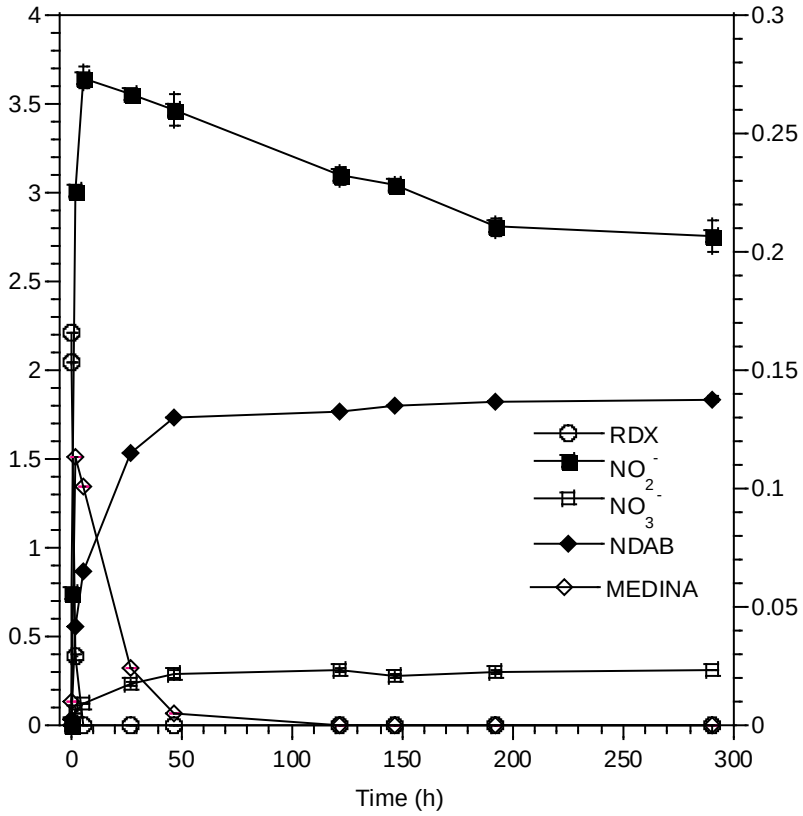

Figure 15. **Time course of aerobic biodegradation of RDX with *Rhodococcus* sp. DN22**

Although NDAB was formed as a dead end product during RDX aerobic incubation with DN22, our previous studies demonstrated that the chemical can be degraded by *Methylobacterium* (Fournier et al. 2005) and by *Phanerochaete chrysosporium* (Fournier et al. 2004) and under strong alkaline conditions (Balakrishnan et al 2003). In the present study we successfully hydrolyzed NDAB (20 mg L^{-1}) at pH 12.3 and room temperature and identified N_2O, HCHO, NH_3, and HCOOH as degradation products. The rate of NDAB hydrolysis was much slower than that of RDX (data not shown). Products distribution suggested that hydrolysis of NDAB occurred *via* initial OH^- attack at the secondary C in $O_2NNH\underline{C}H_2NHCHO$ to first produce the imine $O_2NNH\underline{C}H{=}NCHO$ that upon reaction with water would initially give the α-hydroxynitroamine $O_2NNH\underline{C}H(OH)NHCHO$. The latter is unstable in water and should decompose readily to produce NH_2NO_2 (precursor to N_2O), hemiacetal $CH_2(OH)_2$ (precursor to HCHO) and formamide (precursor to ammonia and HCOOH). We did not detect any nitrite or nitrate anions.

NDAB as we described earlier is recalcitrant to biodegradation by DN22 but NH_2CHO decomposed to NH_3 and HCHO (Fournier et al. 2002). Indeed we found that in the presence of DN22 NH_2CHO biodegraded to first produce NH_3 and HCOOH that were later utilized by the bacteria (Figure 16). Abiotic controls containing NH_2CHO in the absence of DN22 did not produce any significant hydrolysis.

As for NDAB and MEDINA formation it is obvious that if RDX loses $2NO_2^-$ prior to ring cleavage and decomposition it produces NDAB (O_2NNHCH_2NHCHO) exclusively; however if

RDX loses only $1NO_2^-$ then both NDAB and MEDINA ($O_2NNHCH_2NHNO_2$) can potentially form (Figure 17).

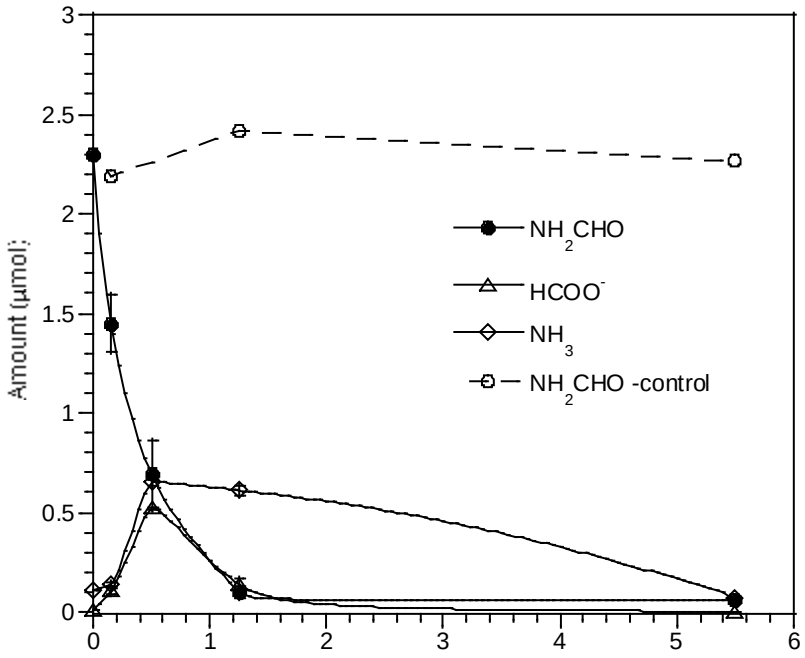

Figure 16. Biodegradation of formamide with resting cells of *Rhodococcus* sp DN22.

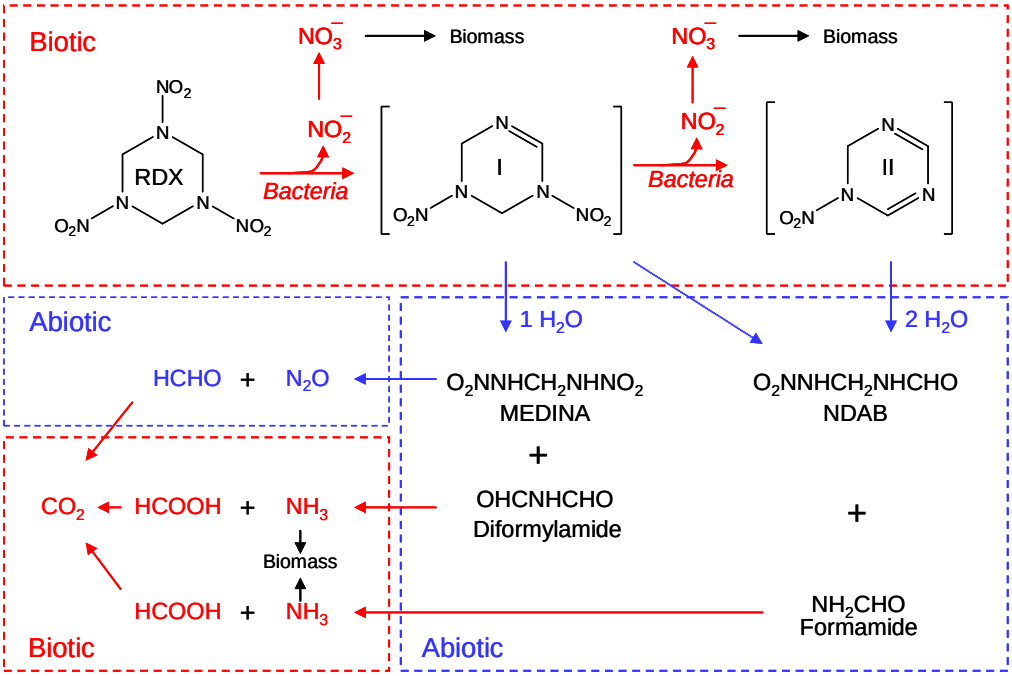

Figure 17. Constructed biotic (red) and abiotic (blue) degradation routes of RDX with *Rhodococcus* sp. DN22

As the above discussion reveals the initial denitration step taking place during RDX incubation with DN22 is the most important step in the whole degradation process. Following denitration, the resulting monodenitrated intermediate **I** and didenitrated intermediate **II** follow a cascade of secondary abiotic and biotic reactions to finally give NO_2^-, NO_3^-, NH_2CHO, NH_3, N_2O, HCHO, HCOOH, and NDAB (Figure 17). As for N_2O we suggest that MEDINA acted as a precursor for its formation.

Figure 17 shows that for each mole of RDX lost 1.7 and 0.1 molar equivalents of NO_2^- and NO_3^-, respectively, a molar ratio reaching 17, were detected. Production of nitrate and nitrite was confirmed by LC-MS showing a mass ion at *m/z* 62 Da and *m/z* 46 Da, respectively (Figure 18A and 5C).

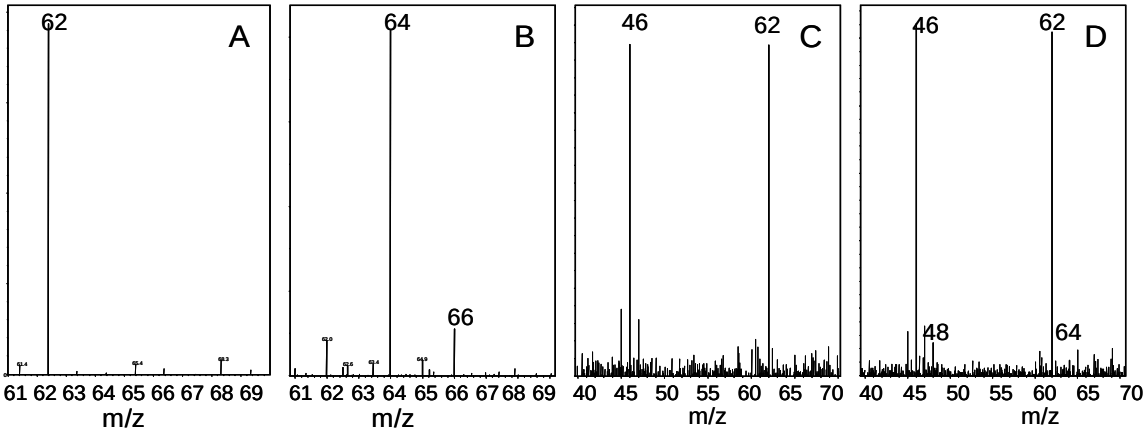

Figure 18. Mass spectra of nitrate anion produced from RDX during incubation in aerobic assays containing *Rhodococcus* sp. DN22 in the presence of unlabeled oxygen ($^{16}O_2$) (A) or $^{18}O_2$ (B), and mass spectra of nitrite and nitrate anions in the presence of ordinary water ($H_2{}^{16}O$) (C) or $H_2{}^{18}O$ (D)

When we incubated RDX with DN22 in the presence of $^{18}O_2$ we detected NO_2^-, with a mass ion at *m/z* 46 Da confirming that NO_2^- originated from RDX without the inclusion of any ^{18}O. Furthermore, we detected two mass ions, one with a major intensity at *m/z* 64 Da representing NO_3^- with the inclusion of $1{}^{18}O$ atom and a less intense ion with *m/z* at 66 Da representing NO_3^- with the inclusion of $2{}^{18}O$ atoms (Figure 18B). A control containing NO_2^- and DN22 in the presence of $^{18}O_2$ gave NO_3^- with two *m/z* values, one at 64 Da and another at 66 Da as was the case with NO_3^- detected during incubation of RDX with DN22. An abiotic control containing NO_2^- and oxygen in the absence of DN22 did not give NO_3^-. We concluded that the NO_3^- detected during RDX incubation with DN22 resulted from bio-oxidation of the NO_2^- originally formed from N–NO_2 bond cleavage in RDX. For example, it has been reported that NO_2^- can biologically oxidize to NO_3^- (Ignarro et al. 1993; Pietraforte et al. 2004). We presumed that the trace amount of NO_3^- that we detected with two ^{18}O atoms originated from biotic oxidation of nitric oxide (NO) (Schopfer et al. 2010) produced from NO_2^- at pH 5.5 in sample prepared without phosphate buffer for LC-MS analysis. It has been shown that under slightly acidic conditions NO_2^- can produce NO through disproportionation (Zweier et al. 1999).

Likewise when we incubated RDX with DN22 in the presence of $H_2{}^{18}O$ we observed NO_2^- with m/z at 46 Da and another mass ion with *m/z* at 62 Da representing NO_3^- with no ^{18}O involvement (Figure 18D). However we detected a trace amount of the mass ions at m/z 48 and

m/z 64 Da representing NO_2^- and NO_3^- with the inclusion of one ^{18}O atom. This experiment indicated that part of NO_2^- originated from RDX might also produce NO (Zweier et al. 1999) which should subsequently auto-oxidize to revert back NO_2^- with one ^{18}O from water (Miller and Grisham, 1995; Goldstein and Czapski, 1995) prior to biological oxidation to NO_3^- (Ignarro et al. 1993). Results from the above $H_2{}^{18}O$ and $^{18}O_2$ labeling experiments indicated that RDX denitration does not involve direct participation of either oxygen or water in its formation, but both water and oxygen play major roles in the subsequent secondary chemical and biochemical reactions of the nitrite anion once released from RDX. However similar to previous studies (Fournier et al. 2002; Bhushan et al. 2003), we found that degradation of RDX with DN22 in the presence of $H_2{}^{18}O$ produces the ring cleavage product NDAB with the inclusion of one ^{18}O from water (data not shown).

Degradation of MNX with *Rhodococcus* sp. strain DN22 – denitration versus denitrosation

MNX has been frequently observed with RDX as a contaminant (Cassada et al. 1999; Beller and Tiemeier, 2002) or as an early degradation product of RDX. For example we detected MNX aerobically during RDX incubation with the fungus *P. chrysosporium* (Sheremata and Hawari, 2000) and anaerobically with *Shewanella halifaxensis* (Zhao et al. 2008). To determine the fate of MNX biodegradation with DN22, we incubated MNX with resting cells of DN22 using conditions similar to those employed with RDX. We found that DN22 degraded MNX but at a slower rate than that of RDX, indicating that if MNX had been a degradation product of RDX by DN22, we would have been able to observe it. Also when we incubated MNX with DN22 we did not observe RDX as an oxidized MNX product. This is in line with our earlier observation showing that DN22 is unable to degrade TNX (Fournier et al. 2002).

The disappearance of MNX with resting cells of DN22 was accompanied with the formation of NO_2^- and NO_3^- (Figure 19) in addition to NH_3, N_2O, HCHO, and HCOOH (data not shown). We also detected NDAB (23%) with approximately one third its yield from RDX (Figure 19) and a trace amount of an intermediate with a $[M–H]^-$ at *m/z* 102 Da matching an empirical formula of $C_2H_5N_3O_2$.

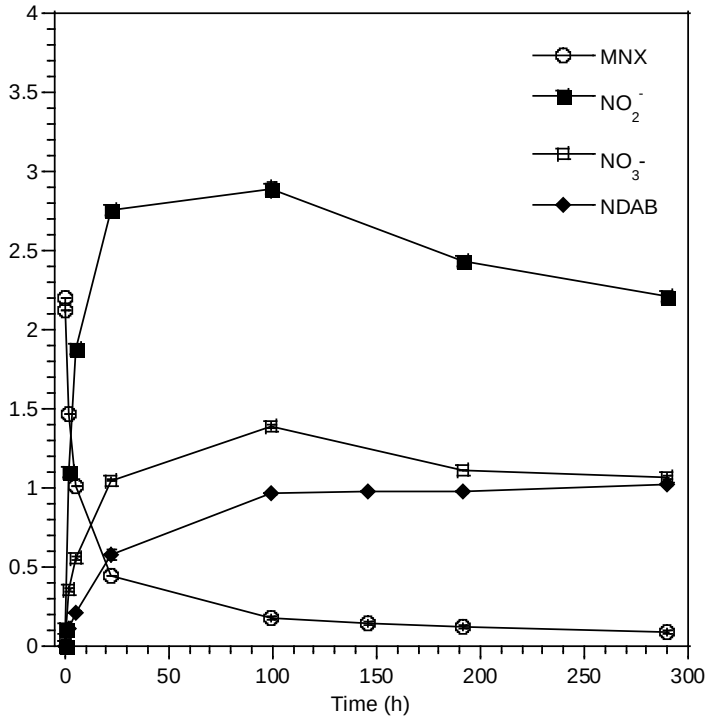

Figure 19. Time course of aerobic biodegradation of MNX with *Rhodococcus* sp. DN22.

Using ring labeled ^{15}N-MNX, the $[M–H]^-$ was observed at *m/z* 104 Da, suggesting the inclusion of two ^{15}N atoms from the inner aza Ns in MNX. We tentatively assigned the metabolite as the nitroso equivalent of NDAB, i.e., 4-nitroso-2,4-diazabutanal (4-NO-DAB, $ONNHCH_2NHCHO$). Although we were unable to observe MEDINA, we detected its suspected decomposition products HCHO that disappeared later and N_2O that persisted (8%). However, both HCHO and N_2O can also be produced from the decomposition of the nitroso derivative of MEDINA, i.e. O_2NNHCH_2NHNO (Figure 20).

The formation of NDAB requires the initial loss of NO whereas the formation of 4-NO-DAB requires the initial loss of NO_2 before MNX decomposition. In support of our hypothesis we detected 1.3 molar equivalent of nitrite and 0.6 molar equivalents of nitrate ions for each disappearing mole of MNX (Figure 19).

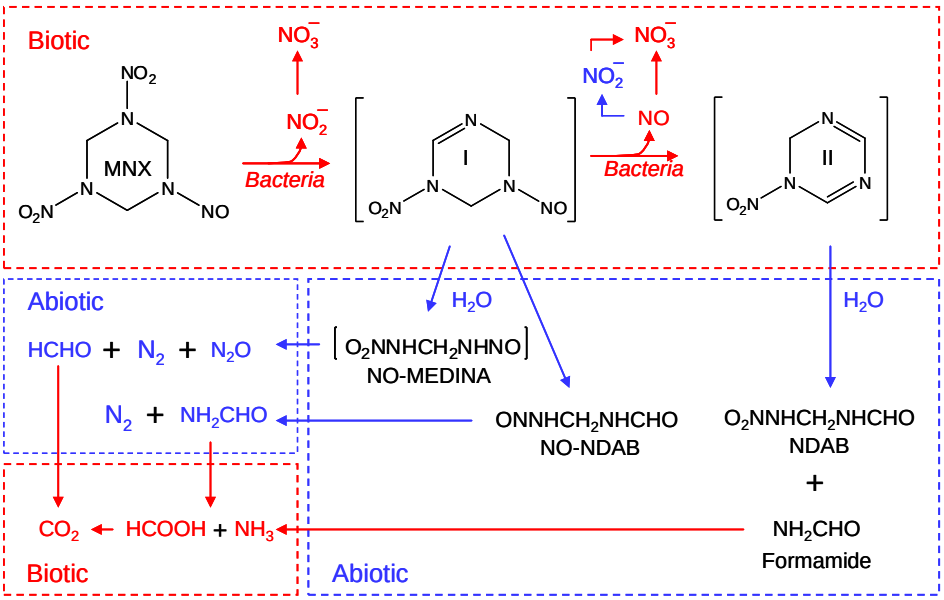

Figure 20. Biotic (red) and abiotic (blue) degradation routes of MNX with *Rhodococcus* sp DN22.

In contrast, in the case of RDX, the stoichiometry of denitration was almost two molar equivalents of nitrite and only trace amounts of nitrate formed for each disappearing mole of RDX (Figure 17). The relatively high nitrate production from MNX was attributed to MNX denitrosation and subsequent oxidation of the resulting NO to nitrate. It has been reported that some microbial flavohemoglobin (flavoHb) can exhibit nitric oxide dioxygenase activity (Schopfer et al. 2010) and oxidize NO to NO_3^- using $^{18}O_2$-labeled oxyheme (flavoHb(Fe^{III}-$^{18}O_2$)) prepared from *E. coli*. (Gardner et al. 2006). In this respect, when we incubated MNX with DN22 in the presence of $^{18}O_2$ we detected NO_3^- with two mass ions: a major one at *m/z* 66 Da incorporating two ^{18}O atoms and another minor one at *m/z* 64 Da incorporating only one ^{18}O (Figure 21A). We attributed the formation NO_3^- with one ^{18}O to the bio-oxidation of the initially formed NO_2^- from MNX to NO_3^- and the formation of NO_3^- with two ^{18}O atoms to bio-oxidation of the initially formed NO (N–NO cleavage) to NO_3^-. Experimental evidences gathered thus far suggested that besides initial denitration N–NO bond cleavage might also take place during MNX incubation with DN22 (Figure 30).

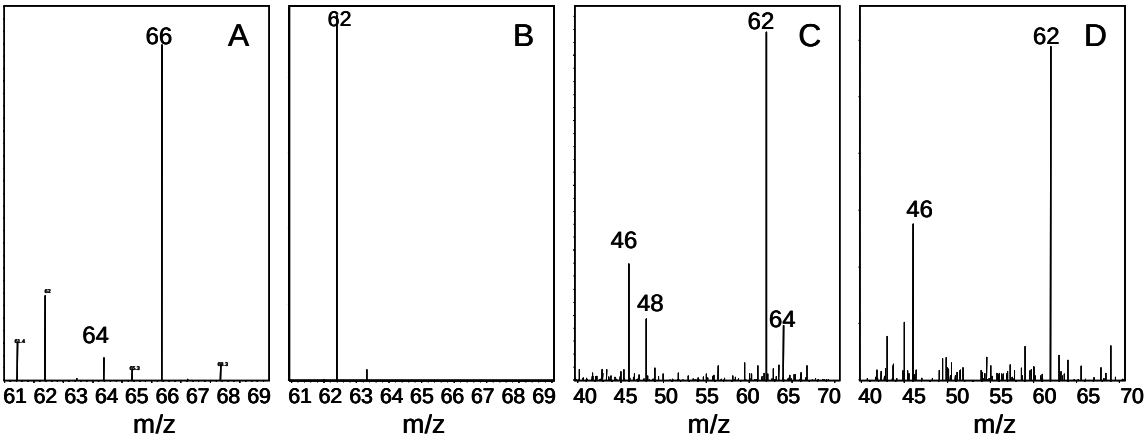

Figure 21. Mass spectra of nitrate anion produced from MNX during incubation in aerobic assays containing *Rhodococcus* sp. DN22 in the presence of labeled $^{18}O_2$ (A) or $^{16}O_2$ (B), and mass spectra of nitrite and nitrate anions in the presence of $H_2{}^{18}O$ (C) or $H_2{}^{16}O$ (D)

When we incubated MNX with DN22 in the presence of $H_2{}^{18}O$ we detected NO_3^- with two different masses: one with major intensity at *m/z* at 62 Da representing NO_3^- without ^{18}O incorporation and another with much lower intensity at *m/z* 64 Da (Figure 21C) representing NO_3^- with the inclusion of one ^{18}O atom. Like for RDX, we concluded that part of NO coming from MNX first auto-oxidized to NO_2^- prior to being biotically oxidized to NO_3^-. Also we detected NO_2^- with two different masses, one at *m/z* 46 Da representing NO_2^- coming directly from MNX and another at *m/z* 48 Da representing nitrite with the inclusion of one ^{18}O confirming the potential auto-oxidation of NO in water to NO_2^-.

Results from the above $H_2{}^{18}O$ and $^{18}O_2$ labeling experiments indicated that MNX can undergo both denitration and denitrosation and both water and oxygen can play major roles in the subsequent secondary chemical and biochemical reactions of both nitrogen species.

Learning more of the initial denitration step leading to RDX and MNX decomposition

We know from the alkaline hydrolysis of RDX that denitration is caused by an OH^- attack on the acidic $-CH_2-$ group of RDX leading to the formation of the unstable 3,5-dinitro-3-cyclohexene whose subsequent decomposition in water gives products distribution similar to that obtained during RDX incubation with *Rhodococcus* sp. DN22, i.e., NO_2^-, NH_3, N_2O, HCHO, and HCOOH (Balakrihnan et al. 2003; McHugh et al. 2002). The chemical insight gained from RDX hydrolysis under alkaline conditions might thus help us understand the initial enzymatic denitration step(s) leading to RDX decomposition during its incubation with DN22 and P450 system XplA/B. In this context one might presume that biotic denitration of RDX might also have been triggered by an enzymatic H^--containing species that first abstracted a proton (H^+) from one of the CH_2 groups in RDX leading to the formation of a carbenyl anion whose denitration would produce the imine intermediate (–HC=N–) (**I**, Figure 1, *a*). **I** might undergo a second denitration to produce intermediate **II**. Likewise decomposition of **I** would then give both NDAB and MEDINA depending on what type of C–N bond in RDX is hydrolyzed first but decomposition of **II** can only give NDAB (Figure 1). However we do not know if DN22/XplA can carry out specific hydride anion (H^-) reaction with RDX. If RDX truly involved initial reaction with H^- one might expect to see hydrogen gas as a product which we did not detect. Initial denitration might also take place through an e-transfer process leading to the formation of a radical anion which upon denitration would give the aminyl radical **III** (Figure 1, *b*). $H^{\cdot}$-atom abstraction from a reducing radical by the aminyl radical **III**, denitrohydrogenation, would give 1,3-dinitro-perhydro-1,3,5-triazine **IV** (Figure 1, *b*). McHugh et al. (2002) reported the synthesis of **IV** by reducing RDX with Na(Hg)/THF/H_2O. **IV** is unstable and thus far has been reported as its nitrated salt that decomposes to MEDINA, HCHO and NH_3 (Lamberton, 1951; Bonner et al. 1972).

Alternatively, RDX intermediates **I** and **II** could be generated by $H^{\cdot}$-abstraction from one of the CH_2 groups in RDX by an XplA enzymatic system in the form of peroxy radical leading first to the formation of a carbenyl centered radical whose denitration would produce intermediate **I** (Figure 22, *a*). A second denitration of RDX by the same mechanism would give intermediate **II** (Figure 22, *a*). Reaction of **I** with water would produce the unstable α-hydroxylamine –NH–CH(OH)– that should trigger ring cleavage and auto-decomposition in water. Recently Guengerich (2001) explained a classical enzymatic carbon hydroxylation route of alkyl amines

through H·-abstraction/oxygen rebound mechanism wherein the resulting α-hydroxyl amine decomposes to produce aldehydes and an amine. The H·-abstraction/oxygen rebound mechanism resembles the α-hydroxylation of the –CH_2– group in RDX leading to its decomposition but in our case the oxygen originated from water and not from air. We thus speculate that a superoxide radical formed from $O_{2(g)}$ by a redox Cytochrome P450 system was involved in hydrogen atom abstraction from one of the CH_2 groups in RDX leading to its decomposition. Strobel and Coon (1971) describe a hydroxylation reaction catalyzed by cytochrome P450 coupled with a superoxide generating system.

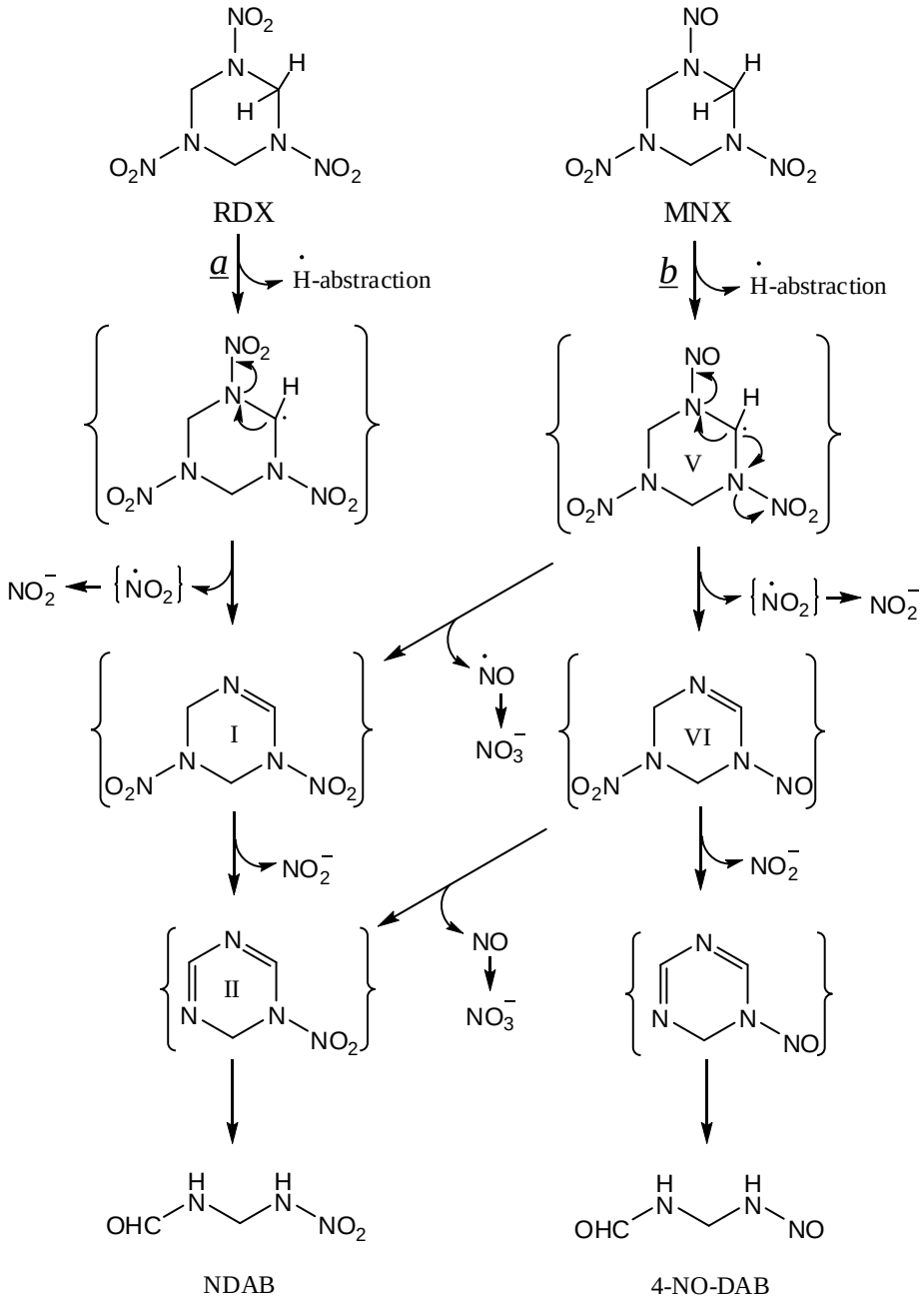

Figure 22. Proposed denitration route of RDX (*a*) and denitrosation and denitration routes of MNX (*b*) with *Rhodococcus* sp. DN22 under aerobic conditions.

As for MNX denitrosation of the carbenyl intermediate (**V**) would give intermediate **I** which in turn should decompose in water to give NDAB (Figure 22, *b*). If MNX carbenyl intermediate undergoes denitration intermediate **VI** would be formed whose decomposition in water should produce the nitroso derivative of NDAB, $ONNHCH_2NHCHO$ (Figure 22, *b*). Indeed we detected both NDAB and 4-NO-DAB during MNX incubation with DN22.

Based on experimental evidences gathered thus far from ^{18}O-labelling experiments and products distribution we suggest that the $H^{\cdot}$-abstraction mechanism (Guengerich, 2001) is the most likely route to initiate denitration and/or denitrosation of RDX and MNX.

Environmental significance of the denitration pathway of cyclic nitroamines

The denitration pathway in Figure 17, summarizing most significant biotic and abiotic reactions involved in RDX degradation with DN22, provides valuable information on how much of the N and C content originally present in RDX can actually be utilized by the microorganism. For example, formation of the dead end product NDAB seizes two Cs out of a total of three in RDX leaving only one C for mineralization as demonstrated by the detection of only 30% mineralization of disappearing RDX. In the MEDINA pathway most of the C in RDX is liberated as HCHO (from MEDINA decomposition) and HCOOH (from diformylamide) that are subsequently mineralized by DN22 (Fournier et al. 2002). The MEDINA pathway mostly occurs under anaerobic conditions and is supported by the fact that high mineralization (60-70%) is frequently observed (Zhao et al. 2002; Shen et al. 2000). Obviously RDX degradation by denitration is of great environmental significance because it can lead to the development of an effective RDX remediation technology.

The denitration pathway should also serve as a template to help in the development of molecular tools to monitor and enhance in situ bioremediation. For example, the pathway clearly shows the actual chemical bonds, i.e., –N–N–, –N–C–, –N–O– that are being attacked or broken during RDX degradation. Such information on the type and order of bond cleavage would be useful in the understanding of stable isotope fractionation (Bernstein et al. 2008) and stable isotope probing (SIP) (Schmidt et al. 2004; Roh et al. 2009).

Finally, products from RDX denitration pathway such as NDAB and nitrite can be employed as useful markers to detect and monitor fate of RDX in the environment. Indeed we detected NDAB in several soils and ground water samples taken from sites contaminated with RDX, e.g. in soil sample collected from an ammunition plant in Valleyfield, Quebec, Canada (Fournier et al. 2004).

Degradation of MNX with XplA

We found that, under aerobic and anaerobic conditions, XplA degraded MNX with the concurrent formation of NO_2^-, NO_3^-, N_2O, and HCHO (Figure 23 and Figure 24) with varying stoichiometric ratio, 2.06, 0.33, 0.33, 1.18, and 1.52, 0.15, 1.04, 2.06, respectively (Table 1). The degradation rate and products distributions under aerobic conditions were closely similar to those observed with *Rhodococcus* sp. strain DN22, confirming involvement of XplA during MNX degradation by DN22 (Halasz et al. 2010).

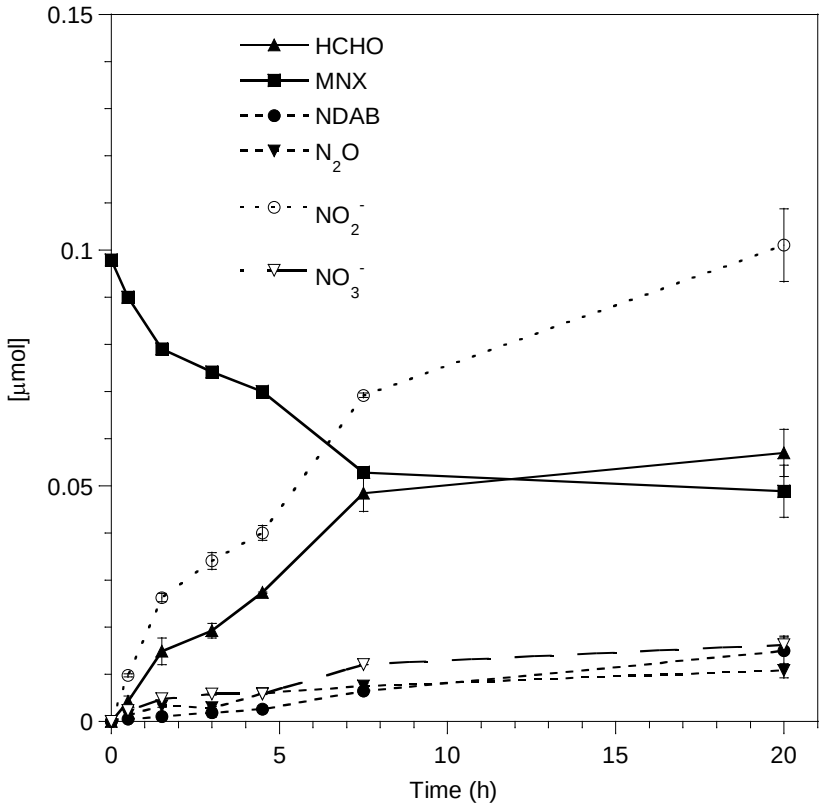

Figure 23. Time course of aerobic biodegradation of MNX by XplA

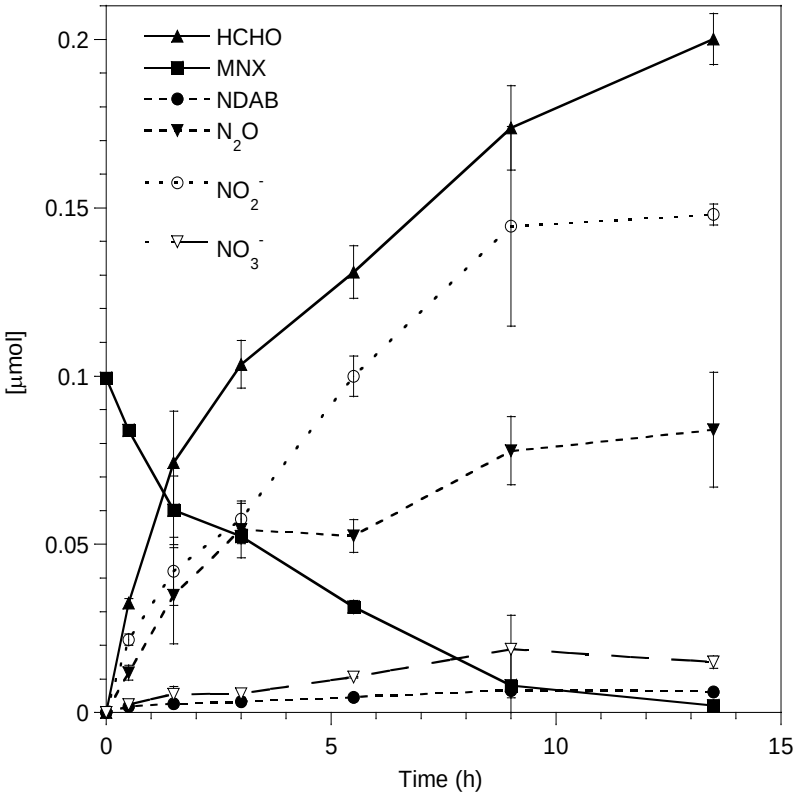

Figure 24. Time course of anaerobic biodegradation of MNX by XplA.

Table 5. Stoichiometric ratio of the products to MNX degraded with XplA under aerobic (49 nmol of MNX, 20h) and anaerobic (97 nmol MNX, 13.5 h) conditions.

Products	NO_2^- (RSD)	NO_3^- (RSD)	N_2O (RSD)	HCHO (RSD)	NDAB (RSD)
Aerobic	2.06 (3.1)	0.33 (0.0)	0.33 (22.9)	1.18 (2.6)	0.30 (8.2)
Anaerobic	1.52 (0.6)	0.15 (10.7)	1.04 (15.7)	2.06 (4.3)	0.06 (4.4)

In addition, we detected the ring cleavage product 4-nitro-2,4,-diazabutanal (NDAB), identified by comparison with a reference material, but with a stoichiometric ratio higher under aerobic than under anaerobic conditions, 0.3 and 0.06, respectively (Table 5).

A trace amount of another intermediate with a $[M-H]^-$ at 102 Da, matching an empirical formula of $C_2H_5N_3O_2$, was detected under aerobic conditions, which was an intermediate detected in an earlier study with MNX and *Rhodococcus* sp. strain DN22 (Halasz et al. 2010). In that study we used uniformly ring labeled ^{15}N-MNX and confirmed the intermediate to be the nitroso-derivative of NDAB, 4-nitroso-2,4-diaza-butanal ($ONNHCH_2NHCHO$, NO-NDAB). We presumed that the present intermediate shown at $[M-H]^-$ 102 Da was also NO-NDAB. Trace amounts of formamide (NH_2CHO) were detected in the samples prepared under aerobic conditions. Ammonium ion (NH_4^+) was detected but could not be quantified because of the strong interference caused by NADPH during analysis. For the same reason, formate production was not determined. Thereby, carbon and nitrogen atoms recoveries reached only 60-73% and 63-66%, respectively, under aerobic and anaerobic conditions.

Although we were unable to observe methylenedinitramine, $O_2NNHCH_2NHNO_2$ (MEDINA), or its nitroso-derivative, O_2NNHCH_2NHNO (NO-MEDINA), the detection of HCHO and N_2O suggested that MEDINA and/or NO-MEDINA was formed but decomposed very rapidly in water under conditions used (Paquet et al. 2011; Halasz et al. 2002) (eqs 1 and 2).

$$O_2NNHCH_2NHNO_2 + 2H_2O \rightarrow (OH)_2CH_2 + 2NH_2NO_2 \rightarrow HCHO + 2N_2O + 3H_2O \quad (1)$$

$$O_2NNHCH_2NHNO + 2H_2O \rightarrow (OH)_2CH_2 + HN{=}NOH + NH_2NO_2 \rightarrow HCHO + N_2 + N_2O + 3H_2O \quad (2)$$

Both hemiacetal ($(OH)_2CH_2$) and nitramide (NH_2NO_2) are unstable in water and should decompose spontaneously to give HCHO and N_2O, respectively (eq 1). In equation 2, decomposition of O_2NNHCH_2NHNO should initially give hydroxydiazene (HN=NOH), in addition to NH_2NO_2 and hemiacetal. It is known that hydroxydiazene (HNNOH) decomposes in water to N_2 (Casewit and Goddard III, 1982). The yield of N_2O in the anaerobic system was 3 fold higher than its yield under aerobic conditions, 1.04 and 0.33 $nmol \cdot nmol^{-1}$ MNX degraded, respectively, which accounted for only half of the calculated yield from $O_2NNHCH_2NHNO_2$. This observation suggests that one of the N-NO_2 (precursor of N_2O) in MEDINA was more likely N-NO (precursor to N_2). Also since we were able to detect MEDINA during RDX incubation with the same enzymatic system (Jackson et al. 2007), we suggest that NO-MEDINA,

rather than MEDINA, was the MNX ring cleavage product whose decomposition in water should produce N_2, N_2O and HCHO (eq 2).

On the other hand, the relatively high stoichiometric ratio of nitrite produced under both aerobic and anaerobic conditions, 2.06 and 1.52, respectively, suggest that the suspected two nitroso intermediates of MNX, namely, NO-NDAB and NO-MEDINA can degrade further to produce nitrite. This is supported by the fact that hydroxydiazene (HN=NOH) in water exists as a nitroso-oxime tautomer with nitrosamide (NH_2NO) (eq 3), which is known to hydrolyze to HNO_2 and NH_3 (Casewit and Goddard III, 1982).

$$HN{=}NOH \leftrightarrow NH_2N{=}O \qquad (3)$$

We detected NO_3^- under both aerobic and anaerobic conditions but with higher stoichiometric ratio in the former case, 0.33, and 0.15, respectively. The formation of NO_3^- can originate from NO formed by the cleavage of N-NO linkage in MNX following its initial denitration. Nitric oxide, NO, is known to undergo aerobic bio-oxidation to NO_3^- (Halasz et al. 2010; Ignarro et al. 1993) and autoxidation to NO_2^- (Awad and Stanbury, 1993). In an earlier study, during incubation of RDX with *Rhodococcus* sp. strain DN22 in the presence of $^{18}O_2$, we observed both NO_2^- and NO_3^- and attributed the small formation of the latter ion to bio-oxidation of NO_2^- to NO_3^- (Halasz et al. 2010). In addition, it is known that in the P450 catalytic cycle, autoxidation of the unstable oxy-ferrous intermediate ($Fe^{2+}.O_2$) can generate a superoxide radical anion ($O_2^{\cdot-}$) (Guengerich, 2001). Reportedly, nitric oxide can react with $O_2^{\cdot-}$ to yield $ONOO^-$, which upon protonation gives the unstable peroxynitrous acid (ONOOH) whose spontaneous decomposition in water would yield nitrate (NO_3^-) (Jourd'heuil et al. 1997). On the other hand, homolytic decomposition of ONOOH can produce nitrogen dioxide free radical ($\cdot NO_2$), which upon dimerization gives dinitrogen tetroxide, N_2O_4. Decomposition of N_2O_4 in water would produce nitrite and nitrate (Augusto et al. 2002). Previously we proposed the formation of $\cdot NO_2$ during denitration of RDX and MNX with *Rhodococcus* sp. strain DN22 (Halasz et al. 2010) and we will explain its formation and role in the degradation process later on in the present study.

Degradation of MNX with XplA-heme

XplA-heme is a truncated protein without the flavodoxin domain, which was substituted by ferredoxin and its reductase partner ferredoxin reductase in replacement of XplB. MNX was efficiently transformed using the combination of [XplA-heme-ferredoxin]/ferredoxin reductase. In the presence of oxygen, 22% of the MNX was transformed after only 5 min (Figure 25). MNX transformation rates progressively decreased and the reaction stopped after 200 min of incubation, with the disappearance of 1.35 μmols of the initial 1.94 μmols of MNX. Among the diverse MNX breakdown products examined, we found significant amounts of NDAB, NO_2^-, and HCHO. NDAB concentration increased throughout the time course, even after MNX transformation had stopped. The molar fraction of NDAB produced to MNX degraded was 0.20 after 200 min of incubation and reached 0.48 after 22 h. Nitrite ions were formed at a molar fraction of 1.9 moles for each disappearing mole of MNX. Only trace amounts of nitrate were formed. HCHO reached a molar fraction of 1.5 at time 120 min (Figure 25).

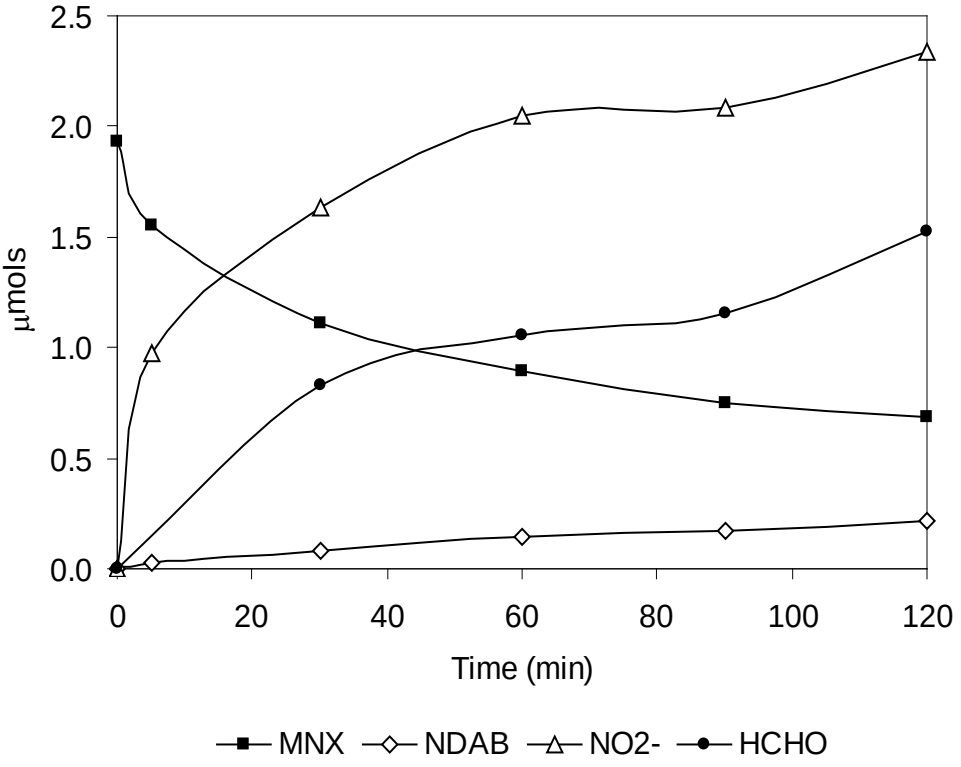

Figure 25. Aerobic transformation of MNX by XplA-heme

The results obtained with XplA-heme incubated aerobically with MNX are in agreement with what we previously observed with *Rhodococcus* sp. DN22 and XplA/XplB system. The major difference is that NO_3^- was found at a molar fraction of 0.5 and 0.33 with DN22 and XplA/XplB, respectively, and only in trace with the enzyme XplA-heme.

Under anaerobic conditions, each disappearing mole of MNX gave 1.4 moles of NO_2^- (Figure 26). HCHO was formed at a molar fraction of 1.7. A similar stoichiometry for NDAB was observed under aerobic and anaerobic conditions, i.e, the concentration increased substantially several hours after MNX transformation had stopped, and reached 0.42 after 18 h. Production of NDAB under anaerobic conditions is in opposition to what we observed using the XplA/XplB system and MNX or RDX (Jackson et al. 2007).

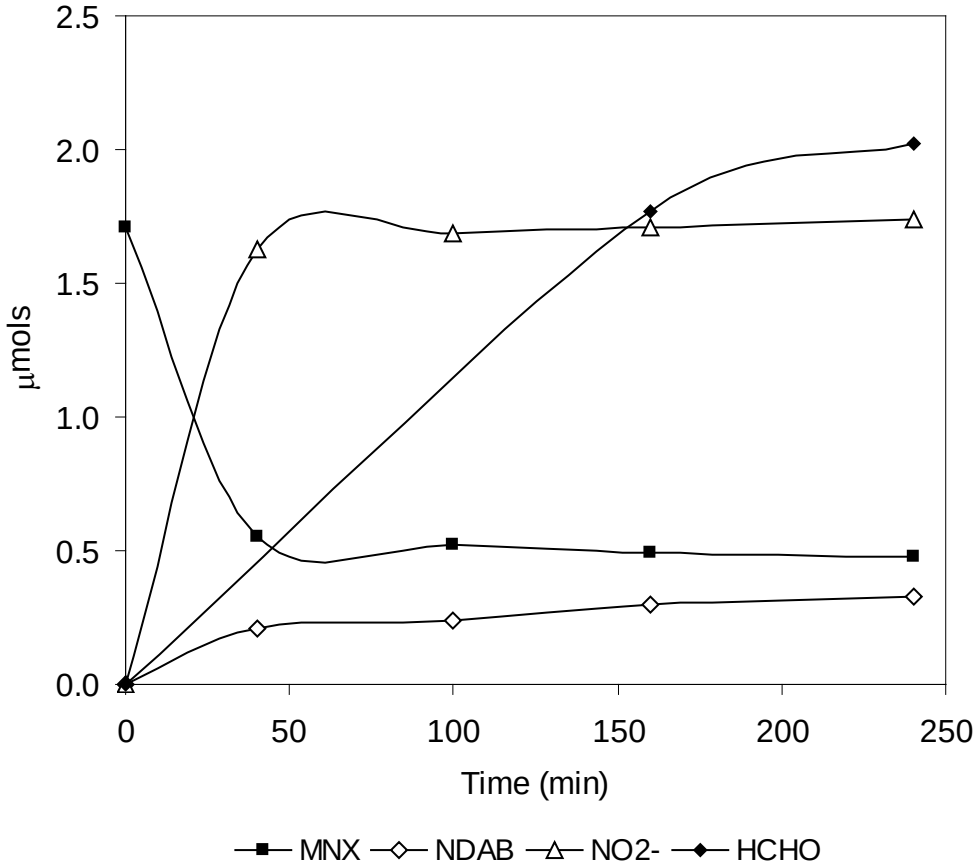

Figure 26. Anaerobic transformation of MNX by XplA-heme

The production of nitrite, HCHO and NDAB under both aerobic and anaerobic conditions in comparable molar ratio (1.9, 1.5, 0.48 and 1.4, 1.7, 0.42, respectively) suggest that the oxygen was not involved in MNX degradation by [XplA-heme/ferredoxin]/ferredoxin reductase, which is contrary to what we observed using XplA with its natural redox partner XplB (Table 5) or with strain DN22. The lack of production of NO_3^- under both conditions suggest that NO has underwent an autoxidation to NO_2^- rather than reacted with a superoxide radical anion ($O_2^{\cdot-}$) producing NO_3^- (see above).

XplA-heme worked efficiently with commercially available and relatively inexpensive redox partners. The products distribution was different than what was obtained with XplB, particularly regarding the production of NDAB. These results suggest the possibility that XplA systems with different redox partners could be engineered to degrade RDX and its nitroso derivatives via selected routes for its use in bioremediation activities.

Relative reactivities of RDX and its nitroso products MNX, DNX and TNX with XplA

When we incubated RDX, MNX and TNX separately with XplA under aerobic and anaerobic conditions we found that the enzyme degraded both RDX and MNX but not TNX. The initial removal rates of RDX and MNX were 357 and 72 $nmol \cdot h^{-1} \cdot nmol^{-1}$ protein under aerobic conditions and 472 and 118 $nmol \cdot h^{-1} \cdot nmol^{-1}$ protein under anaerobic conditions, respectively. The present data showed that the anaerobic degradation rates of both chemicals were higher than the aerobic rates, suggesting that molecular oxygen might not be needed to initiate degradation.

Also the data clearly showed that under both aerobic and anaerobic conditions, MNX degradation was slower than RDX. This is consistent with our previous finding that the dissociation constant (K_D) of XplA heme domain with MNX is about twice the value of the one calculated with RDX (~24.2 µM and 11.4 µM, respectively). High K_D with MNX would imply higher K_M (Michaelis-Menten constant) and, likely, lower k_{cat} (maximum turnover rate) values and, in general, lower activity (Sabbadin 2010).

In other experiments, RDX, together with its three nitroso derivatives, was incubated with XplA under aerobic and anaerobic conditions (Figure 27).

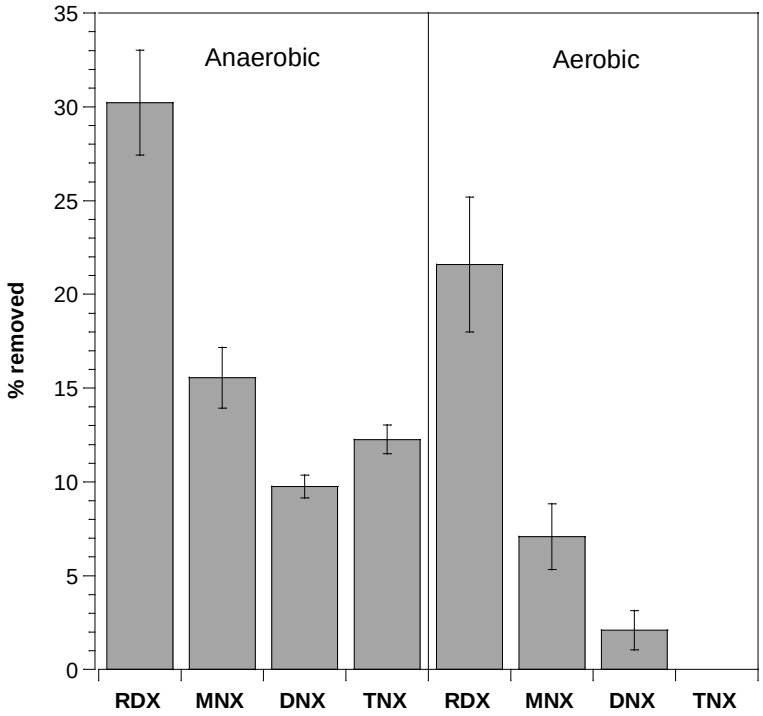

Figure 27. RDX and its nitroso derivatives removal from mixture incubated with XplA for 1h under anaerobic and aerobic conditions.

In aerobic assays, RDX and two of its nitroso derivatives MNX and DNX degraded with initial rates equaled to 126, 40, and 11 $nmol \cdot h^{-1} \cdot nmol^{-1}$ of protein, respectively, lower than their removal rates when incubated separately with the enzyme. TNX $(CH_2NNO)_3$, which does not contain $N\text{-}NO_2$, did not degrade aerobically with XplA.

In anaerobic assays, under otherwise identical conditions, the four chemicals RDX, MNX, DNX, and TNX degraded with initial rates of 180, 91, 51, and 69 $nmol \cdot h^{-1} \cdot nmol^{-1}$ of protein, respectively (higher than those observed under aerobic conditions). This showed that the successive replacement of $N\text{-}NO_2$ by N-NO in RDX reduced the removal rate of the chemical. We also found that TNX can only degrade with XplA under anaerobic conditions and in the presence of a co-substrate containing $N\text{-}NO_2$ functionality (Table 2). A reactive intermediate possibly coming from degradation of an $\text{-}N\text{-}NO_2$ containing substrate, e.g., RDX or MNX might have initiated TNX degradation (discussed below).

Table 2. Percent of RDX, MNX and TNX removed after 1h incubation with XplA under anaerobic conditions. Initial concentrations of RDX, MNX and TNX were 147 µM, 135 µM and 127 µM, respectively.

Mixture	RDX (%)	MNX (%)	TNX (%)
RDX and TNX	47	na*	20
MNX and TNX	na*	36	8

* not applicable

Experimental data gathered thus far prove that with XplA (1) the heterocyclic compound with the highest number of $-NO_2$ groups reacts faster, i.e. rates decreased in the order RDX>MNX>DNX and (2) denitration, N-NO_2 bond cleavage, is favored over denitrosation, N-NO bond cleavage, under both aerobic and anaerobic conditions. Conversely to biologic degradation with XplA, abiotic degradation of RDX and its nitroso products with highly reactive organically-complexed iron(II) species showed reaction rates in the order TNX>DNX>MNX>>RDX (Kim and Strathmann, 2007). As we mentioned earlier, XplA degraded RDX via initial denitration and its nitroso derivatives via denitration and/or denitrosation, which is different from what was proposed for the Fe(II) reaction. In the latter case, RDX is suggested to degrade via sequential reduction of the N-NO_2 groups to the corresponding N-NO functionalities. Interestingly, in a much earlier study using *Clostridium bifermentans* HAW-1, we found the following degradation rates for RDX and its nitroso derivatives MNX and TNX: 28.1, 16.9, and 7.5 µmol h^{-1} g(dry wt) $cells^{-1}$, respectively (Zhao et al. 2003). MNX denitration as major route and continuous reduction to DNX and TNX as minor degradation route have been proposed (Zhao et al. 2003).

Insights into the initial steps involved in the degradation of MNX: denitration versus denitrosation.

Aerobic degradation Earlier we investigated MNX biodegradation with *Rhodococcus* sp. strain DN22 (Halasz et al. 2010) using conditions similar to those employed with RDX (Fournier et al. 2002) and demonstrated that both denitration (N-NO_2 bond cleavage) and denitrosation (N-NO bond cleavage) can occur before ring opening. In the present study, we investigated the degradation of MNX by the rhodococcal P450 XplA. During the aerobic incubation with XplA, we detected nitrite and nitrate ions in stoichiometric ratio equaled to 2.06 and 0.33, respectively, for each disappearing mole of MNX. The comparatively high yield of nitrite (2.06) suggested that the first step in the MNX degradation was possibly denitration caused by hydrogen atom abstraction followed by $\cdot NO_2$ elimination as was the case with DN22 (Halasz et al. 2010) (Figure 28).

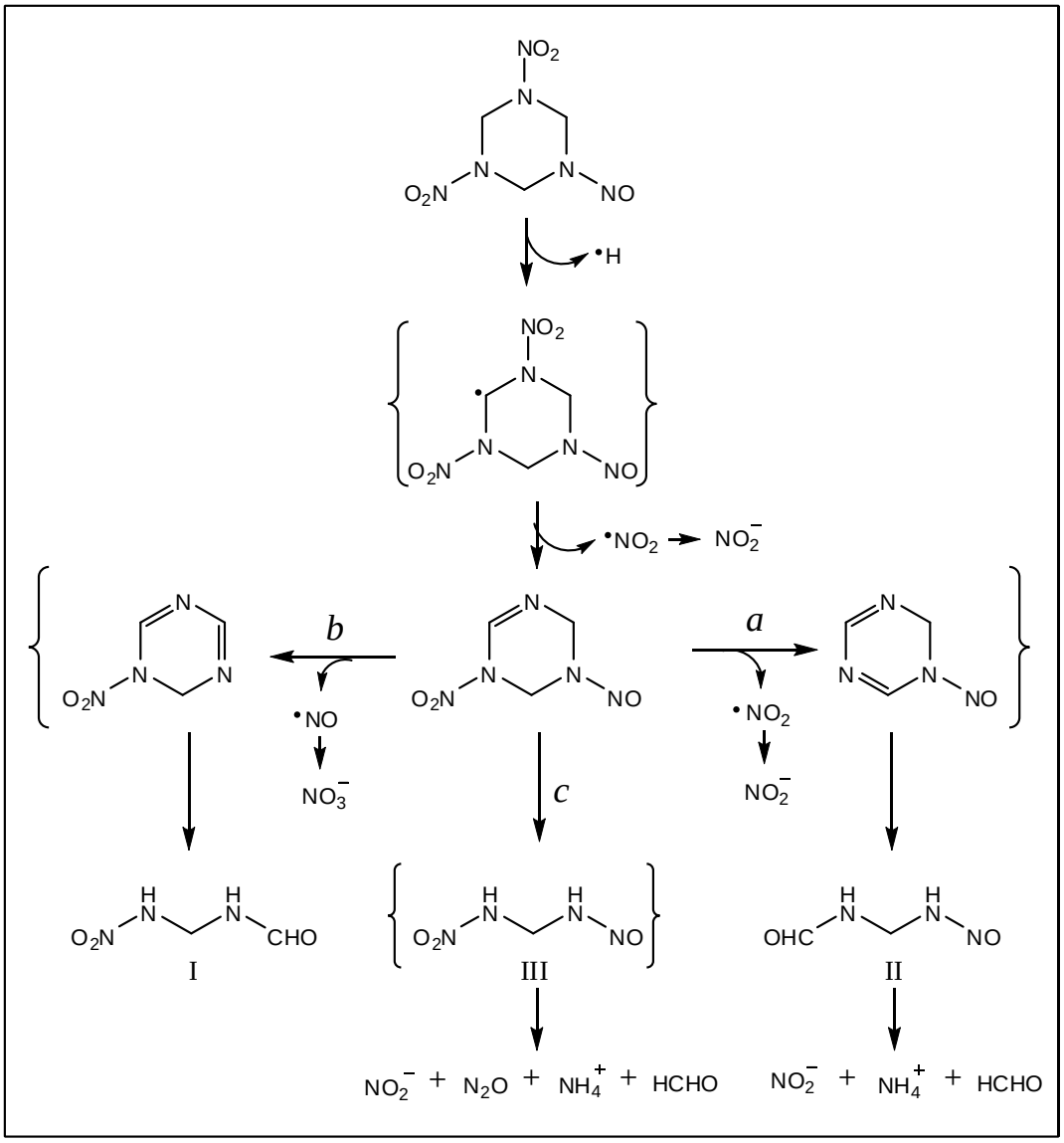

Figure 28. Proposed aerobic degradation routes of MNX by XplA. Compounds in brackets were not detected.

Following this key initial denitration step, MNX can either undergo further denitration (Figure 28, path *a*) or denitrosation (Figure 28, path *b*) before ring cleavage. In line with this explanation, we detected nitrate anion and the key ring cleavage product NDAB (I) and its nitroso-derivative NO-NDAB (II) (Figure 28, paths *a* and *b*). We also detected N_2O. From earlier studies, we know that N_2O can be formed from the decomposition of MEDINA ($O_2NNHCH_2NHNO_2$, eq 1), an RDX ring cleavage product (Halasz et al. 2002). We speculate here that in the case of MNX, it is more likely that N_2O originated from the nitroso-derivative of MEDINA (O_2NNHCH_2NHNO, III), which should undergo spontaneous decomposition in water to give N_2O and HCHO that were both detected (Figure 28, path *c*).

Anaerobic degradation Previously we found that degradation of RDX by XplA under anaerobic conditions is initiated by monodenitration followed by ring cleavage to produce MEDINA (Jackson et al. 2007). In a subsequent review article (Halasz and Hawari, 2011), we

elaborated further on the anaerobic formation of MEDINA from RDX and suggested the occurrence of denitrohydrogenation followed by ring cleavage to give MEDINA, which, being unstable in water, decomposes to HCHO and N_2O (eq 1). In the present study, for each mol of MNX reacted anaerobically with XplA we detected 1.52 and 0.15 moles of nitrite and nitrate, respectively. In addition, we detected HCHO and N_2O in stoichiometric ratio equaled to 2.06 and 1.04, respectively. The formation of one mole of N_2O tends to suggest that MNX, after initial denitration, underwent ring cleavage to give NO-MEDINA ($ONNHCH_2NHNO_2$, III) as the key ring cleavage product whose degradation would give N_2O, N_2, NH_3 and HCHO (Figure 5A). As we explained in equation 3, intermediate III can exist in equilibrium with its hydroxydiazenyl tautomer ($HONNCH_2NHNO_2$, IV) (Figure 29A).

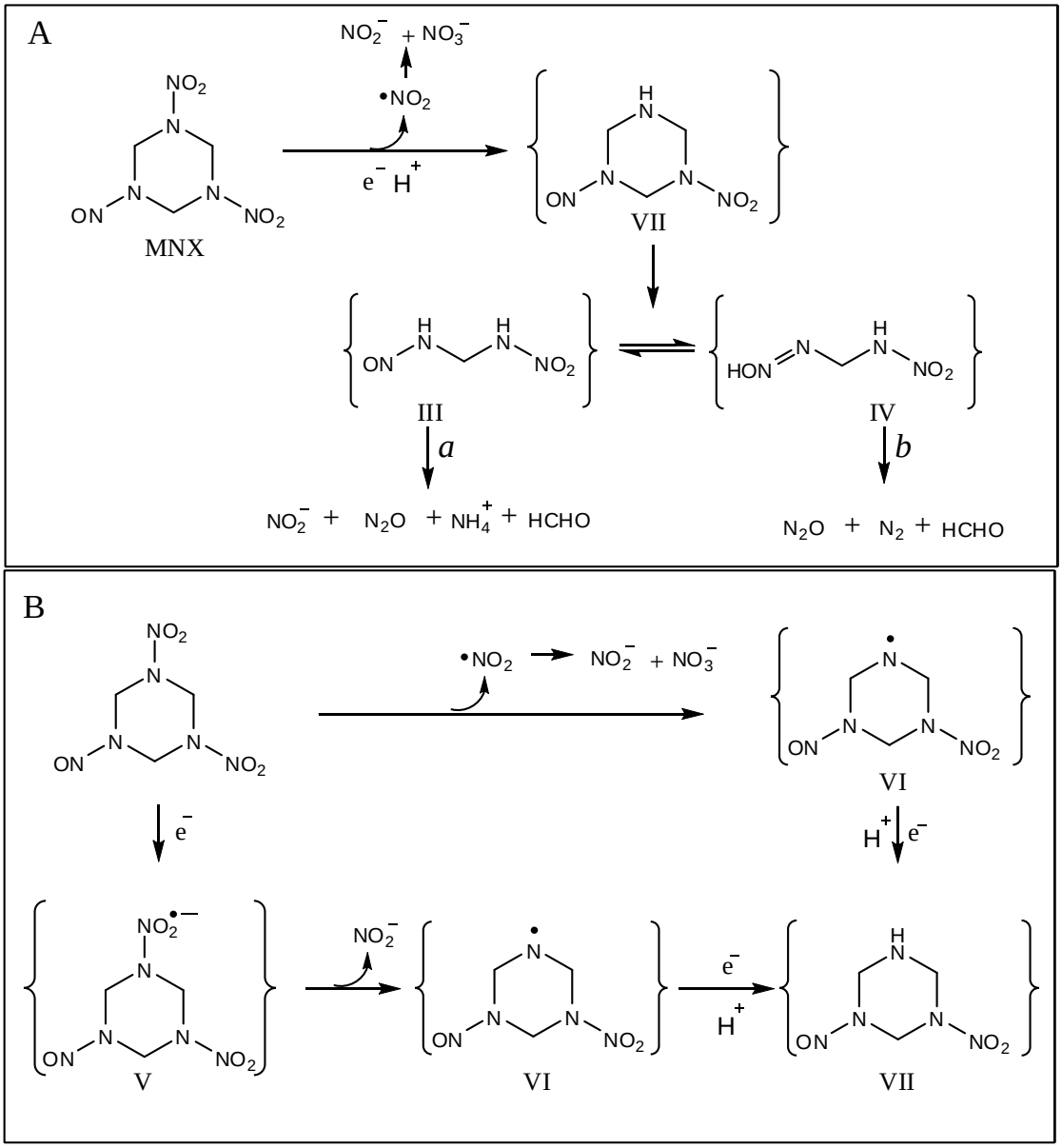

Figure 29. Proposed anaerobic degradation route of MNX by XplA. Compounds in brackets were not detected.

Decomposition of tautomer IV should produce N_2 but we were unable to analyze the gas because of interference from the nitrogen gas in the air. However, we detected nitrite with stoichiometric ratio of 1.52, which was approximately 50% higher than the yield calculated based on the cleavage of only one N-NO_2 bond in MNX. These experimental findings suggested that about half of NO-MEDINA was present as a nitrosamide tautomer (III) that decomposed to NO_2^- and NH_4^+ (Figure 29A).

Considering all of the above experimental evidences we suggest that, under anaerobic conditions, XplA reduced MNX to initially form the unstable intermediate 1-nitroso-3-nitro-perhydro-1,3,5-triazine (VII), which should decompose to give NO-MEDINA (III) and its tautomer IV (Figure 29A and 7B). Indeed, McHughes et al. (2002) reported that reduction of RDX with Na(Hg) process via denitrohydrogenation leads to the initial formation of the unstable denitrohydrogenated intermediate 1,3-dinitro-perhydro-1,3,5-triazine whose decomposition gives MEDINA.

The remaining challenge here is to know how initial denitration of MNX (and other substrates investigated in this study) took place. Based on our earlier discussion, we propose two routes for the possible formation of 1-nitroso-3-nitro-perhydro-1,3,5-triazine (VII) (Figure 29B). One route involved direct homolysis of –N–NO_2 resulting in the formation of the $\cdot NO_2$ and aminyl radical (VI). The other route involved the formation of MNX anion radical (V), which upon loss of nitrite would also produce the aminyl radical (VI) (Figure 29B). Hydrogen atom abstraction by VI would lead to the formation of 1-nitroso-3-nitro-perhydro-1,3,5-triazine (VII).

Finally, the potential involvement of $\cdot NO_2$ and the aminyl radical (VI) in the degradation pathways of MNX (or RDX (Bhushan et al. 2002a) can help explain the degradation of TNX when the latter is incubated with XplA in the presence of a N-NO_2 containing substrate. A free radical generated from degradation of MNX (and either RDX or DNX) might thus be responsible for initiating TNX degradation. For example hydrogen abstraction by either $\cdot NO_2$ or aminyl radical from the –CH_2– in TNX, $(CH_2NNO)_3$, would destabilize the molecule causing it to decompose.

Environmental significance

The nitroso derivatives of RDX are toxic and need to be removed from the environment (Zhang et al. 2008). Understanding their transformation pathways should help to develop efficient remediation strategies that completely remove RDX and its nitroso products from contaminated sites. Aerobic XplA-containing *Rhodococcus* have been isolated from RDX-contaminated soils (Seth-Smith et al. 2002) and from a microaerophilic aquifer (Bernstein et al. 2011). Because RDX degradation by *Rhodococcus* strains was shown possible under extremely microaerophilic conditions (Fuller et al. 2010), it is reasonable to presume that *Rhodococcus* can degrade the anaerobically formed nitroso in micro-oxic environments. They would also degrade the nitroso compounds that may migrate to the oxic zone (Sagi-Ben Moshe et al. 2010).

The cytochrome P450 XplA was shown to degrade MNX and DNX, and also to degrade TNX in the presence of RDX and MNX but only under anaerobic conditions. MNX is a key degradation product of RDX and is detected in most groundwater and soil showing the presence of RDX (Beller and Tiemeier, 2002; Sagi-Ben Moshe et al. 2010, Paquet et al. 2011). We established that XplA degraded MNX by two distinctive pathways, one pathway occurring under aerobic (Figure 28) and another under anaerobic (Figure 29) conditions, preferentially cleaving the N-NO_2 bonds over N-NO. These pathways are complimentary to the pathways we recently reported for RDX (Halasz et al. 2010; Halasz and Hawari, 2011). Knowledge of the type and

order of bond cleavage would help in the development and application of stable isotope fractionation and stable isotope probing tools recently considered important in the understanding of the fate of N-containing explosives in the environment (Sagi-Ben Moshe et al. 2010; Bernstein et al. 2008; Schmidt et al. 2004; Roh et al. 2009). In a recent study we successfully detected RDX transformation products, including MNX and the ring cleavage products NDAB, NO_2^-, NO_3^- and N_2O in contaminated groundwaters, as a sign of past RDX contamination and *in situ* natural attenuation (Paquet et al. 2011). In the present MNX study, we also detected NDAB and some characteristic products such as NO_2^-, NO_3^- and N_2O. Since the three N-oxide compounds can also originate from other processes in the field, we can apply ^{15}N and ^{18}O stable isotope analyses as a sensing tool to differentiate between compounds derived from the cyclic nitramines (RDX and MNX) and those formed *via* other processes and use data to monitor and enhance *in situ* remediation and natural attenuation.

Task 3. Determine the diversity of *xplA* in the environment and possible evolutionary origin

This task was combined with Task 6.

Task 4. Determine the mechanism of horizontal gene transfer of xplA

For the plasmid transfer, three potential recipient strains were chosen: *Rhodococcus* sp. CW25 (known to be able to heterologously express *xplA*), *Rhodococcus* sp. NCIM9784 (a commercial strain) and *Pseudomonas fluorescens* (a gamma proteobacteria able to heterologously express *xplA*). Antibiotic selection and absence of RDX degradation were tested for the different recipient strains in order to select potential transconjugants (Table 6). First, the selection of transconjugants was performed using a single antibiotic selection and on the acquired ability to grow on RDX as the sole nitrogen source.

Table 6: Antibiotic resistance of strains used for catabolic plasmid conjugation experiments

Strain	RDX	Rif10	Kan30	Cm35
R. sp. 11Y	+	-	-	-
R. sp. CW25	-	+	+	-
R. sp.NCIM9784	-	-	+	-
P. fluo. F113	-	+	Not tested	Not tested

Tests were done by streaking bacteria from a rich and non-selective medium onto selective medium. +: resistance and growth, -: no growth, R.: *Rhodococcus*, P. fluo: *Pseudomonas fluorescens*, Rif 10: rifampicin 10mg/ml, Kan 30: Kanamycin 30mg/ml, Cm 35: Chloramphenicol 35mg/ml

Transconjugants were only obtained with *Rhodococcus* sp. CW25 as the recipient strain, but they did not survive the subsequent purification steps on selective media. This result suggested that a mix of strains (donor and recipient) grew conjointly on the selective medium. Thus we tried to improve the conjugation experiments by using more bacteria (1 ml and 25 ml) to select for potentially rare conjugation events. Selection of recipient strains (*Rhodococcus* sp. CW25) with newly acquired RDX degradation capability was performed on agar plates containing RDX as sole nitrogen source. Counter selection of the donor strain (*Rhodococcus* sp. 11Y) was performed with a double kanamycin and rifampicin selection. Serial dilutions of the mating experiments were also used to avoid antibiotic depletion by the bacterial mass; however, the

obtained clones did not survive the further purification steps, suggesting once again that they were not genuine transconjugants.

Task 5. Investigate the regulation and transcription of xplA/B.

454 pyrosequencing of Rhodococcus rhodochrous sp. 11Y

Genomic DNA from *R. rhodochrous* 11Y was used for 454 pyrosequencing. This was performed at the Technology Facility at the University of York. A total of 23963 sequences were obtained, with an average length of 226 bp (Figure 30). The sequence assembly released with the Roche software created 1825 contigs, of which 167 were larger than 500 bp long. Comparative genomic analyses of these sequences using the *Rhodococcus jostii* RHA1 reference genome were performed with the Roche software. *R. jostii* RHA1 possesses one chromosome representing 80 % of the entire genome and three plasmids. An 80 % identity cut-off was used to compare and assess the presence of homologous sequences between the two genomes. 15 % of the 23963 *R. rhodochrous* 11Y reads and 23 % of the 1825 contigs were mapped on the RHA1 genome. RHA1 chromosomic sequences represented 90 % of this mapping, showing a slight overrepresentation in comparison to the plasmidic sequences. Only 26 of the 1825 contigs of *R. rhodochrous* 11Y were mapped onto the RHA1 plasmids. Interestingly, those plasmid sequences were not randomly distributed, but corresponded to a gene cluster encoding a metabolic pathway for the beta-oxidation of fatty acids previously predicted as a genomic island of foreign origin in RHA1(McLeod et al., 2006). These results indicated that RHA1 and 11Y are likely to harbor different plasmids. Only a quarter of the 11Y reads were mapped on the RHA1 genome sequence, despite the fact that they belong to the same genus. Mapped sequences were highly represented on the chromosome and suggested that they might belong to the core genome.

When the 1825 contigs were blasted against the NCBI databank, only 55 % of the best blast hits were *Rhodococci* sequences (Figure 30A). Often, the best blast hits were with other actinomycetal genera (*Mycobacterium* (13 %), *Nocardia* (8 %), *Frankia* (6 %)). This suggests that actinomycetal bacteria shared a pool of common functions that can be possibly transferred between different genera. Moreover, 7 % of the best blast hits were with proteobacterial sequences suggesting, in these cases, a potentially broader range of lateral gene transfer occurs.

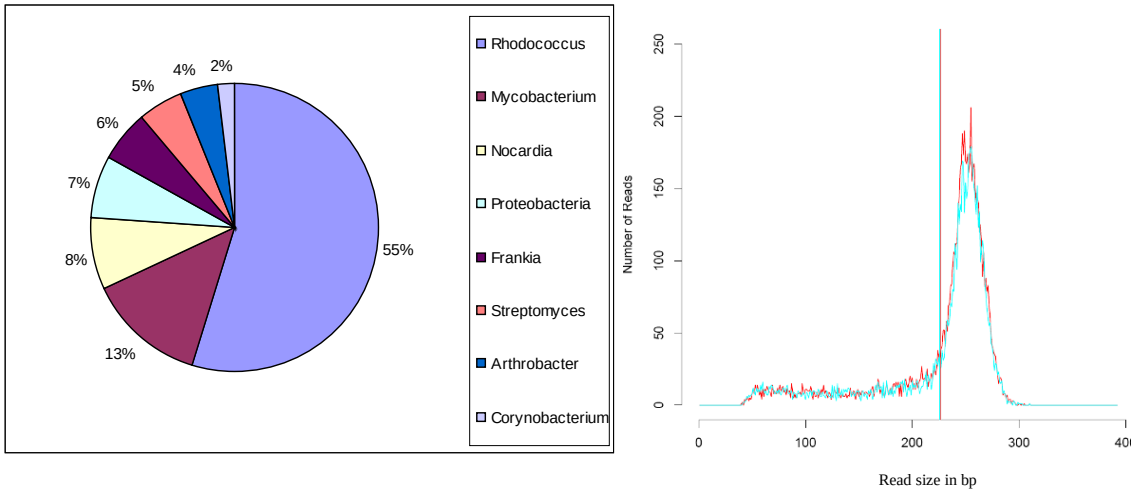

Figure 30: A graphic representation of the *R. rhodochrous* 11Y 454 sequencing.

The vertical line indicates the average size of reads. B. Representation of the genera with the best blast hit with 1825 contigs 11Y sequences. Only sequences bigger than 50 bp with a nucleotide identity of more than 40 % were taken into account.

Degradation of different compounds

From the 454 'snap shot' pyrosequencing of the *R. rhodochrous* 11Y genome, we have been able to identify genes potentially involved in the degradation of different compounds. For instance, a phenol 2-monoxygenase and a phenol hydrolase with 94 % identity to 482 nt respectively 82 % to 430 nt of a *Rhodococcus spp.* were identified, indicating a potential for phenol degradation. Using a similar approach, we identified genes that might be involved in benzoate, camphor and taurine degradation. 11Y was cultured in minimum media containing the different carbon sources as described above as sole carbon and/or nitrogen sources. We showed that *R. rhodochrous* 11Y can use phenol, benzoate and camphor as sole carbon sources and taurine as sole nitrogen source.

Cosmid library construction

A cosmid library of 960 clones in the pWEB cosmid vector, with an average insert size of estimated 40 kb has been conserved in glycerol at -80 °C. The *R. rhodochrous* 11Y genome is estimated to be 8 Mb and this library should cover almost 99 %. Using PCR, 768 clones were screened for the presence of *xplA* and ten of them found to harbor *xplA*.

R. rhodochrous 11Y cosmid snap shot sequencing

One of these clones was sub-cloned in pGEM-T (Promega) and used for 'snap shot' sequencing. The 96 inserts were amplified with the T7 and Sp6 primers and sequenced with the Sp6 primer. Good quality sequences were assembled with the 454 Roche software and 26 contigs and 15 singletons generated. The best BlastX matches are presented in Table 7.

Table 7: Best BlastX (NCBI) matches of the 'snap shot' sequencing of a *R. rhodochrous* 11Y cosmid insert harbouring the gene *xplA*

Contig/ clone	Nb of reads	Length	Blast homology
Contig 1	3	737 bp	71% putative plasmid partitioning protein ParA *Rhodococcus opacus*
Contig 2	2	697 bp	51 % hypothetical protein *Rhodococcus opacus* on 130AA
Contig 3	2	559 bp	91 % flavoprotein involved in K+ transport *Gordonia bronchialis*
Contig 4	3	930 bp	63 % hypothetical protein *Rhodococcus erythropolis* on 70 AA
Contig 5	5	823 bp	97 % transcriptional regulatory protein *Microbacterium sp.* MA1
Clone 77	1	194 bp	Low homology with hypothetical protein
Contig 7	9	254 bp	91% on 30AA with CrcB protein homolog *Rhodococcus opacus* B4
contig 8	2	279 bp	Low homology with hypothetical protein
contig 9	3	301 bp	Low homology with hypothetical protein
contig 10	3	660 bp	60 % cell wall-associated hydrolase *B multivorans* on 69 AA
contig 11	2	428 bp	No homology
contig 12	2	657 bp	100 % *xplA*
contig 13	3	720 bp	76 % flavoprotein involved in K+ transport *Gordonia bronchialis*
contig 14	2	750 bp	100 % xplB
contig 15	2	1237 bp	40 % on 180AA with replication protein and 73% on 125AA with hypothetical
contig 16	2		81% hypothetical protein MAV_0276 *Mycobacterium avium* 104
Clone 17	1	546 bp	64% on 140AA GAF like transcriptional activator of acetoin/glycerol metaboli
Clone 51	1	502 bp	nothing significant
contig 19	6	1555 bp	33 % on 104 AA with hypothetical protein *P. fluorescens* SBW25
contig 20	2	303 bp	nothing significant
contig 21	2	500 bp	72% with Cell wall-associated hydrolase *Roseobacter sp*.
contig 22	3	650 bp	nothing significant
contig 23	3	646 bp	37 %hypothetical protein MsilDRAFT_1691 *Methylocella silvestris*
contig 24	4	535 bp	54% on 125 AA with replication protein *Gordonia westfalica*
contig 25	4	609 bp	nothing significant
contig 26	9	771 bp	85 % helicase associated protein *Gordonia bronchialis*
Clone9	1	625 bp	43% putative helicase Rhodococcus erythropolis
Clone28	1	783 bp	48% replication protein *Gordonia westfalica*
Clone34	1	784 bp	50% replication protein *Gordonia westfalica*
Clone35	1	789 bp	57% hypothetical protein RHA1 *Rhodococcus sp*

Clone71	1	770 bp	43% Hypothetical protein NCgl1611 *Corynebacterium glumaticum*
Clone83	1	472 bp	70% ATPase, ParA type *Rhodococcus sp.* RHA1

Genome walking and comparative genomics of RDX degradation genes

Three *R. rhodochrous* 11Y cosmids containing the *xplA* gene were used as the template for genome walking. Internal *xplA* primers (Table 8. Primers used to amplify genomic island in the isolates) were designed to obtain sequence information up- and downstream from *xplA*. With this new sequence information, further primers were designed to continue the genome walking up- and downstream of *xplA* (Table 8. Primers used to amplify genomic island in the isolates). This was repeated several times.

Table 8. Primers used to amplify genomic island in the isolates

Primer name	Primer sequence 5'-3'
GAF-F	CGATTCCGTATCCGACCTC
TranscRp-504R	GATGTTCTCCGGTTGATCG
RegulatoryPrt-89F	GGTTCACATGGCTTTTCACC
SensorK-292R	CTATCGCATCGCTCAGGAGT
SensorK-129F	CATTCCGTCTATTCCGGTTC
SensorK-1087R	CGTGGTCGTGACAGTCATCT
Sensork-1035F	GATTCGGTCGAACGGGTA
Carbesterase-167R	AGAGTCGGGCACATGACAC
MarR-194R	GCACTGTTGAGTCCGAGATG
HypoPrt-453F	GGTCTCGCAACACACTGAAC
Carbesterase-6F	ACGTCGGAATTCAGTGTCGGGCGGACC
Permease-6R	GAGTCGAAGAGGGCACTCAG
Permease-7F	CTGTGTGGTGTGGTGATGGT
Permease-7R	CTACTCCCCGGTCTTCTTCGGAAT
Permease-8F	ACTACATCGTGCTGCTGTCC
Dihydro-8R	GTCGAGCATATGCACGTCGGGGATACG
Dihydro-9F	GATGTCAACGAATGGACGAT
xplB-9R	GTCGATCCGAAGTGGAACAC
xplB-10F	CGGTGATGATGCGTGAACT
xplA-10R	TCTCCGTAGGTGGAGGTGAC
xplB-11F	ACCC GACATATGACACCCGAGATGGAG
xplA-11R	TCAGATAGCCGAAAGCGACT
xplA-12F	CACGCGTCCTACAACTACCC
SSD12R	AACAGCTCCTCACGGTAAGC
xplA13F	ATCGTCCTGTCCTGAAAACC
AMP13R	GTTGTGGCAGGTGTTGAGTT
AmMP14F	ATCAGCGATGGGACGATAC
AMP14R	ATGCCCAGGTGAACGTGT

AMP15F GTGATGTACGAGGGCAAGC

In total, a region of 15 kb of DNA was sequenced and compared with the published sequence of *Microbacterium* sp. MA1, another bacterium able to degrade RDX (Andeer et al., 2009).

Microbacterium MA1 and *R. rhodochrous* 11Y shared a genomic island spanning over 15 kB containing the gene *xplA*. The genomic island was found to be highly identical in the two species with the exception of a transposable element found in MA1 and five single nucleotide polymorphisms located in *xplA*. Moreover, sequencing revealed that the first gene located upstream in the genomic island is highly similar to a GAF protein found in *Gordonia bronchialis*. **GAF** domains are motifs found in cyclic **G**MP-regulated cyclic nucleotide phosphodiesterases, some **A**denylyl cyclases and the bacterial transcription factor **F**hlA. The GAF-like protein in MA1 was found to be truncated but of full length in 11Y (Figure 31).

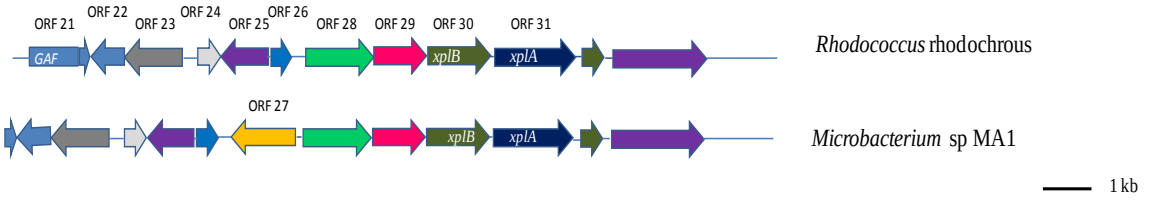

Figure 31: *xplA* gene cluster alignment of *R. rhodochrous* 11Y and *Microbacterium* MA1.

The synteny of the genes in both organisms is the same with the exception of a transposable element (ORF27) and a truncated GAF protein in MA1 (ORF21).

Determine the length of the xplA-operon

Softberry-BProm was used to analyze the sequence from *marR* to *xplA* for putative promoter sites. Within this region three putative promoter sites were predicted; one upstream of xplB (-10 box TGTAACAAT, -35 box TTACAT, putative transcription factor binding site soxS AACTGTAA), one upstream of the permease (-10 box CCCTATGTT and the -35 box TTCCGG) and one within *xplA* (-10 box CGTCACGAT, -35 box TCGCCG, putative transcription factor binding site rpoD17 GGTCCTACA).

To establish the transcription start site and determine which genes are part of the *xplA/xplB* operon primer extension analysis was used. Two putative promoter sites were targeted: one site, predicted using the fruitfly promoter search program upstream of the putative regulator MarR, and another site, predicted using Softberry-BPROM upstream of the permease as described above. Four 6-carboxyfluorescein-labelled (FAM) primers were designed ranging between 65 and 147 bases downstream of the predicted promoter sites and tested by PCR for efficiency using a forward primer close to the desired sequence.

Primer extension was performed by extracting RNA from *R. rhodochrous* 11Y grown in MM containing 180 μM RDX to OD_{600}= 0.5. Each labeled primer was used separately to reverse transcribe the region of interest and analyze the fragment for its length. The fragment analysis was performed using the Technology Facility at the UoY. No labeled fragments could be detected when using either of the two primers designed to amplify the region upstream of the putative regulator *marR*. Two products around 114 bp and 200 bp were obtained using the

primers designed to regions 65 and 147 bases respectively downstream of the predicted promoter site. The lengths of the fragments map the promoter to the promoter site as predicted by the software Softberry-BPROM.

Fragment analysis using primers to reverse transcribe the region upstream of the putative permease was repeated. Therefore the reverse transciptase reaction for the targeted promoter sites was performed by replacing dGTP with deazaGTP. The use of deazaGTP reportedly reduces the production of hairpin structures and results in a more accurate size determination of the fragments.

When using the primer, which is 147 bases downstream of the predicted promoter site, two fragments were identified; one as obtained previously with a length of 204 bases and one with a length of 569 bases, which was not obtained when using dGTPs (Figure 32). When using the primer which is 65 bases downstream of the predicted promoter site no fragment was identified. Experiments were repeated again; however, the fluorescent signal was too low to allow judgment of the fragment lengths obtained.

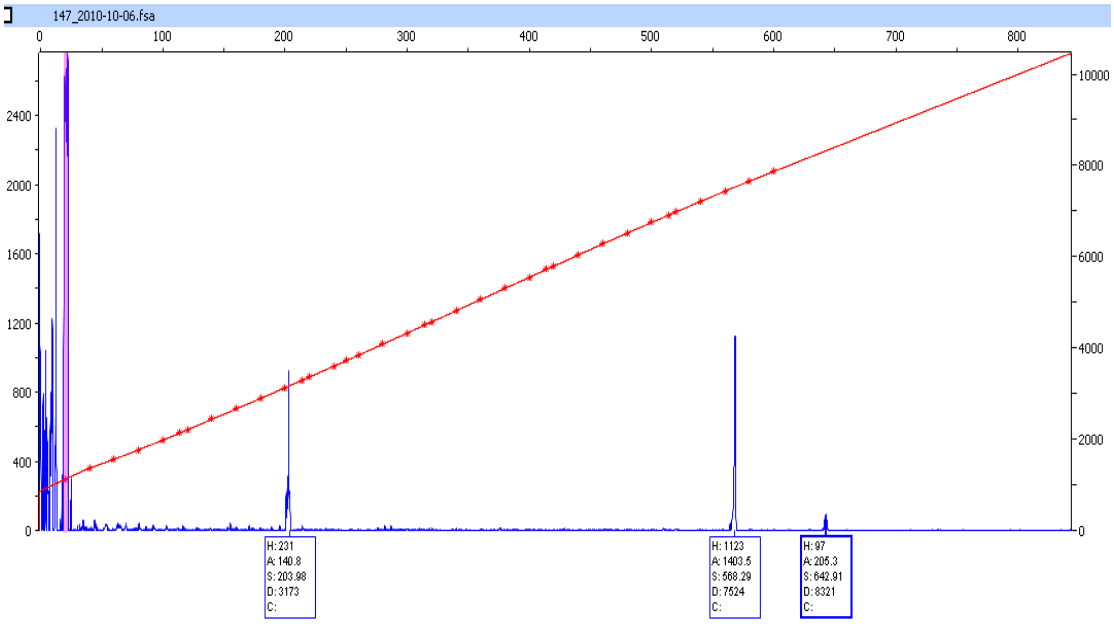

Figure 32: Fragment detection using the Peak Scanner Software.
Two signals representing fragments of 204 and 569 bases respectively were measured.

Additionally, we targeted a further putative promoter site, predicted using Softberry-BPROM upstream of XplB.

A 6-carboxyfluorescein-labelled (FAM) primer 88 bases downstream of the predicted XplB promoter site was designed to perform the primer extension analysis. One product of around 77 bases was obtained, mapping the predicted transcription start site after the ATG start codon of xplB **(**Figure 33**).**

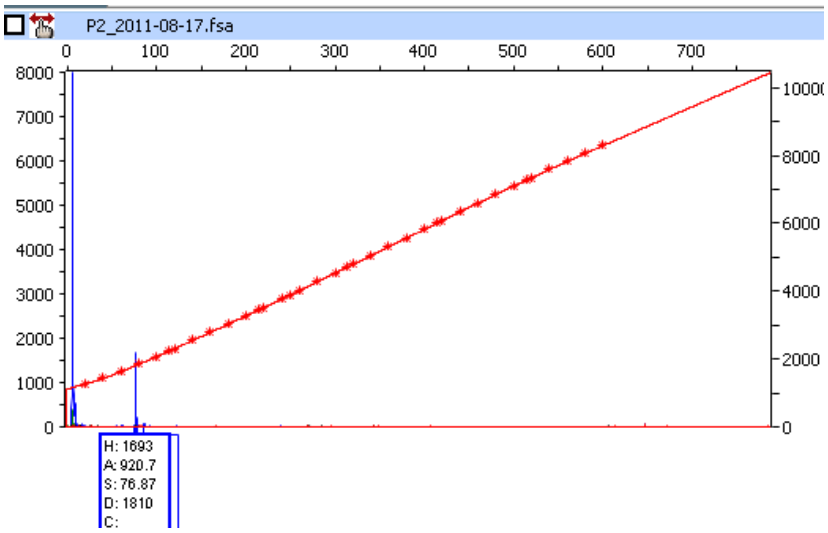

-10

- AAGAAC**TGTAACAA**TAGAGTATTTGG**ATG**GACAT**C**ATGAGTGAAGTGGACGTGGCA
- CCGCGCGTGGCGGTGGTCGGCGCGGGACCGTCGGGTTGTTTCACCGCACAGCAACTCC

Figure 33: Primer extension analysis for transcription start site upstream of xplB.

(A) Fragment analysis using the Peak Scanner Software. (B) Putative promoter site upstream of xplB. Bold: start codon *xplB*, blue text: location of primer 88, red letter c: predicted start site

To verify the results above described Rapid Amplification of cDNA Ends (RACE) PCR was performed. The RACE PCR technology enables the identification of 5' ends of mRNA (cDNA) molecules representing the transcription start sites. Sequence analysis of the PCR product obtained when the promoter upstream of the permease was targeted, mapped the transcription start site to the promoter site as predicted by the software Softberry-BPROM and obtained by primer extension analysis (Figure 34). No product was obtained when the predicted promoter sequence upstream of xplB was targeted.

Figure 34: Promoter region upstream of the permease verified by primer extension and RACE PCR

The xplA operon characterization

Genes involved in one metabolic pathway are often clustered, and therefore genes adjacent to *xplA* may be involved in the metabolism of xplA. Moreover, the fact that the genes adjacent to *xplA* are on a same putative transposable element in *Microbacterium* suggested a potential role for RDX uptake. The first gene of the *xplA* cluster encodes a permease (ORF 29, Figure 35), a

class of protein involved in membrane transport. Similarly, a putative regulatory protein (ORF 27) upstream of the permease may be involved in regulating *xplA* expression. In order to investigate the roles of both genes in RDX metabolism expression studies were performed and overexpressing and knock out strains engineered.

An ORF was identified by primer walking, upstream of the *xplA* operon with a Helix-Turn-Helix protein domain. Best blast matches in databanks were with *Microbacterium* MA1 (100 % with the exception of the start codon), *Gordonia bronchialis* DSM 43247 (61 % in AA) and a *marR* family transcriptional regulator of *R. erythropolis* (50 %). PFAM research indicated that this ORF belonged to the MarR family. MarR could have a role in regulating expression of *xplA* and was therefore cloned and expressed for the use in gel shift assays. Moreover, knock out strains of this putative regulator were constructed. In order to confirm the function of XplA and B in the metabolism of RDX knock out strains lacking *xplA* and *xplB* were engineered.

Figure 35 gives a schematic representation of the gene cluster and DNA regions deleted in the knock-out strains.

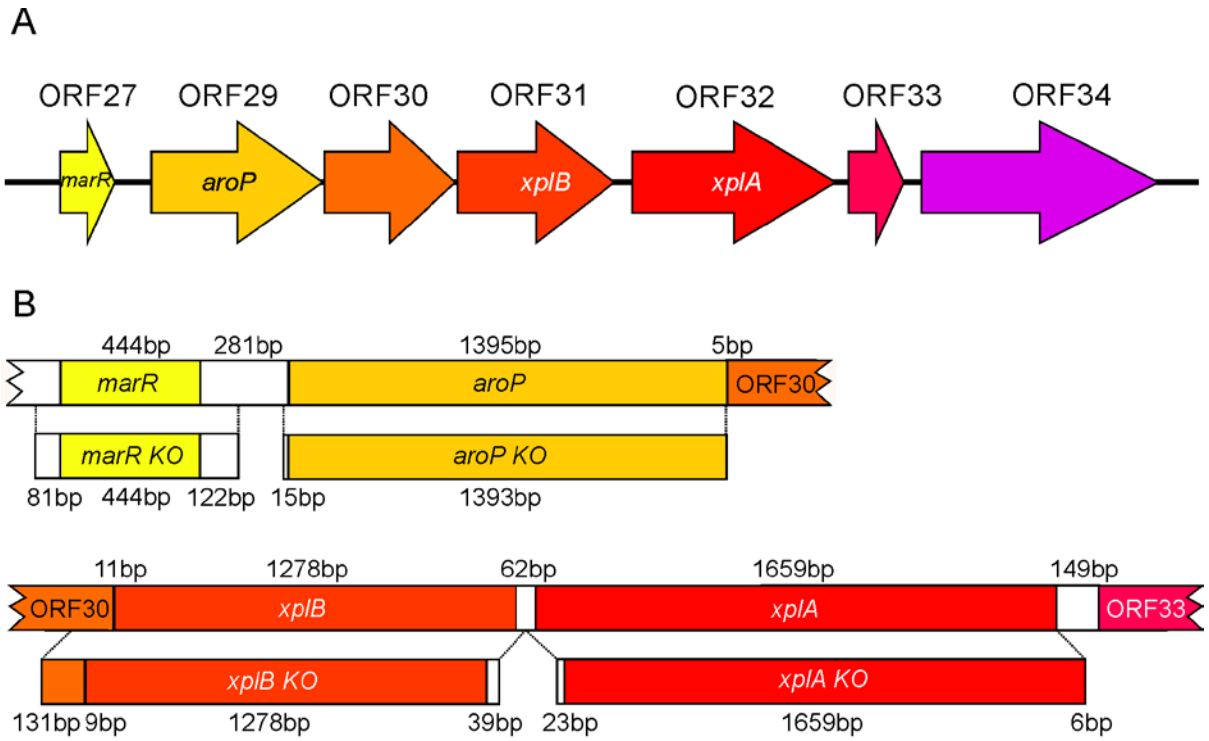

Figure 35. Organization of the RDX degradation gene cluster in *R. rhodochrous* 11Y.

(A) Scaled diagram of the putative *xplA*/*xplB*-containing operon. ORF27, putative transcriptional regulator with homology to regulatory protein MarR; ORF29, *aroP*, putative transporter with homology to amino acid permease from *Mycobacterium vanbaalenii* PYR-1; ORF30, putative dihydrodipicolinate reductase; ORF31, *xplB*, encodes a flavodoxin reductase partner for *xplA*; ORF32, *xplA*, encodes novel cytochrome P450 (CYP177A1, XplA) with flavodoxin domain; ORF33, Aldehyde dehydrogenase C-terminus domain protein ; ORF34, AMP-binding protein (propionyl /acetyl-coA ligase). (B) Scaled diagram showing DNA regions deleted in *xplA*, *xplB*, *marR* and *aroP* knock-out (KO) strains. Non-coding regions are represented by white boxes.

Studies evaluating permease expression

The messenger RNAs from cells of 11Y grown in media with or without RDX were extracted. Real time PCR analyses with primers designed to amplify *xplA*, permease and *gyrB* and *atpD* genes as internal control showed that the *xplA* and the permease genes are expressed to basal levels in the absence of RDX, but 16 and 27 fold more, respectively, in its presence (Figure 36).

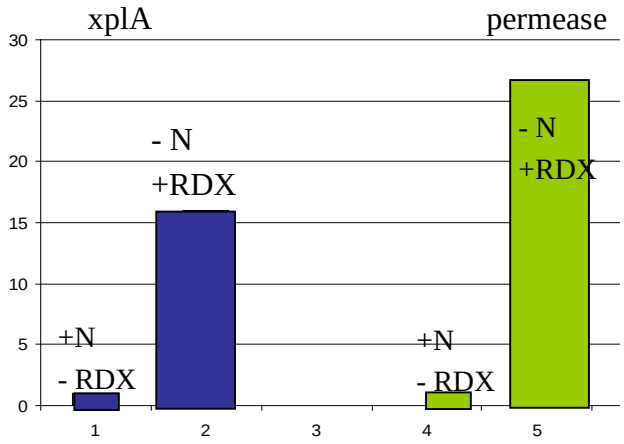

Figure 36: Level of expression of the xplA and permease genes

Overexpression studies of the permease

The permease gene was cloned in the expression vector pETYSBLic 3C and expressed in *E. coli* rosetta 2. After induction, the membrane protein fraction was tested by Western Blot analysis (targeting the HIS-tag of the cloned permease) for the presence of permease. A ~40 kDa immunoreactive protein was present in the membrane fraction of all of the tested clones. The molecular weight was slightly smaller than the predicted molecular weight (49 kDa), however, it is a common phenomenon that membrane proteins migrate faster in SDS-PAGE gels (data not shown). These results indicated that the 11Y permease was expressed and targeted to the *E. coli* membrane.

An artificial operon with the permease and *xplA* cloned together was constructed in the same vector and transformed into *E. coli*. RDX degradation tests indicated that the rates were lower in strains expressing the two genes in comparison to those expressing only *xplA* (Figure 37).

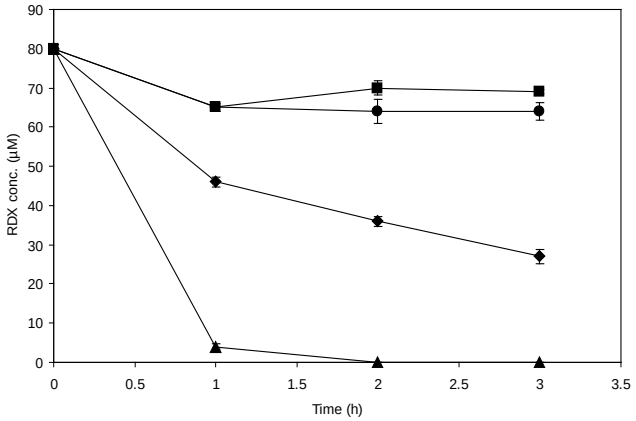

Figure 37: Resting cell incubations (HPLC).

XplA expressing clone (triangles), XplA co-expressed with permease clone (diamonds), permease expressing clone (squares) and Rosetta 2 with empty vector (circles). Error bars show one standard deviation for triplicate samples**.**

The permease knock out strain

The permease gene was deleted in *R. rhodochrous* strain 11Y using the plasmid pK18mobsacB containing sucrose sensitive and kanamycin resistance markers, and a homologous area flanking up- and downstream regions of the target gene. Following conjugation and plasmid transfer into *R. rhodochrous* strain 11Y a crossover adjacent to the homologous region occurred leading to the transfer of the sucrose sensitive marker gene. Successful recombinants are unable to grow on sucrose and can be sustained by replicate plating on agar containing kanamycin. Permease knockout mutants were identified by PCR amplification using primers specific to a region upstream and downstream of the permease gene. The permease knock out was further characterized in growth experiments and resting cell assays.

Growth experiments revealed that RDX degradation and growth rates for the knockout and wild-type strains were nearly identical. Additionally, resting cell assays showed no difference in the RDX removal rates between the permease knockout and wild-type strains (Figure 38).

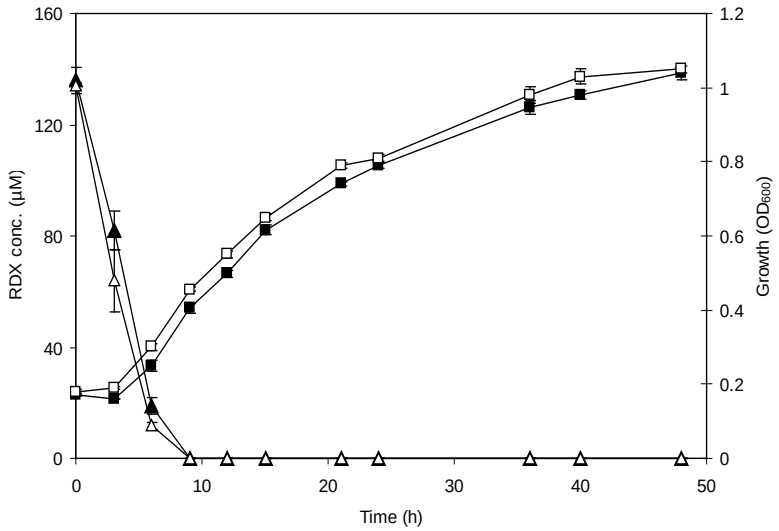

Figure 38: Growth of the permease knock out strain and WT on RDX as a sole nitrogen source.

RDX concentration for WT (closed triangles) and permease knockout strain (open triangles). OD_{600} for WT (closed squares) and permease knockout strain (open squares). Error bars show one standard deviation for triplicate samples**.**

To investigate whether the putative permease knock out strain has higher affinity towards RDX when RDX is present at low concentrations, the knockout and wild-type strains were incubated in MM containing 40 µM RDX and grown for 8 hours.

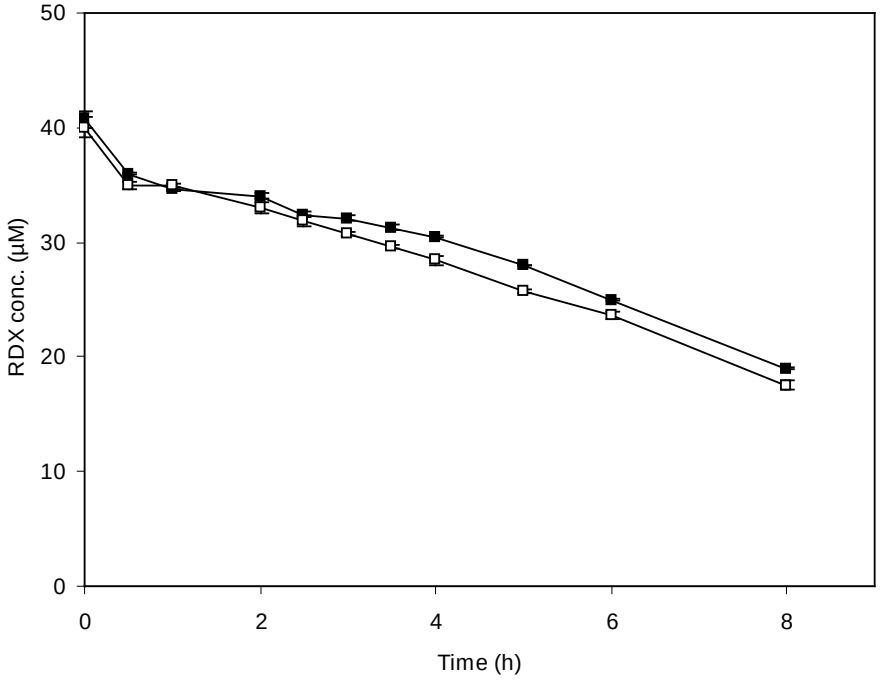

Figure 39: RDX removal by the permease knock out and wild type strains at lower RDX concentration**.** RDX concentration for WT (closed squares) and *permease* knockout strain (open squares). Error bars show one standard deviation for duplicate samples.

There was no significant differences in RDX degradation in either of the strains (Figure 39Crude extract assays

A putative regulator MarR was identified upstream of the transcription start site of the *xplA* operon and may be involved in controling *xplA* expression. To characterize potential DNA MarR interactions gel shift assays with crude cell extract and purified MarR were performed.

A PCR product of 715 bp, located upstream the operon was used in EMSA binding experiments with *R. rhodochrous* strain 11Y crude protein extracts. Protein mixtures were obtained from cells grown in rich medium (LB) or in minimum medium with RDX as sole source of nitrogen. DNA probes incubated with proteins extracted from cells grown in LB showed a band shift in comparison with the control DNA without protein (Figure 40). No band shift was observed for DNA probes in the presence of protein extracted from cells grown in RDX medium. These preliminary results suggested that proteins might bind to the regulatory regions of the operon in the absence of RDX. In the presence of RDX, these proteins might bind RDX, which prevents DNA binding. Altogether these results suggest that the expression of the *xplA* operon might be repressed under “normal” conditions. In presence of RDX, this repression might be removed and enable expression of *xplA*.

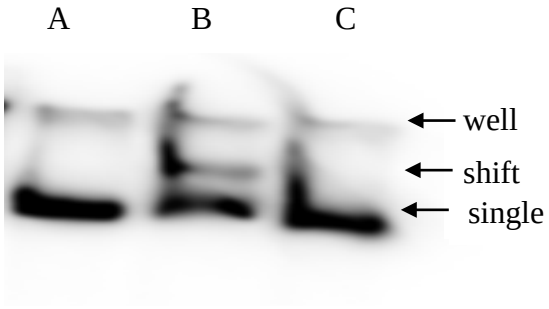

Figure 40: EMSA with 11Y crude extract.

EMSA was performed with (A) no protein, (B) protein crude extract from cells grown in rich medium, (C) protein crude extract with cells grew in RDX minimum medium.

Gel shift assays using purified protein

The MarR putative regulator was cloned and expressed for gel shift assays. Sequence analysis did not reveal any classical "ATG" start codon in frame. However, an alternative GTC start codon in frame was identified. Lic-primers were designed to amplify the full length gene (534 nt). The gene was cloned and the protein expressed with the expression vector pETYSBLic 3C in *E. coli* Rosetta 2 for optimal expression of potentially rare codons. The crude extract fractions were analyzed on SDS-page gels and showed over-expression of the 19.5 KDa cloned protein in comparison to non-induced controls (Figure 41A). The His-tagged over expressed protein was then purified with nickel affinity resin. The purifications steps were optimized to increase protein purity. Routinely, a first wash with addition of 50 mM imidazole in the buffer

was used to elute the non-specifically bound proteins. The His-tagged protein was then released with 250 mM imidazole (Figure 41B). A probe of 327 bp between the *xplA* operon start codon and the potential MarR regulator was used for EMSA experiments. No shift was observed in EMSA experiment conducted with this probe and the purified MarR regulator (Figure 41C). This suggests that experiment conditions are not optimal and further optimizations could be tried in the future. It may also suggest that the expressed protein is actually not involved in *xplA* operon regulation.

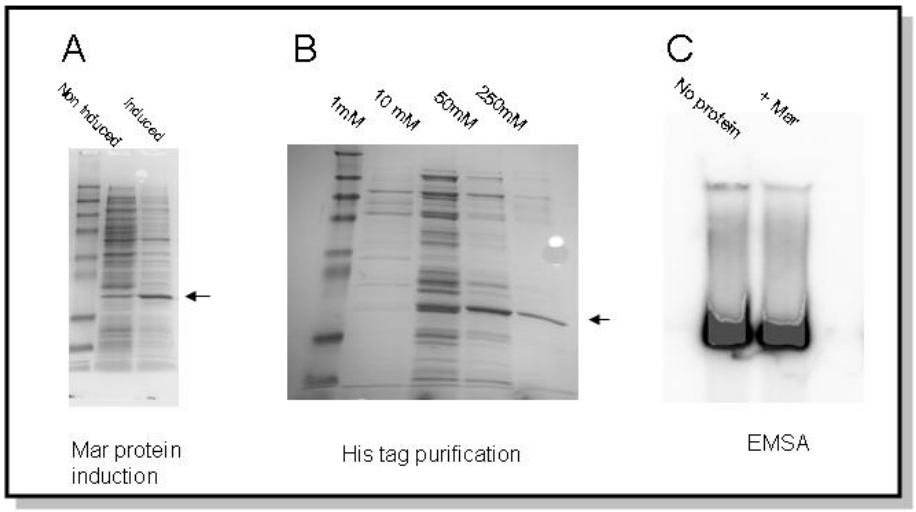

Figure 41: EMSA using purified protein.

A. Induction of the MarR protein in *E. coli*. First and second lanes show protein band pattern without and with IPTG induction. B. SDS page gel of the successive imidazole washings for the HIS-tag purification of the overexpressed MarR protein. C. EMSA result performed with the purified MarR protein. The first lane is the control without protein and the second the binding reaction. The arrow symbol indicates the position of the expressed MarR protein.

Characterization of the MarR knock out strain

A comparison of RDX degradation and growth of the wild-type and regulator knockout strains in the presence of alternative nitrogen sources

Studies have shown that RDX degradation by whole cells was delayed in the presence of alternative nitrogen sources (Nejidat et al., 2008, Jung et al., 2011). To investigate whether the RDX degradation in the wild-type and regulator knockout strains is also affected by the presence of alternative nitrogen sources, growth experiments were performed with different nitrogen sources.

Cells were grown in MM contained RDX only or RDX with additional nitrogen sources (nitrite/nitrate) and RDX degradation was monitored over the incubation time. For the wild-type strain, RDX was degraded at the fastest rate when no alternative nitrogen source was supplemented in the medium, with 91 % of RDX removal after 12 h of incubation (Figure 42). The presence of alternative nitrogen sources delayed the RDX degradation in wild-type. In the presence of KNO_3 or $NaNO_2$, approximately 59 % and 49 % of the RDX was degraded, respectively, within 12 hours after inoculation.

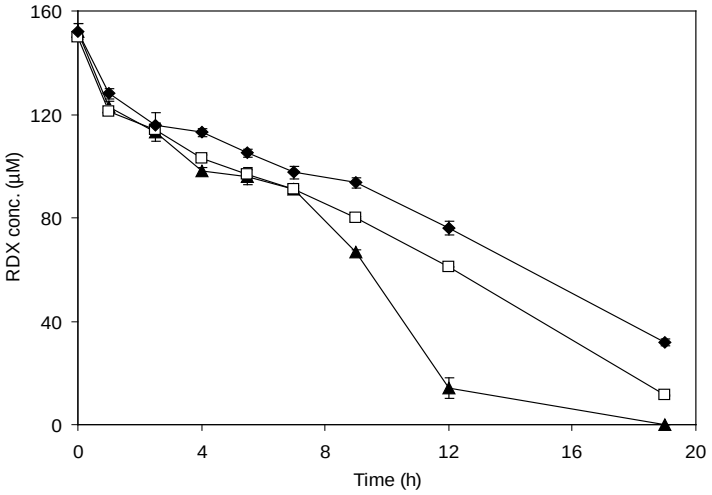

Figure 42: Effect of nitrogen on RDX degradtion in strain 11Y wild type.
RDX alone (closed triangles), supplemented with 5 mM of KNO3 (open squares) and NaNO2 (closed diamonds). Error bars show one standard deviation for duplicate samples.

The growth of wild-type cells was monitored by measuring the optical density (OD) at 600 nm. While cells in medium containing RDX-only and RDX supplemented with nitrite grew at a similar rate, cells in medium containing RDX supplemented with nitrate grew faster (Figure 43).

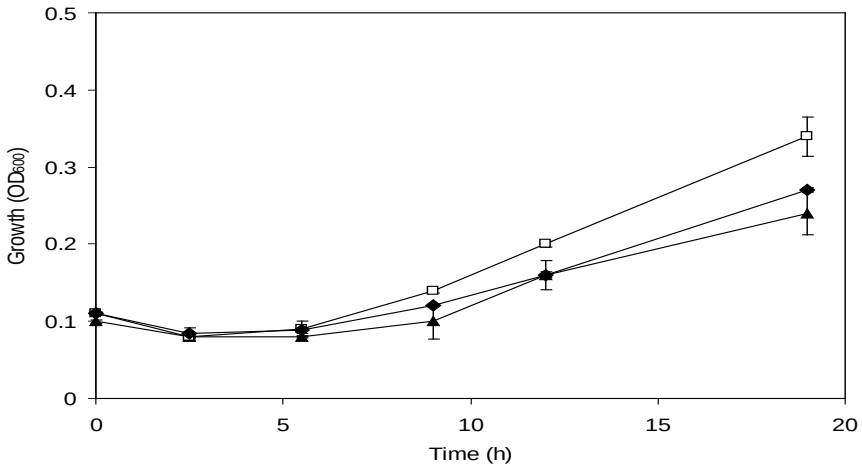

Figure 43: Growth profile of strain 11Y wild-type.
RDX alone (closed triangles), supplemented with 5 mM of KNO3 (open squares) and NaNO2 (closed diamonds). Error bars show one standard deviation for duplicate samples.

The effect of nitrite and nitrate on RDX degradation by the regulator knockout strain was found to be similar to wild-type (Figure 44).

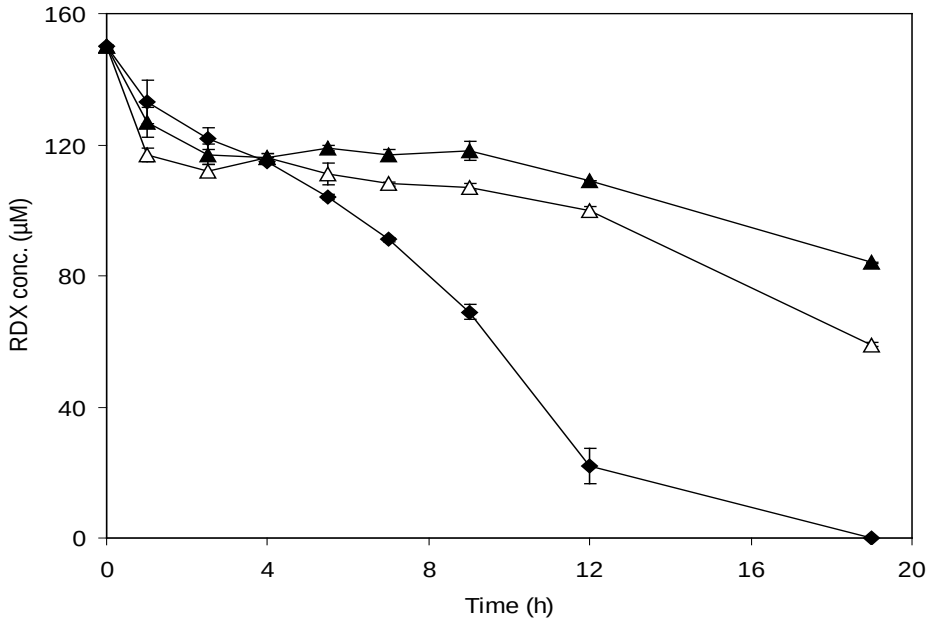

Figure 44: Effect of nitrogen on RDX degradation by growing cells of the regulator knock out strain. RDX-alone (closed diamonds), supplemented with 5 mM of KNO3 (open triangles) and NaNO2 (closed triangles). Error bars show one standard deviation for duplicate samples.

While the regulator knockout in medium containing RDX-only and RDX supplemented with nitrite grew at similar rates, cells in medium containing RDX supplemented with nitrate grew slightly faster (Figure 45).

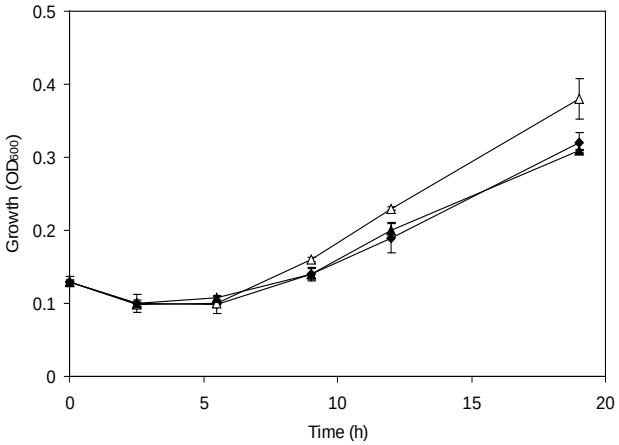

Figure 45: Growth profile of the regulator knock out lines.

RDX alone (closed diamonds), supplemented with 5 mM of KNO3 (open triangles) and NaNO2 (closed triangles). Error bars show one standard deviation for duplicate samples.

When the RDX degradation rates of both wild-type and putative regulator knockout strains, grown in medium containing the same nitrogen sources (RDX-only, RDX + KNO_3 or RDX + $NaNO_2$), were compared, a similar RDX degradation rate was observed to that grown in medium contained RDX-only (Figure 46A). However, in medium containing RDX + KNO_3 and RDX + $NaNO_2$, the RDX degradation rate for the knockout strain was slower than wild-type (Figure 46 B and C)

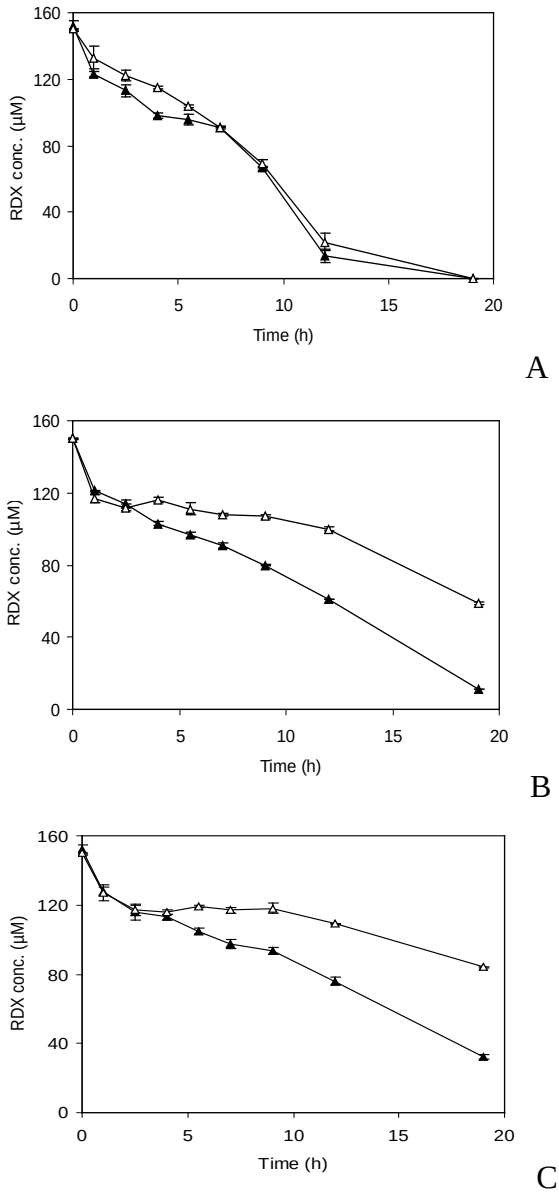

Figure 46: Comparison of RDX degradation between regulator knockout and wild-type strains.

Strains 11Y WT (closed triangles) and regulator knockout (open triangles) were incubated in MM contained different nitrogen source: (A) RDX-alone, (B) RDX and KNO3, (C) RDX and NaNO2. Initial concentration for RDX and other nitrogen sources (KNO3 or NaNO2) was 150 µM and 5 mM, respectively. Error bars show one standard deviation for duplicate samples.

Characterization of the xplA knockout strain

To investigate whether there are any additional RDX degrading gene(s) present in strain 11Y, the *xplA* knockout strain was constructed.

The *xplA* knockout and wild type strains were incubated in MM, with RDX as a sole nitrogen source at a concentration of 150 µM, over 48 h of incubation. Growth of the strains and RDX

removal throughout the incubation time were monitored. HPLC analysis revealed that whilst the wild-type strain 11Y removed all of the RDX in the MM within 8 h, no RDX removal was observed with the knockout strain over 48 h of incubation (Figure 47). The growth of the *xplA* knockout strain reached an OD_{600} of 0.6 after 48 h of incubation which is probably due to the carry-over of nitrogen source from inoculum (LB-grown cells) or the knockout strain utilized nitrogen from dead cells for growth.

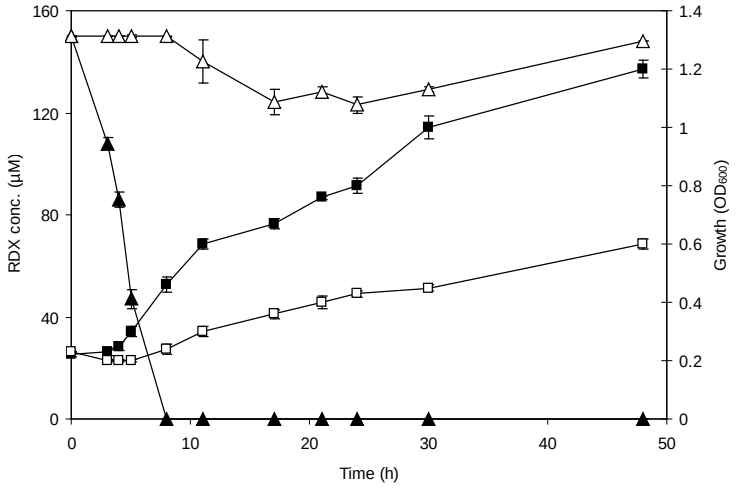

Figure 47: Growth of the xplA knock out strain and wild-type on RDX MM.
RDX concentration for wild-type (closed triangles) and xplA knockout strain (open triangles). OD600 for wild-type (closed squares) and xplA knockout strain (open squares). Error bars show one standard deviation for triplicate samples.

Western blot analysis

To check that XplA was absent in the knockout strain, western blot analysis was carried out; no XplA was detected in the knockout cell free extract (Figure 48) while the positive control (11Y wild-type) showed a band of correct molecular weight (60 kDa).

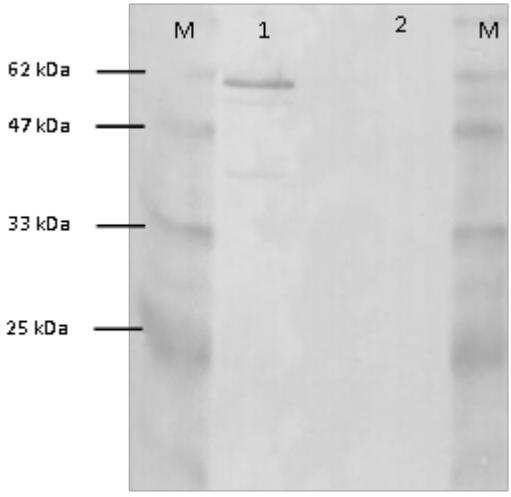

Figure 48: Western blot analysis of cell free extracts of xplA knockout and wild type strains.

(M): Protein marker. (1): WT cell free extracts (0.1 g/mL). (2): *xplA* knockout cell free extracts (0.1 g/mL).

Growth of the xplA knockout strain on RDX dispersion agar

RDX dispersion agar is a MM, agarose-grade agar containing RDX over the solubility limit. The agar has a white, opaque appearance due to insoluble RDX crystals. All of the RDX degrading bacteria isolated so far produce a zone of clearance, where the opacity disappears, around the edge of the colony. The mechanism behind the zone of clearance still remains unknown and to investigate this, the *xplA* knockout strain was grown on RDX dispersion agar supplemented with an additional nitrogen source (NH_4Cl, KNO_3 or $NaNO_2$). The results demonstrated that there was no zone of clearance formed by the *xplA* knockout strain in the RDX dispersion agar supplemented with another nitrogen source (NH_4Cl, KNO_3 or $NaNO_2$) (Figure 49). This shows that the formation of a zone of clearance by the wild-type strain has a direct relationship to XplA activity.

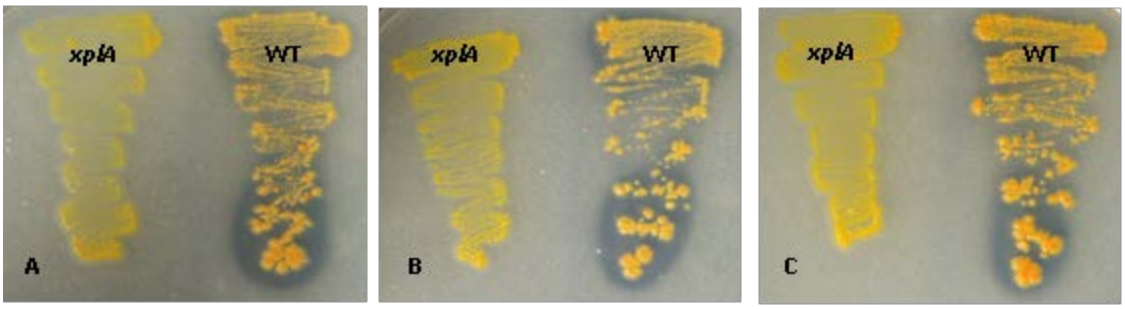

Figure 49: The xplA knockout and wild-type strains on RDX dispersion agar.

Agar was supplemented with 5 mM of RDX and 250 µM of (A) NH4Cl; (B) KNO3 and (C) NaNO2. Strains were allowed to grow at 30 °C for 2 weeks.

Characterization of the xplB knockout strain

To determine whether XplB is the sole reductase partner for XplA, an *xplB* knockout strain was constructed. Sequencing analysis confirmed that *xplB* had been removed and that the coding sequence of the neighboring *xplA* gene was unaltered. To compare the RDX-degrading ability of the *xplB* knockout strain with that of the wild-type, both strains were grown in MM containing 150 µM RDX as the sole nitrogen source. The growth (OD_{600}) and RDX removal were monitored over the 48 h of incubation time (Figure 50). The *xplB* knockout strain removed RDX at a rate of 3.1 µM/h and removed all the RDX within 48 h with the OD_{600} reaching 1.0 after 48 h. The wild-type removed RDX at the faster rate of 18.8 µM/h.

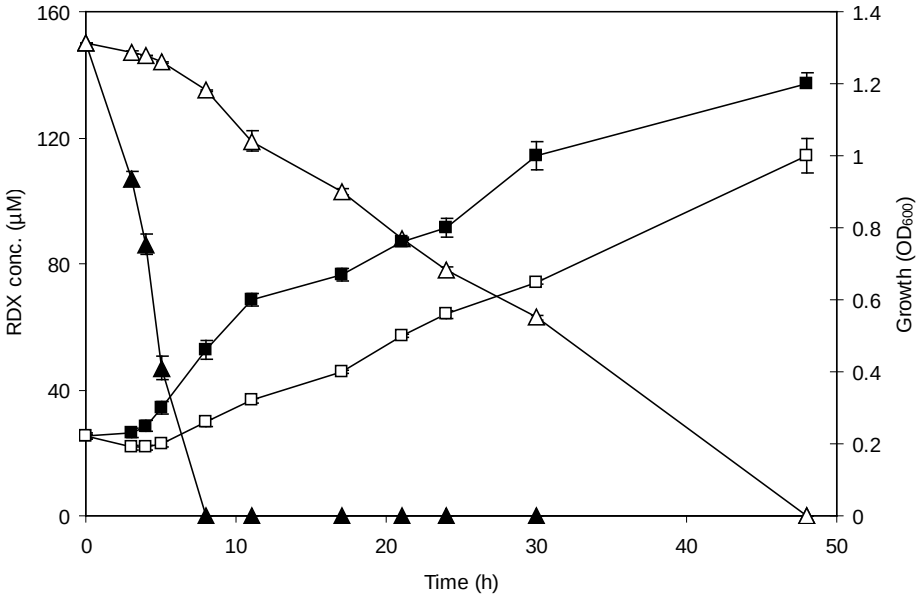

Figure 50: Growth of the xplB knock out and wild-type strains on RDX as a sole nitrogen source.

RDX concentration for wild-type (closed triangles) and xplB knockout strain (open triangles). OD600 for wild-type (closed squares) and xplB knockout strain (open squares). Error bars show one standard deviation for triplicate samples.

Studies under nitrogen-limiting conditions and RDX

Earlier studies suggested that RDX degrading activity in strain 11Y is induced by RDX (Seth-Smith, 2002). To investigate whether expression of XplA in strain 11Y is induced when cells are exposed under nitrogen-limiting/starving conditions or to RDX as sole nitrogen source, cells were grown under a range of nitrogen conditions, then analyzed. Cells were grown overnight in medium containing the nitrogen sources described below (Table 9) to OD_{600} 0.3-0.5, the cells were harvested and grown in fresh medium for a further 3 hour incubation. Cells were harvested, washed twice and used for these subsequent experiments: resting cell assays, western blot analysis, cell free extract activity assays and quantitative real time PCR.

Table 9: Growth conditions for expression studies on *R. rhodochrous* 11Y

Treatment	Overnight Growth Conditions	3h Growth Conditions
(a)	5 mM KNO_3	5 mM KNO_3
(b)	750 µM KNO_2	450 µM KNO_2
(c)	750 µM KNO_3	450 µM KNO_3
(d)	750 µM KNO_3	no nitrogen
(e)	750 µM KNO_3	150 µM RDX
(f)	250 µM RDX	150 µM RDX
(g)	750 µM Glutamine	450 µM NH_4Cl
(h)	5 mM Glutamine	5 mM NH_4Cl

Resting cell incubations were performed in MM supplemented with 100 µM RDX and 100 µM kanamycin at 30 °C, over 60 minutes (Figure 51). Cells treated with (b) 5 mM KNO_3 (closed squares) had the lowest RDX removal rates. Cells treated in (a and c) nitrogen-limiting (open triangles and closed circles) and (d) starving (open diamonds) conditions were able to take up RDX more quickly than cells grown in (b) nitrogen rich medium (5 mM KNO3). Interestingly, the RDX uptake rates were further increased in (e and f) cells grown overnight and/or treated for 3 h in RDX (closed triangles and open squares). The cells with the longest pre-incubation exposure to RDX (f) (closed triangles) demonstrated the highest RDX uptake of all the treatments.

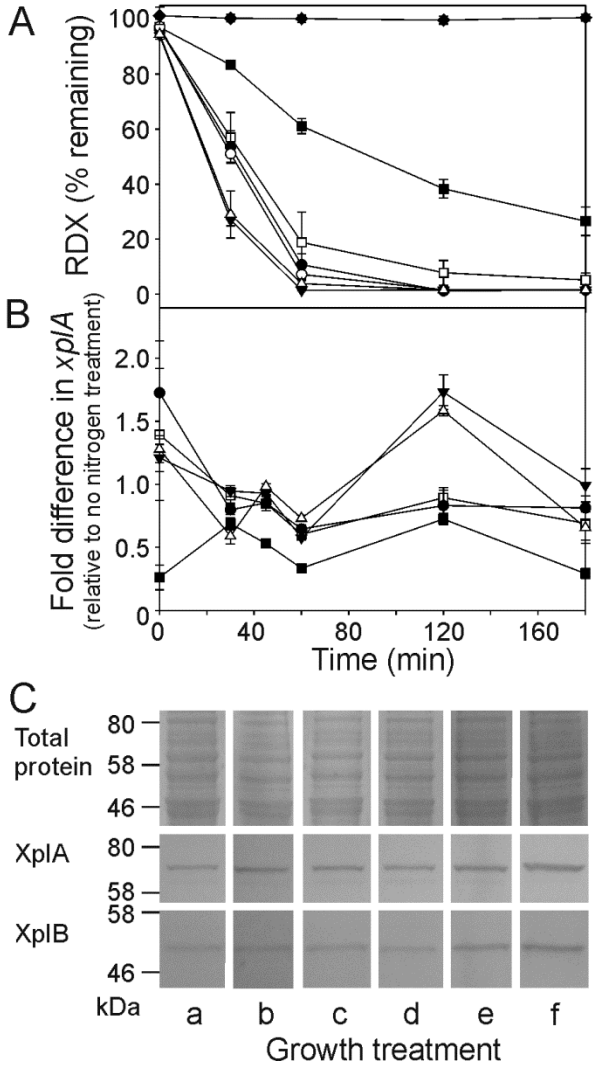

Figure 51: Effect of nitrogen sources on RDX removal and XplA expression in wild type *R. rhodochrous* 11Y

(A) Resting cell assays. Growth conditions were: (●) overnight in 5 mM NH4Cl then 3h in 5 mM NH4Cl (treatment (a));(○)750 µM KNO3 then 5 mM KNO3 (treatment (b)); (▼)750 µM NH4Cl then 450 µM NH4Cl (treatment (c)); (△)750 µM KNO3then 450 µM KNO3 (treatment (d)); (■)750 µM KNO2 then 450 µM KNO2 (treatment (e)) (□) 250 µM RDX then 150 µM RDX(treatment (f)); (◆) No nitrogen control. Results are se of three biological replica. (B)

Expression levels of *xplA* after 2 hour resting cell assay, relative to treatment d. Levels were normalized to *gyrB* expression and results are se of four biological replica. (C) Western blots of protein levels after 2 h.

To investigate the effect of the different nitrogen regimes on gene expression, xplA transcript was measured by qPCR over the treatment time of three hours. As shown in Figure 51B, there was little change in xplA expression in the treatments without RDX.

The transcript levels of *xplA* in cells treated under different nitrogen conditions throughout the 3 hours incubations were monitored (Figure 51B). The *xplA* transcript levels of cells treated with high nitrogen source (5 mM KNO_3) were generally low throughout the incubation time (closed squares). Cells treated with low nitrite/nitrate, no nitrogen or RDX had higher XplA transcript levels than high-nitrogen treated cells. In the cells supplied with RDX (treatments e and f) there was a two- to three-fold increase in transcript after 2 h, relative to cells cultured in medium without nitrogen. No increase in transcription was seen in the low nitrogen-treated and nitrogen-starving cells.

Following transcript expression analysis, protein and activity levels were measured in *R. rhodochrous* 11Y cells after growth in the conditions described in Figure 52 On western blots of crude extracts probed with XplA antibody (Figure 51C), in agreement with the *xplA* expression levels, the strongest signal was seen from cells supplied with RDX as sole nitrogen source (treatments e and f). The XplA levels detected in the remaining treatments (a – d) were approximately similar to each other. To relate protein levels with XplA activity, crude extracts were assayed by following the oxidation of NADPH at 340 nm. The activity of XplA from cells supplied with RDX as the sole nitrogen source (treatment f) was 6.9 ± 0.5 nmol NADPH. $mg^{-1}.min^{-1}$, cells supplied with RDX for 3 h (treatment e) had 1.5 ± 0.7 nmol NADPH. $mg^{-1}.min^{-1}$. No XplA activity was detected in the treatments supplied with alternative nitrogen regimes (treatments a-d). (Figure 52).

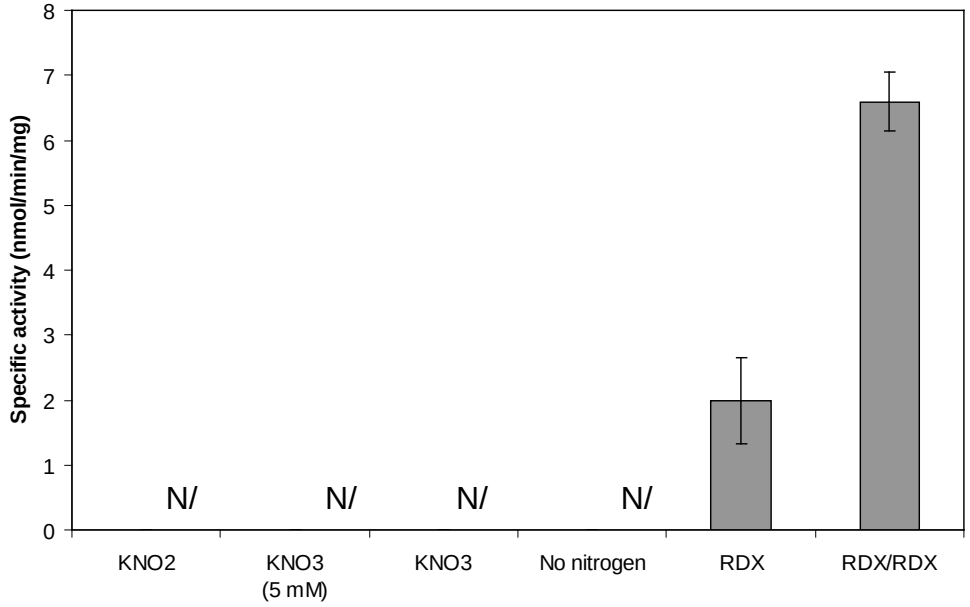

Figure 52: Specific XplA activity in cells treated with different nitrogen sources.
RDX (condition (e) in Table 5.2); RDX/RDX (condition (f) in Table 5.2). Results are mean of three technical replicates of two biological measurements. N/D: Not detected.

Additional resting cell assays were set up to measure *xplA* expression when grown in low (750 µM) or high (5mM) NH_4Cl, a reduced nitrogen source. Furthermore, experiments were performed to confirm that 5 mM of a nitrogen source is reflecting an unlimited nitrogen supply.

Cells were grown in MM but with glutamine (750 µM or 5 mM) as nitrogen source. Cells were grown overnight to an OD_{600} of approximately 0.3, pelleted and resuspended to 0.1g/ml in phosphate buffer (40 mM, pH 7.0). Cells were used to inoculate 250 ml MM containing either 450 µM or 5 mM NH_4Cl and incubated shaking for a further 3h at 30 °C. Resting cell assays were performed a described in section Resting cell assay 2.

Figure 53 shows the RDX removal in NH_4Cl grown cells compared to KNO_3 and RDX grown cells. When cells were grown in low concentrations of NH_4Cl similar removal rates to RDX grown cells were measured. High concentrations of NH_4Cl reduced RDX removal significantly ($p>0.5$) and at a similar rate to 5 mM KNO_3 grown cells.

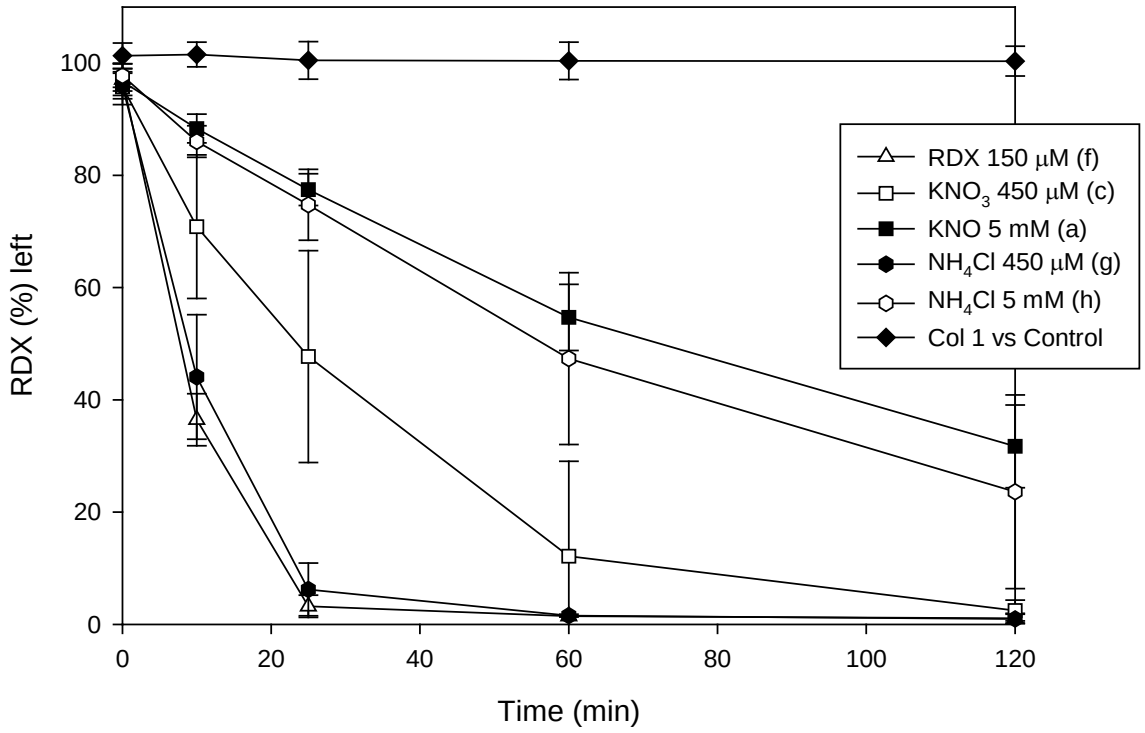

Figure 53: Effect of nitrogen sources on RDX removal and XplA expression in wild type *R. rhodochrous* 11Y (2)
Resting cell assays. Growth conditions were: (▼) overnight in 5 mM KNO_3 then 3h in 5 mM KNO_3 (treatment (a)); (●) 750 µM KNO_3 then 450 µM KNO_3 (treatment (c)); (△) 250 µM RDX then 150 µM RDX (treatment (f)); (◆) No bacteria control; (⬢)750 µM Glutamine then 450 µM NH_4Cl (treatment (g)); (⬢)5 mM Glutamine then 5 mM NH_4Cl (treatment (h)). Results are ± se of three biological replicas.

To test if 5 mM nitrogen source represents a non-limiting nitrogen concentration under the conditions tested experiments were set up using 5 mM or 20 mM KNO_3. As shown in **Error! Reference source not found.** RDX removal in cells grown in 5 mM or 20 mM KNO_3 occurs to a similar rate and therefore growth of cells in 5 mM KNO_3 can be considered as growth in an unlimiting nitrogen source.

Construction of a random mutagenesis library of *R. rhodochrous* 11Y

Generating the mutants

A random mutagenesis library of *R. rhodochrous* 11Y using a Tn5 transposition complex was constructed to obtain additional information about genes involved in RDX metabolism. Electrocompetent cells were transformed with the <KAN-2>Tnp Transposome (Epicentre), allowing the insertion of the Tn5 transposon into the genome. Potential candidates can then be identified using inverse PCR (iPCR) (Figure 54).

Cells were grown on LB agar and on agar with the addition of 1 mM RDX. Colonies with slower growth on agar containing RDX, or cells with severely reduced ability to grow on RDX or unable to form a ‘zone of clearance’- produced by removal of precipitated RDX in agar medium- were selected. These colonies were transferred again onto agar containing RDX and LB, and re-screened eliminating false positives. The Tn5 insertion was confirmed by performing a whole cell PCR on these clones using primers designed to amplify the kanamycin gene.

In total 2870 colonies have been screened for their reduced ability to grow on RDX. A total of 11 mutants were selected for their normal growth on LB medium, but reduced growth on RDX or MM containing NH_4Cl. Resting cell assays were performed to further characterize these mutants. Preliminary data gave encouraging results, as some of the mutants showed a reduced ability to remove RDX however, these results could not be confirmed in the subsequent assays.

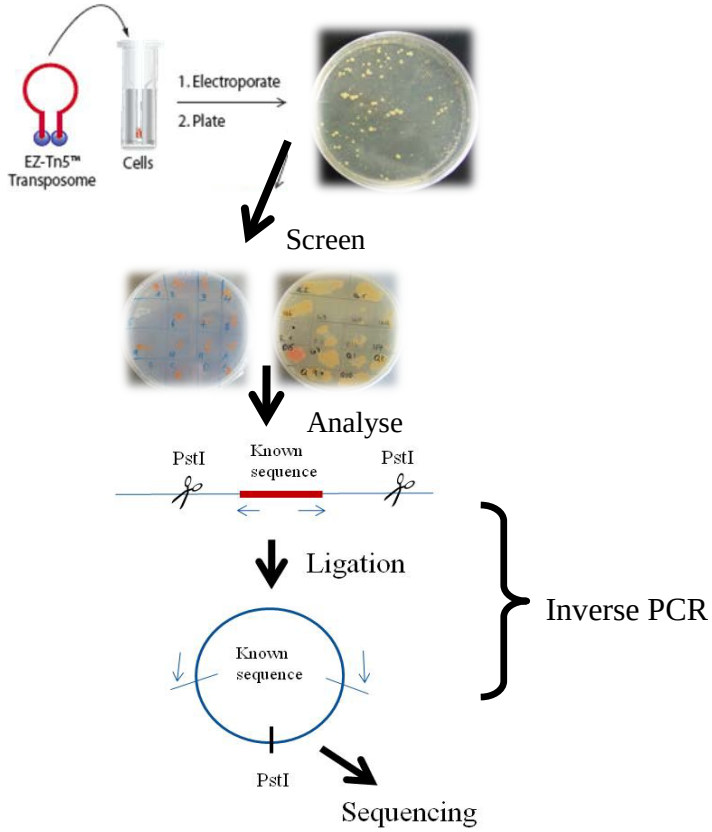

Figure 54: Schematic representation of the Tn5 mutagenisis and characterization of mutants

Characterization of the promoter site upstream of the permease: Dynabead assays

As described previously in this report a promoter site was identified upstream of the permease, and *xplA* expression was found to be induced under nitrogen limiting conditions and can be further enhanced by RDX treatment.

Inducible promoters are controlled by interaction with transcription factors or are dependent on ligands altering the secondary structure of the mRNA to enable translation. To investigate if DNA binding proteins initiating expression, binding assays with crude extracts from *R. rhodochrous* 11Y to an immobilized promoter specific DNA probe homologue to the region of interest will be performed. Any bound proteins specific to the regulatory site can then be identified using MALDI-TOF MS peptide mapping.

A promoter specific double stranded DNA probe was labeled with biotin, immobilized onto Streptavidin coupled magnetic beads and incubated with *R. rhodochrous* 11Y crude extracts as described in Materials and Methods. Binding of protein to the promoter specific sample was determined by SDS PAGE, followed by identification using MALDI-TOF. Probes treated with crude extracts obtained from cells grown with RDX or low amounts of KNO_3 (750 μM) showed a prominent band at 14 kDA; one prominent band around 60 kDa was identified in the RDX treatment and another (about 60 kDa) was seen in the KNO_3 treatment. Peptide mapping determined that the 14 kDa sample relates to Streptavidin, whereas the band in the RDX treatment was identified as Elongation factor Tu [*Mycobacterium leprae*] and in the KNO3 treatment as Keratin & a single peptide match to 60 kDa chaperonin [Rhodococcus sp. A]. None

of the identified proteins could be related to DNA binding proteins suggesting unspecific binding. Additionally, streptavidin with a molecular weight of 60 kDa was degraded during treatment and run therefore at around 14 kDa.

2D-Gel electrophoresis

A 2D-Gel electrophoresis was performed, to explore potential genes involved in RDX metabolism. Therefore, cells of *R. rhodochrous* were grown to an OD_{600} of 0.8 in MM containing either 250 µM RDX or 750 µM NH_4Cl. Cells were lysed by sonication and the soluble protein fraction cleaned up using the ReadyPrep 2D clean up kit (Biorad). Protein samples of both treatments were submitted to the protein production facility of Technology Facility at the University of York to check the quality and suitability of the protein sample prior performing the 2D-Gel electrophoresis.

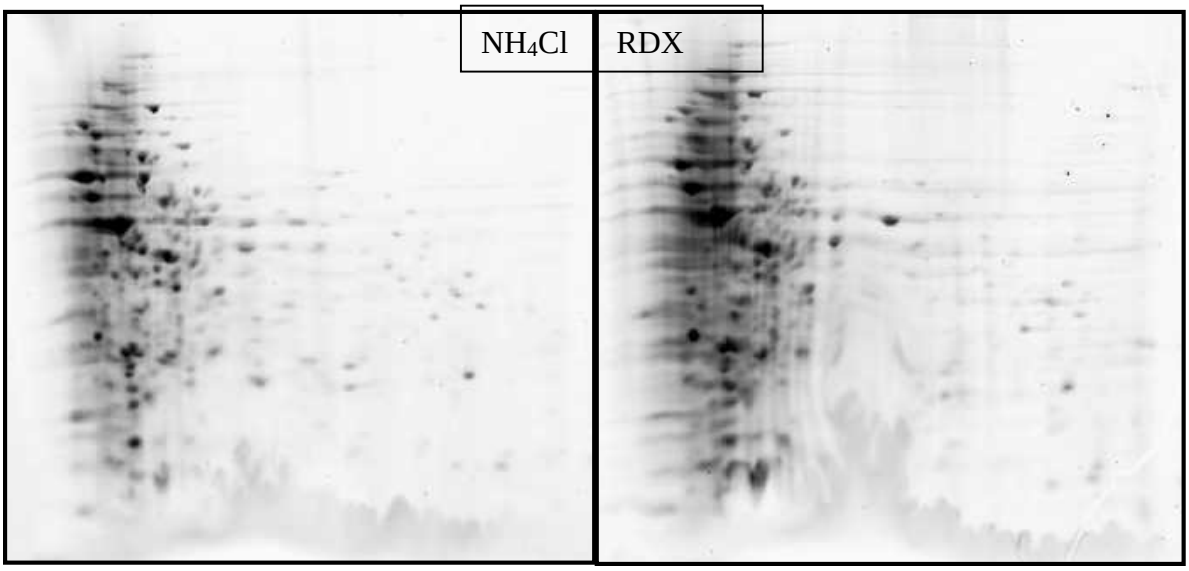

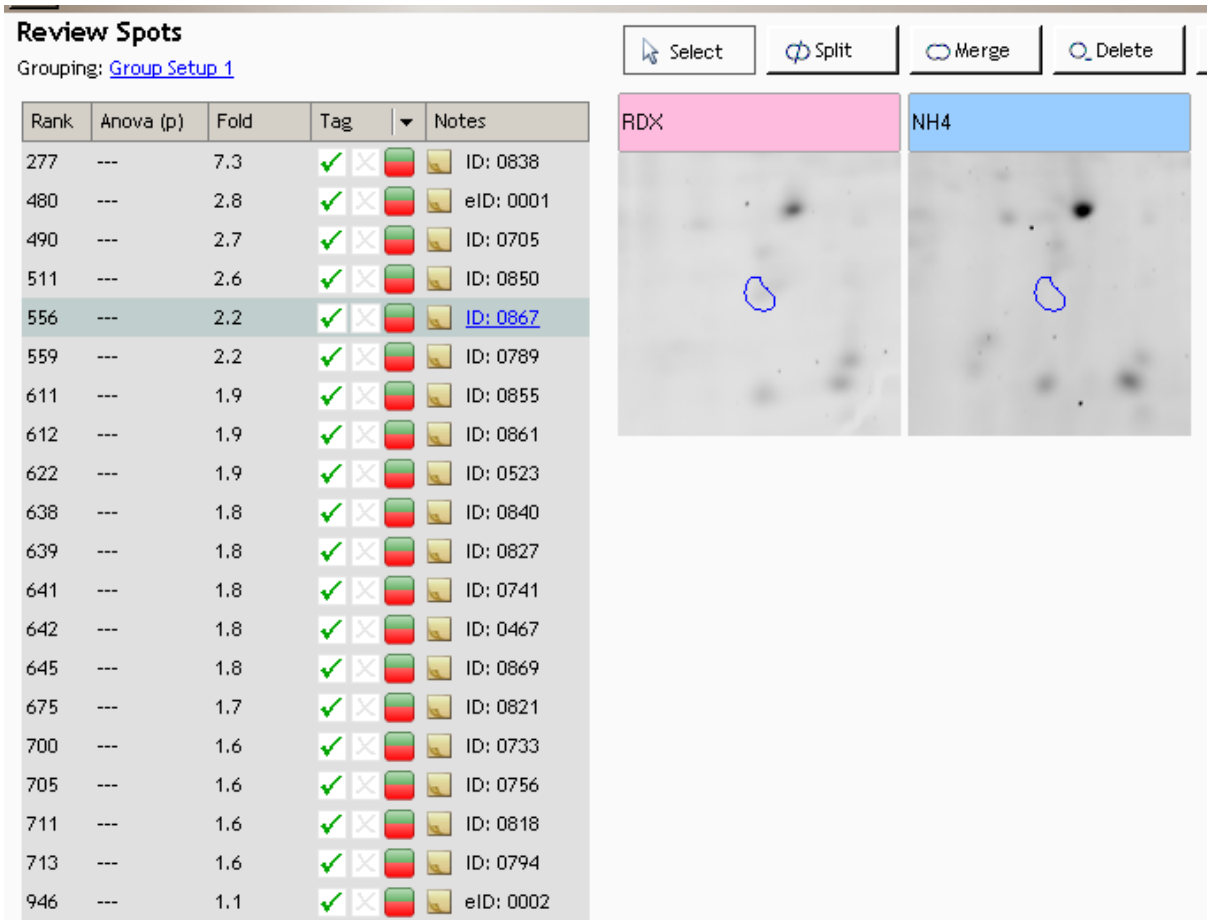

Figure 55: 2-D Gel electrophoresis

Samples of the two different treatments were compared and spots evaluated for their presence in the RDX treatment, but absence in the NH_4Cl treatment. Spots were excised and analyzed using peptide mapping.

Table 10: Peptide matches for spots present in the RDX treatment

Brackets indicate the fold change in the RDX treatment over NH_4Cl. The number following allocates a corresponding “rank” (Figure 55)

(7.3) 227 - No Match
(2.8) 480 - Single peptide matches to diguanylate cyclase and delta-1-pyrroline-5-carboxylate dehydrogenase.
(2.7) 490 - dihydrodipicolinate reductase
(2.6) 511 - 30S ribosomal protein S6
(1.9) 611 - cold shock protein.
(1.9) 612 - Single peptide match with to putative cold shock protein
(1.9) 622 - NDMA-dependent methanol dehydrogenase
(1.8) 641 - peptidyl-prolyl cis-trans isomerase (rotamase) and CarD family transcriptional regulator with a single peptide match to hypothetical protein RHA1_ro03329 [Rhodococcus jostii RHA1].
(1.8) 642 - glutamine synthetase
(1.8) 645 - nicotinate-nucleotide pyrophosphorylase and delta-1-pyrroline-5-carboxylate dehydrogenase
(1.7) 675 - Single peptide match to nitrogen regulatory protein P-II
(1.6) 700 - Two single peptide matches to Superoxide dismutase from different species.
(1.6) 705 - Two single peptide matches to elongation factor Tu.
(1.6) 713 - Single peptide matches to bacterioferritin, unnamed protein (extracellular metal-dependent peptidase [Idiomarina baltica OS145]) and methyl-accepting chemotaxis sensory transducer.

Gels were analyzed for protein spots present in the RDX but absent or of reduced level in the NH4Cl treatment (Table 10). Fifteen spots were found; proteins were extracted and subjected to digestion with trypsin, MS/MS and a Mascot database search. Searching the data against the NCBI database restricted to bacteria (Eubacteria) (7002453 sequences) has produced the matches listed in Table 11.

Table 11: Proteins increased after treatment with RDX as identified in the 2-D Gelelectrophoresis

Diguanylate cyclase	**Second messenger signaling in bacteria.** Their activity is responsible for the condensation of two GTP molecules into the signaling compound cyclic di-GMP.
Delta-1-pyrroline-5-carboxylate dehydrogenase	((S)-1-pyrroline-5-carboxylate + NAD^+ + 2 H_2O > L-glutamate + NADH + H^+ **Nitrogen metabolism**
Dihydrodipicolinate reductase	**Dihydrodipicolinate reductase** is an enzyme found in bacteria and higher plants which is involved in the biosynthesis of diaminopimelic acid, a component of bacterial cell walls, and the essential amino acid L-lysine
NDMA-dependent methanol dehydrogenase	Expressed during degradation of thiocarbamates and atrazine. Catalyzes the oxidation of alcohols (including methanol) with the concomitant reduction of N,N'-dimethyl-4-nitroso-aniline (NDMA), aldehydes or ketones
Peptidyl-prolyl cis-trans isomerase (rotamase)	Protein folding
1-pyrroline-5-carboxylate dehydrogenase	**Nitrogen metabolism**
Nitrogen regulatory protein P-II	PII helps regulate the level of glutamine synthetase in response to nitrogen source availability. **Nitrogen metabolism**
Superoxide dismutase	Superoxide dismutases a class of enzymes that catalyze the dismutation of superoxide into oxygen and hydrogen peroxide.
Elongation factor Tu.	Translation
Bacterioferritin	Iron storage proteins
Methyl-accepting chemotaxis sensory transducer.	Bacterial receptor that mediate chemotaxis to diverse signals, responding to changes in the concentration of attractants and repellents in the environment by altering swimming behaviour

Fifteen spots were found with the following matches when screened against the database: 30S ribosomal protein S6, dihydrodipicolinate reductase, cold shock protein, putative cold shock protein, NDMA-dependent methanol dehydrogenase, glutamine synthetase, nitrogen regulatory protein P-II, superoxide dismutase and bacterioferritin, single peptide matches to diguanylate cyclase and delta-1-pyrroline-5-carboxylate dehydrogenase. peptidyl-prolyl cis-trans isomerase (rotamase), transcriptional regulator, hypothetical protein, nicotinate-nucleotide pyrophosphorylase, delta-1-pyrroline-5-carboxylate dehydrogenase, and elongation factor Tu. Interestingly, XplA or XplB were not identified, these proteins might be within the pool of peptide sequences that could not be matched due to low abundance. To confirm the significance of these data the experiment would have to be repeated; however, none of the identified proteins seems to have and specific involvement in RDX metabolism and therefore no further experiments were performed.

Task 6. Discover new bacteria capable of degrading RDX and determine the enzymes involved (combined with Task 3)

In order to isolate RDX degraders from complex bacterial soil communities, we set up enrichment cultures of the different sampling areas:

1. UK: Otterburn and Longtown
2. Belgium: two enrichment sites
3. Training range Senne

UK: Otterburn and Longtown

Twenty two different spots from the Otterburn site were used to perform selective enrichments with RDX and HMX as sole nitrogen sources. Although only a few of the cultures exhibited growth, all cultures were subcultured after eight days. The 22 initial cultures were monitored for growth over a further 20 days; however, no further increase in biomass, despite growth in those cultures originally observed, was seen. None of the subcultures gave significant growth in comparison to the controls after more than eight days of culturing and no colonies were observed after inoculation on selective plates. Likewise, the five samples from the containment building from Farnborough did not grow during the selective enrichment.

For the Longtown site, triplicate of six soil samples were used in selective enrichment with RDX. Only one out of the six samples gave significant growth in comparison to the controls (Figure 56).

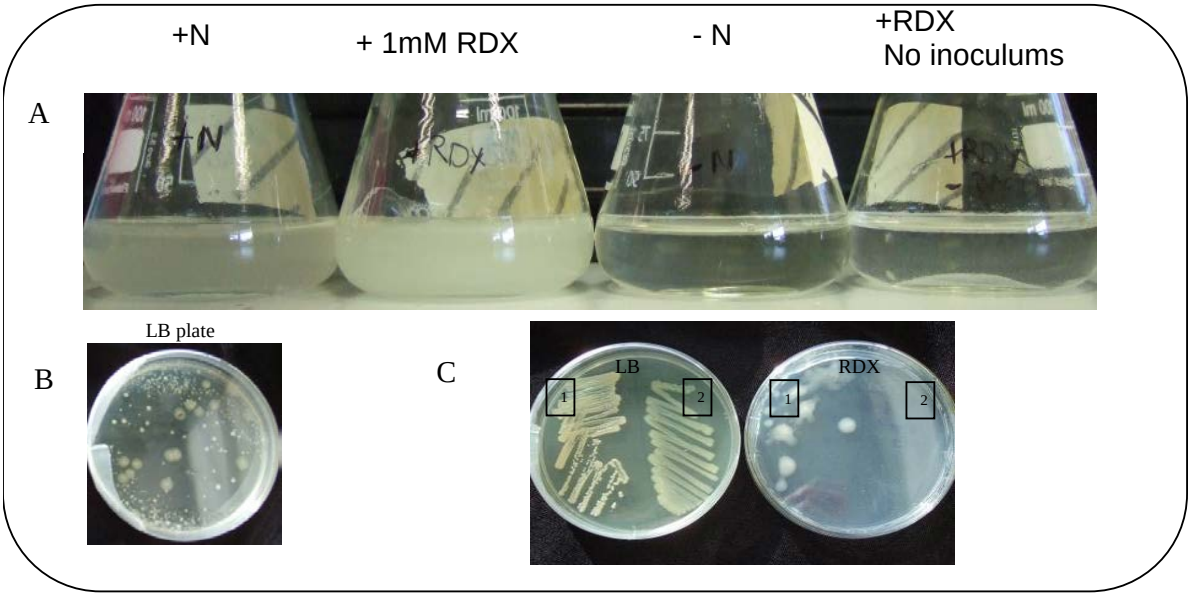

Figure 56: Bacterial growth in selective enrichment cultures and on agar

A. Example of positive growth in minimal media containing RDX during selective enrichment experiments. B. Example of selection step on LB rich medium after spreading of a mixed culture. C. Example of a purification step of two different phenotypes (1 and 2) after step B on LB and RDX plate

After three subcultures, serial dilutions were spread on RDX selective medium and single colonies were purified several times. However, after several days and despite the purification steps, some of the colony streaks exhibited two different colony phenotypes. These mixed cultures were then suspended in a small volume of LB and spread on LB agar to separate the different phenotypes (Figure 56 B). The different colony phenotypes were purified on LB plates and then on MM agar containing RDX. This further round of purification resulted in only one colony type was still able to grow on RDX (Figure 56 C). Thirteen representative pure isolates able to grow on RDX were selected. Their taxonomic position was assessed by 16S rDNA analyses. Phylogenetic trees (**Figure 57**) revealed that all the isolates were identical and belonged to the genus *Rhodococcus*. From a taxonomical point of view, they are different from the *Rhodococcus sp*. type strain 11Y, but more closely related to previously characterized RDX degrading strains isolated by the UoY group (HS strains) and to the non-RDX degrading *R. erythreus* and *R. baikonurensis* species. The presence of the *xplA* gene was found in all the isolates by PCR amplification and sequence comparison revealed no variation with previously known *xplA* sequences.

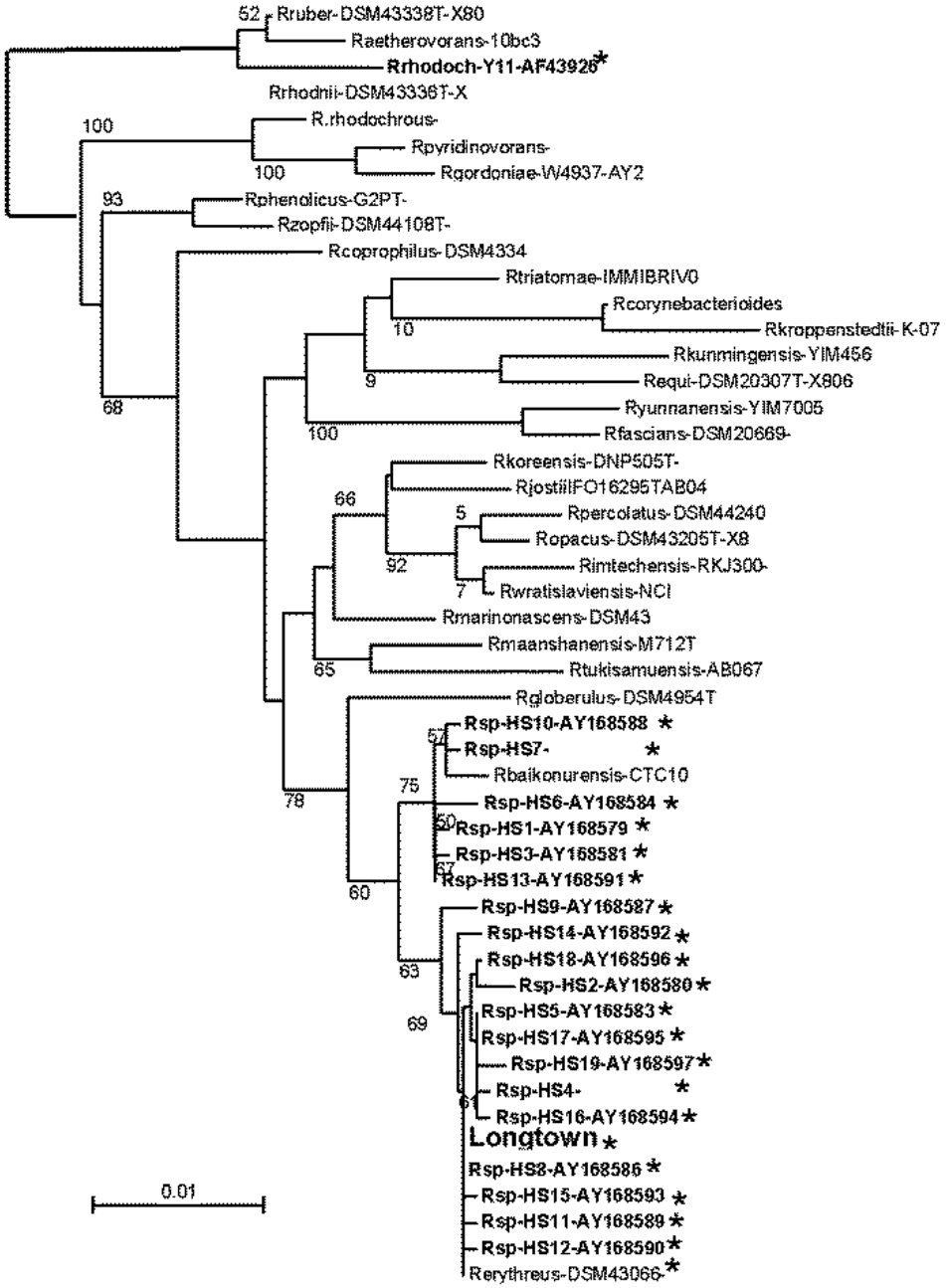

Figure 57: 16S rDNA phylogenetic tree of the *Rhodococcus* genus (Error! Reference source not found.**).**

* indicates the RDX degrading strains. The position of the longtown isolates is shown by a reference sequence named Longtown.

RDX biodegradation of new isolates

The ability of the 13 strains isolated from the Longtownsite to degrade RDX was tested in a biodegradation assay as described in Resting cell assay 1 and compared to those of the

Rhodococcus sp. type strain 11Y (Figure 58). The 13 Longtown isolates showed a good rates of biodegradation (20-40 % in 1h), but these were lower in comparison to 11Y (50 % in 1h).

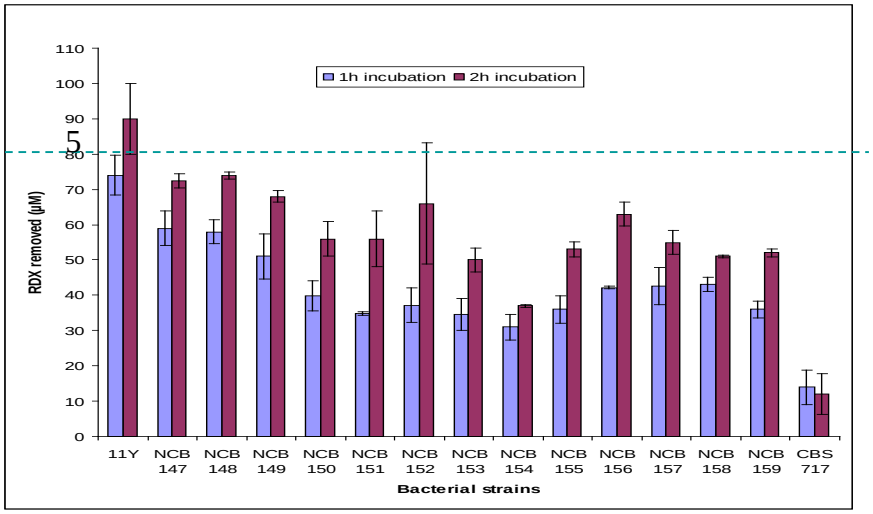

Figure 58: Biodegradation of 13 Longtown strains in comparison to 11Y.

CBC717 is a strain that cannot degrade RDX. The initial concentration of RDX was 160 µM in the medium.

Selective enrichment studies from soils obtained from a, UK MoD ordnance demolition site at Longtown

RDX contaminated soil samples obtained from Longtown were analyzed again in order to find more isolates able to degrade RDX. Enrichments were performed as described in Material and Methods (Enrichment method 2). One of the isolates was confirmed to be *Rhodococcus aetherivorans.*

Selective enrichment studies from soils obtained from a Belgium demolition site

Enrichments were done as described in Materials and Methods. Enrichment method 2 isolated *Rhodococcus erythropolis* and *Rhodococcus* sp. LB-BS. Enrichment method 4 identified *Microbacterium* sp. C-12. No RDX degrading bacteria were found when using leucine as a carbon source.

Characterisation of the new isolated RDX-degrading bacteria

Overlapping primers were designed based on the *R. rhodochrous* 11Y and on the *Microbacterium* MA1 sequence to amplify up- and downstream regions of the xplA/B genecluster. Primers are listed in and approximate locations are shown in Figure 60.

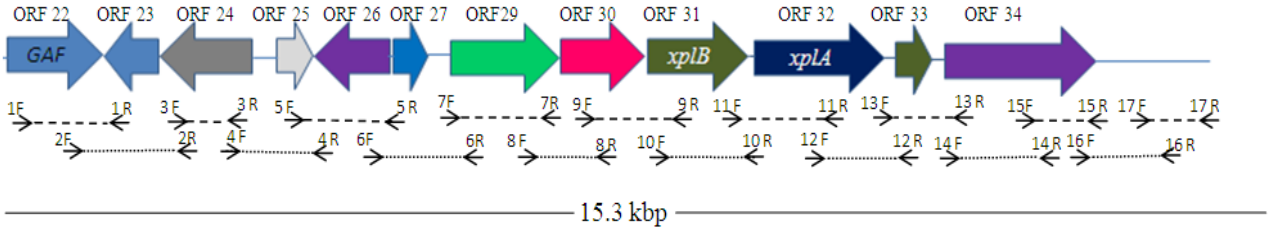

Figure 59: Scheme representing the primer pair locations on the RDX degrading gene cluster in *Rhodococcus rhodochrous* 11Y.

The arrows represent the approximate primers location on the gene cluster. F represents forward primers (5′→3′). R represents reverse primer (3′→ 5′). The lines represent the region which primers are amplifying.

ORF 22:GAF

ORF 23: transcriptional regulatory protein

ORF 24: Putative sensor kinase

ORF 25: Conserved hypothetical protein

ORF 26: Putative carboxylesterase

ORF 27: Putative regulatory protein (MarR)

ORF 29: Permease

ORF 30: Dihydrodipicolinate reductase

ORF 31: XplB

ORF 32: XplA

ORF33: Succinate-semialdehyde dehydrogenase (NADP+)

ORF 34: AMP-binding enzyme

Figure 60: Schematic illustration of the location of the primers used to sequence the xplA/B genecluster

Sequencing analysis revealed that the genomic island harboring xplA and B stretches from ORF 21 to ORF 34. The genomic island is in all analyzed species highly conserved and to 99% identical on nucleotide level. Five single nucleotide polymorphism (SNP) were identified, two in *xplB* and three in *xplA*, located in the heme containing N terminal domain of *xplA*. *Microbacterium* MA1 has additionally ORF28, a transposable element not found in all other isolates tested (Figure 61).

Table 12: Primer sequences to gene walk the xplA/B gene cluster

Primer name	Primer sequence 5'-3'
GAF-F	CGATTCCGTATCCGACCTC
TranscRp-504R	GATGTTCTCCGGTTGATCG
RegulatoryPrt-89F	GGTTCACATGGCTTTTCACC
SensorK-292R	CTATCGCATCGCTCAGGAGT
SensorK-129F	CATTCCGTCTATTCCGGTTC
SensorK-1087R	CGTGGTCGTGACAGTCATCT
Sensork-1035F	GATTCGGTCGAACGGGTA
Carbesterase-167R	AGAGTCGGGCACATGACAC
MarR-194R	GCACTGTTGAGTCCGAGATG
HypoPrt-453F	GGTCTCGCAACACACTGAAC
Carbesterase-6F	ACGTCGGAATTCAGTGTCGGGCGGACC
Permease-6R	GAGTCGAAGAGGGCACTCAG
Permease-7F	CTGTGTGGTGTGGTGATGGT
Permease-7R	CTACTCCCCGGTCTTCTTCGGAAT
Permease-8F	ACTACATCGTGCTGCTGTCC
Dihydro-8R	GTCGAGCATATGCACGTCGGGGATACG
Dihydro-9F	GATGTCAACGAATGGACGAT
xplB-9R	GTCGATCCGAAGTGGAACAC
xplB-10F	CGGTGATGATGCGTGAACT
xplA-10R	TCTCCGTAGGTGGAGGTGAC
xplB-11F	ACCC GACATATGACACCCGAGATGGAG
xplA-11R	TCAGATAGCCGAAAGCGACT
xplA-12F	CACGCGTCCTACAACTACCC
SSD12R	AACAGCTCCTCACGGTAAGC
xplA13F	ATCGTCCTGTCCTGAAAACC
AMP13R	GTTGTGGCAGGTGTTGAGTT
AmMP14F	ATCAGCGATGGGACGATAC
AMP14R	ATGCCCAGGTGAACGTGT
AMP15F	GTGATGTACGAGGGCAAGC

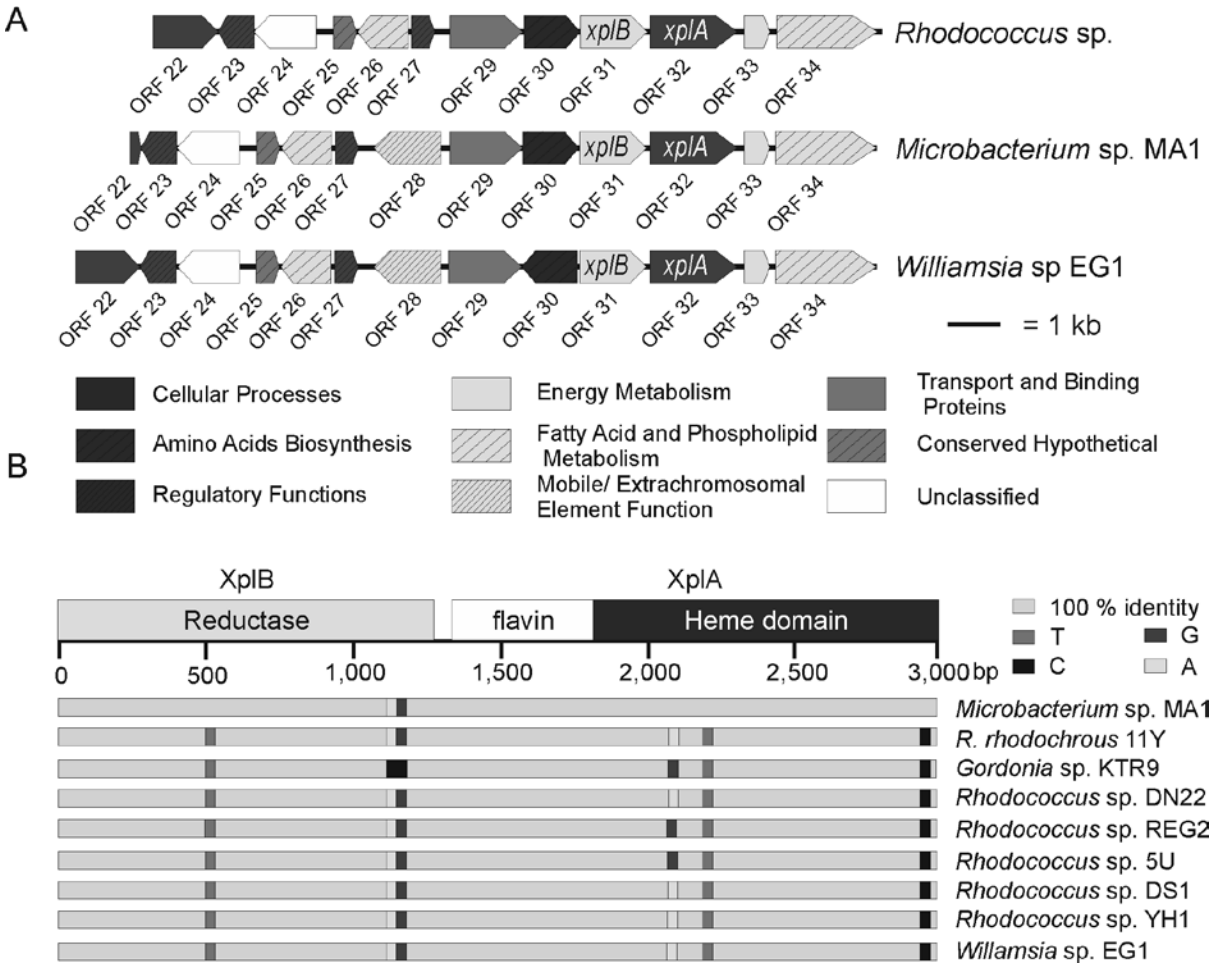

Figure 61: Sequence comparison Belgium, UK and US isolates.

Phylogentic tress constructed for the *xplA*-heme-domain of all isolates showed a closer relation between the Belgium and North America isolates, than UK and Belgium isolates. It was also observed that the SNPs between those isolates are not geographically dependent as *Williamsia* and *Rhodococcus.* sp DN22 isolated in North America and Australia respectively, have shown to be identical with United Kingdom isolates.

Analysis of the Gordonia sp. KTR9 XplB-glutamine synthetase fusion

Sequence analysis revealed that *Gordonia* sp. KTR9 encodes XplA, and an XplB-glutamine synthetase (XplB/GlnA) fusion. In order to understand the functionality of the XplB/GlnA fusion, we cloned and expressed recombinant protein in *E.coli*. Figure 62 shows SDS-PAGE of crude extracts expressing XplB/glnA. When the *xplB/glnA* in pET-28a(+) was assayed for nitrite release from RDX, a high reductase activity was observed. Thus we cloned into pGEX 4T-3, the vector originally used to express XplB, where this background activity was not seen. Preliminary assays on crude extracts of the XplB/GlnA fusion protein showed that RDX, measured using hplc, disappeared from the assay mix. Therefore, we tried to purify the XplB/GlnA fusion for more detailed assays. However, although the XplB/glnA protein was purified (Figure 63), we

were unable to detect any activity. Spectral measurements indicated that the flavin became lost during the purification process.

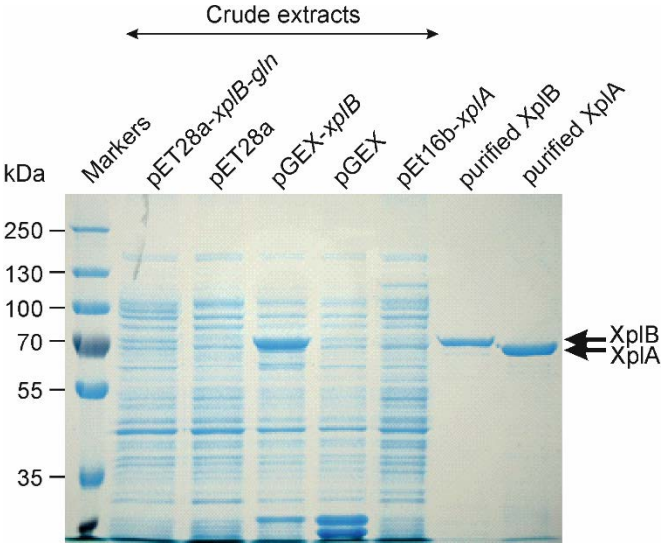

Figure 62: SDS-PAGE analysis showing purification of GST tagged XplB/GS, XplB and XplA.

XplB-Gln and XplB were expressed in *E. coli* BL-21(DE3), XplA was expressed *E. coli* Rossetta 2.

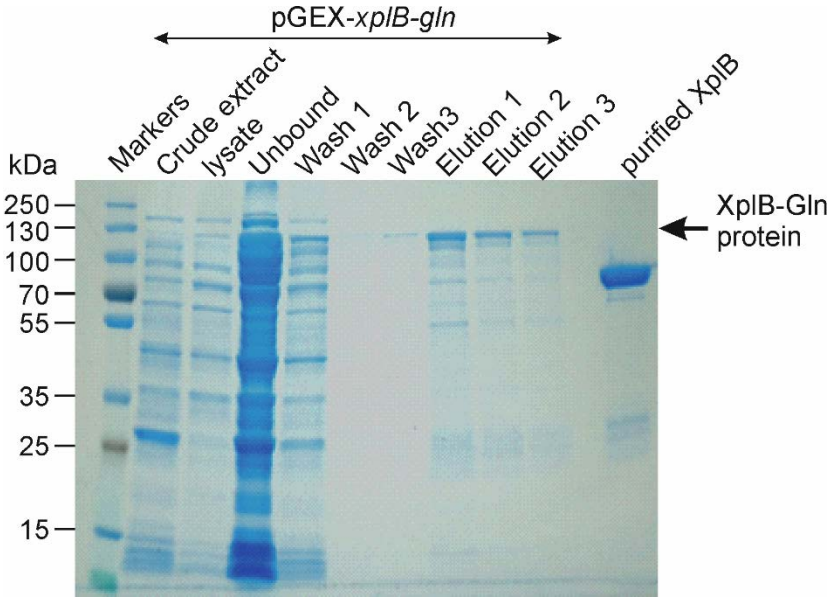

Figure 63. Purification of GST tagged XplB-Gln expressed in *E. coli* BL-21(DE3).

Evolution of XplA

We are investigating a potential XplA homologue in *Gordonia terrae* strain NBRC 100016. While all our RDX-degrading bacteria isolated so far share >99.9% identify across XplA, the putative XplA homologue in *G. terrae* strain NBRC 100016 has only 45 % identity. However, *G. terrae* strain NBRC 100016 is the only bacterium recorded to date that shares the fused

flavodoxin cytochrome P450 arrangement that was previously unique to all xplA-containing bacteria. *Gordonia terrae* strain NBRC 100016 does not grow on minimal agar medium supplemented with RDX as the sole nitrogen source, and following incubation in minimal liquid medium, with RDX as sole nitrogen source, there was no significant removal of RDX over seven days. We have cloned this XplA homologue, and expressed it in *E.coli* Rosetta2 and proteomics and biochemical studies on this unusual protein are now on going.

Spectral analysis on the purified protein showed the characteristic Soret peak of a cytochrome P450 at ~420. Correct folding of the protein was confirmed by reducing the protein with sodium dithionite and observing a shift in the peak to~390 nm. On subsequent carbon monoxide binding, the peak shifted to 450 nm. A spectral shift from 420-390 nm was not observed upon RDX addition which indicates that the enzyme cannot use RDX as a substrate.

In addition to the cytochrome P450 from *Gordonia terrae* strain NBRC 100016, , another uncharacterized cytochrome P450 from the recently sequenced *Gordonia polyisoprenivorans* NBRC16320 genome was also identified, The amino acids sequence of this protein (Accession number H0RGL8) has 48 % sequence identity to the XplA heme domain. Interestingly, the sequence alignment of the protein with XplA revealed that six out of ten amino acids located in the active site of the of XplA are conserved between them. We have cloned this uncharacterized cytochrome P450 into pET-16b. Following the removal of the N- terminus encoding region, soluble expression was achieved. Currently we are focused on increasing the solubility of the protein and investigating whether a site-directed mutagenesis program would create RDX activity.

Conclusions and Implications for Future Research/Implementation

Task 1

Our efforts to develop a functional screen for genes from the soil metagenome were unsuccessful. Technical controls consisting of several orders of magnitude dilution of *P. putida* KT2440 transformed with *xpl*BA DNA only with KT2440 with empty vector demonstrated the efficacy of the strategy of enriching RDX-degrading clones by growth on RDX as sole source of nitrogen (Figure 14). We developed efficient methods of packaging large fragments of partially digested DNA in vectors. These vectors contained RBS and xplB. However, we were unable to enrich clones from the partially digested DNA of any of the known RDX degraders; *Rhodococcus* 11Y, *Microbacterium* MA1, or *Mycobacterium* MA2 in either competent *E. coli* Rosetta-gami B or *P. putida* KT2440 as hosts. Transformation of KT2440 with vectors containing *xpl*BA plus increasing amounts (1kbps and 2.4kbps) of DNA sequence upstream of the *xpl*BA cassette from MA1 yielded growth on RDX that was significantly lower than KT2440 containing the vector with only *xpl*BA itself. These clones were unable to form colonies on RDX as sole N. The 1kbps region upstream of *xpl*BA contains the gene for dihydroxy-picolinicacid (DHP) reductase. This result suggests that there may be a toxic effect of the expression of the DHP reductase or that expression of *xpl*BA in the vector was inhibited by the upstream DNA.

In hindsight it appears that functional screening of metagenomes for activities of specific genes or operons is likely to be highly dependent on host capabilities and on unknown effects of DNA regions from donors in the microbial community contributing the metagenome on the host expression systems.

Task 2

Previously we demonstrated that *Rhodococcus* sp. strain DN22 can degrade RDX aerobically *via* initial denitration to mostly yield the ring cleavage product NDAB. In the present study we degraded RDX with strain DN22 in the presence of $^{18}O_2$ and $H_2{}^{18}O$ to understand the role of oxygen and water in the key denitration step leading to RDX decomposition. We also investigated degradation of MNX (hexahydro-1-nitroso-3,5-dinitro-1,3,5-triazine), a key RDX initial product and frequently found as contaminant with RDX, with DN22 under similar conditions. DN22 degraded RDX and MNX giving NO_2^-, NO_3^-, NDAB, NH_3, N_2O, and HCHO with NO_2^- / NO_3^- molar ratio reaching 17 and *ca*. 2, respectively. In the presence of $^{18}O_2$, DN22 degraded RDX and produced NO_2^- with *m/z* at 46 Da that subsequently oxidized to NO_3^- containing one ^{18}O atom, but in the presence of $H_2{}^{18}O$ we detected NO_3^- without ^{18}O. A control containing NO_2^-, DN22, and $^{18}O_2$ gave NO_3^- with one ^{18}O, confirming biotic oxidation of NO_2^- to NO_3^-.

Treatment of MNX with DN22 and $^{18}O_2$ produced NO_3^- with two mass ions, one (66 Da) incorporating two ^{18}O atoms and another (64 Da) incorporating only one ^{18}O atom and attributed their formation to bio-oxidation of the initially formed NO and NO_2^-, respectively. In the presence of $H_2{}^{18}O$, we detected NO_2^- with two different masses, one representing NO_2^- (46 Da) and another representing NO_2^- (48 Da) with the inclusion of one ^{18}O atom suggesting auto-oxidation of NO to NO_2^-. Detection of NDAB and its nitroso equivalent, i.e., 4-nitroso-2,4-diazabutanal (4-NO-DAB) suggest that double denitration and denitration followed by denitrosation of MNX simultaneously occurred.

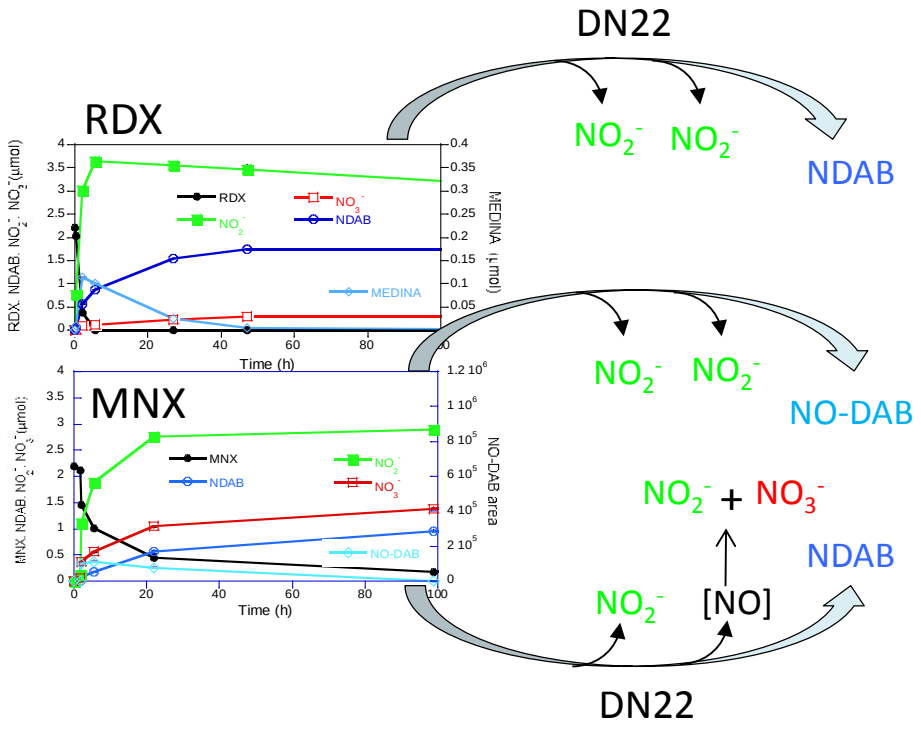

Task 3

This task was combined with task 6.

Task 4

The unsuccessful transfer of the plasmid could be explained by the fact that i) the experiment conditions were not optimal, ii) the rarity of this kind of event, iii) a plasmid incompatibility with the recipient strain. The lack of transconjugants able to grow on RDX could also be explained by the fact that bacteria that have acquired the catabolic plasmid may not have been able to express XplA. Thus, we cannot conclude about the possible transfer or acquisition of the catabolic plasmid of 11Y in natural conditions. Nevertheless, the 454 genome draft sequencing (described below) showed the presence in *Rhodococcus sp*. type strain 11Y of genes potentially involved in plasmid transfer (*e.g*. traA), which is an indication that 11Y is able to transfer plasmid by conjugation.

Moreover, (Jung et al., 2011) demonstrated the successful conjugational transfer of pGKT2, a *xplA*-containing plasmid isolated from Gordonia sp. KTR9 to *Rhodococcus jostii* RHA1, suggesting that *xplA* was most likely acquired and transferred by conjugation to other species.

Task 5

A major task of this work was to identify the origin of XplA, its natural substrate, regulation of the xplA gene cluster and to identify genes potentially involved in the metabolism of RDX, which can be altered to improve RDX degradation in the field.

Sequencing information from a 454 snap shot sequencing of the *R. rhodochrous* 11Y genome allowed the identification of genes potentially involved in the degradation in phenol, benzoate and champhor. The construction of a cosmid library allowed sequencing the xplA- gene cluster and identifying up- and downstream boarders in 11Y and *Microbacterium* MA1. Subsequently, this information could be applied to other RDX-degraders isolated in this study (Task 6). Furthermore, we identified genes potentially involved in the metabolism of RDX and tested by construction of knock out strains their performance when grown in RDX and in a range of different nitrogen sources. *xplA* knock out mutants lost their ability to metabolise RDX indicating that *xplA* is the only gene responsible in the first step of RDX degradation. *xplB* knock out mutants were able to removed RDX, possible by using another endogenous reductase; however, the speed of RDX removal was significantly decreased. This effect has been noted previously (Jackson et al., 2007) and expression of both XplA and B increased RDX removal by plants significantly.

Overexpression and deletion of the permease *aroP* showed no de- or increase in RDX removal, implying no involvement of *aroP* in RDX uptake.

The family of MarR transcriptional regulators is involved in the regulation of a wide variety of cellular processes including detoxification of aromatic aldehydes (Fiorentino et al., 2007) quinones (Leelakriangsak et al., 2008) and the biodegradation of aminophenol (Tropel and van der Meer, 2004). The MarR family regulators have the ability to bind chemical compounds such as 2,4-dinitrophenol or salicylate (COHEN et al., 1993). We hypothesized that the putative transcriptional regulator termed *marR*, might be involved in the regulation of *xplA*, and created *marR* knock-out mutants.

In resting cells assays, the rate of RDX removal by the *marR* knock-out was slower than that of the wild-type cells when grown in nitrogen-excess concentrations of KNO_3 (treatment a); suggesting that MarR may be involved in the detection of high nitrogen however, no other differences were observed.

Resting cell incubations of *R. rhodochrous* 11Y have shown that although activity towards RDX is present in the absence of RDX, activity significantly increased when cells were grown with RDX or low concentrations of NH_4Cl supplied as the sole nitrogen source, suggesting that *xplA* expression is rather a response to low nitrogen levels than RDX specific linking (Indest et al., 2010, Nejidat et al., 2008).

The regulation of RDX degrading genes in *Rhodococcus* strain 11Y has parallels with the regulation of genes encoding atrazine degradation in *Pseudomonas* sp. strain ADP (García-González et al., 2003, Govantes et al., 2010). *Pseudomonas* sp. strain ADP is able to use atrazine as the sole nitrogen source (García-González et al., 2003). Transcription of *atzR*, a regulator that activates the atrazine gene cluster (*atrDEF*), is switched on by a metabolite of atrazine degradation, cyanuric acid, and by nitrogen limitation, and this control is thought to link to central nitrogen metabolism in *Pseudomonas* sp. (Hervas et al., 2008, Govantes et al., 2010)

Analysis of the *R. rhodochrous* 11Y sequence identified two putative promoter regions, one upstream of *aroP* and one upstream of *xplB*. For the putative promoter region upstream of *xplB*, primer extension analysis and RACE PCR did not amplify any products. Furthermore, the -10 sequence is only eleven bases from the ATG start codon of *xplB*, a distance that does not leave much space for RNA polymerase binding prior to translation. Primer extension analysis and RACE PCR did confirm the BPROM-predicted transcription start site upstream of *aroP*.

The construction of a Tn5 insertion library of 11Y was successful but while initial screenings for mutants with decreased RDX removal were promising, subsequent analysis failed to confirm the first observed inhibition in RDX removal.

2D-Gel electrophoresis of 11Y grown in either 250 μM RDX or 750 μM NH4Cl identified some proteins upregulated after RDX treatment involved in nitrogen metabolism; however, no RDX-specific proteins as XplA were found, suggesting that the chosen treatment, as shown for the resting cell assays, results in a similar response and expression of xplA and related proteins arguing that XplA expression is linked to the central nitrogen metabolism and not a specific response to RDX.

Task 6

Enrichment studies identified number of RDX degrading bacteria isolated from contaminated soil from England. Belgium and Ukraine. All isolates were gram positive bacteria and belong to the *Rhodococcus* clade with the exception of Microbacterium isolated from Belgium soil.

The different enrichment conditions have not allowed the isolation of gram negative bacteria, or bacteria degrading RDX with an enzyme other than xplA.

RDX degrading bacteria have so far only been isolated from the explosives contaminated site at Longtown. Our isolates are identical in 16S rDNA, which suggests that they form a monoclonal population. They constitute a closely related but different genotype in comparison to the other RDX degrader *Rhodococcus* isolated in the UK. These results indicated that in the UK, *Rhodococcus* so far remains the main genus found to biodegrade RDX.

The evolutionary origin of XplA is still unclear. So far XplA is the only enzyme which actively degrades RDX. Both *xplA* and *xplB* are part of a high GC content gene cluster which is about 15 kb in size and nearly identical amongst *Rhodococcus* spp, isolated from United Kingdom, Ukraine, United States, Belgium and Israel. The region is also highly conserved in two known genera of actinomycetes: *Microbacterium* sp. MA1 and *Williamsia* sp. EG1. The high sequence identity of the regions flanking *xplA/xplB* indicates that they are part of the larger

genomic island and have a single evolutionary origin, The machinery mechanism of transferring the gene cluster around the world is not yet understood yet, however the finding that the XplA genomics island is limited to actinomycetes suggests that there is a specific transfer system, possible via phages.

Literature cited

Andeer, P., Stahl, D., Bruce, N. & Strand, S. 2009. Lateral transfer of genes for hexahydro-1,3,5-trinitro-1,3,5-triazine (RDX) degradation. *Appl Environ Microbiol*, **75,** 3258-62.

Andeer, P., Stahl, D. A., Lillis, L. & Strand, S. E. 2013. Identification of microbial populations assimilating nitrogen from RDX in munitions contaminated military training range soils by high sensitivity stable isotope probing. *Environ Sci Technol*, **47,** 10356-63.

Augusto, O.; Bonini, M.G.; Amanso, A.M.; Linares, E.; Santos, C.X.; De Menezes, S.L. Nitrogen dioxide and carbonate radical anion: Two emerging radicals in biology. Free Rad. Biol. Medic. 2002, 32, 841-859.

Awad, H.H.; Stanbury, D.M. Autoxidation of NO in aqueous solution. Int. J. Chem. Kinet. 1993, 25, 375-381.

Balakrishnan, V.; Halasz, A.; Hawari, J. The alkaline hydrolysis of RDX, HMX and CL-20: New insights into the degradation pathway obtained by the observation of new degradation products. Environ. Sci. Technol. 2003, 37, 1838-1844.

Balakrishnan, V.K.; Monteil-Rivera, F.; Halasz, A.; Corbeanu, A.; Hawari, J. Decomposition of the polycyclic nitramine explosive, CL-20, by Fe^0. *Environ. Sci. Technol.* **2004**, *38*, 6861-6866.

Beller, H.R.; Tiemeier, K. Use of liquid chromatography/tandem mass spectrometry to detect distinctive indicators of in situ RDX transformation in contaminated groundwater. *Environ. Sci. Technol*. **2002**, *36*, 2060-2066.

Bernstein, A.; Ronen, Z.; Adar, E.; Nativ, R.; Lowag, H.; Stichler, W.; Meckenstock, R.U. Compound-specific isotope analysis of RDX and stable isotope fractionation during aerobic and anaerobic biodegradation. *Environ. Sci. Technol.* **2008**, *42*, 7772-7777.

Bernstein, A.; Adar, E.; Nejidat, A.; Ronen Z. Isolation and characterization of RDX-degrading *Rhodococcus* species from a contaminated aquifer. *Biodegradation* **2011**, *22*, 997-1005.

Bhatt, M.; Zhao, J.-S.; Halasz, A.; Hawari, J. Biodegradation of hexahydro-1,3,5-trinitro-1,3,5-triazine by novel fungi isolated from unexploded ordnance contaminated marine sediment. *J. Ind. Microbiol. Biotechnol*. **2006**, *33*, 850-858.

Bhushan, B.; Halasz, A.; Spain, J.C.; Thiboutot, S.; Ampleman, G.; Hawari, J. Diaphorase catalyzed biotransformation of hexahydro-1,3,5-trinitro-1,3,5-triazine (RDX) *via* N-denitration mechanism. *Biochem. Biophys. Res. Commun*. **2002a**, *296*, 779-784.

Bhushan, B.; Halasz, A.; Spain, J.C.; Thiboutot, S.; Ampleman, G.; Hawari, J. Biotransformation of hexahydro-1,3,5-trinitro-1,3,5-triazine (RDX) catalyzed by a NAD(P)H: nitrate oxidoreductase from *Aspergillus niger*. *Environ. Sci. Technol.* **2002b**, *36*, 3104-3108.

Bhushan, B.; Trott, S.; Spain, J.C.; Halasz, A.; Hawari, J. Biotransformation of RDX by cytochrome P450 2B4: Insights into the mechanisms of RDX biodegradation by *Rhodococcus* sp strain DN22 *Appl. Environ.Microbiol.* **2003**, *69*, 1347-1351.

Bhushan, B.; Halasz, A.; Hawari, J. Effect of iron(III), humic acids and anthraquinone-2,6-disulfonate on biodegradation of cyclic nitramines by *Clostridium* sp. EDB2. *J. Appl. Microbiol*. **2006**, *100*, 555-563.

Bonner, T.G.; Hancock, R.A.; Roberts, J.C. The N-nitroxymethyl derivatives of 1,3-dinitoperhydro-1,3,5-triazine, piperidine, and succinimide. *J. Chem. Soc. Perkin Trans. 1*. **1972**, 1902-1907.

Bonsor, D., Butz, S. F., Solomons, J., Grant, S., Fairlamb, I. J., Fogg, M. J. & Grogan, G. 2006. Ligation independent cloning (LIC) as a rapid route to families of recombinant biocatalysts from sequenced prokaryotic genomes. *Org.Biomol.Chem.*, **4,** 1252-1260.

Broadbent, S., van der Woude, M. & Aziz, N. 2010. Accurate and simple sizing of primer extension products using a non-radioactive approach facilitates identification of transcription initiation sites. *Journal of Microbiological Methods*, **81,** 256-258.

Bröker, D., Arensk̈otter, M. & Steinbüchel, A. 2008. Transfer of megaplasmid pKB1 from the rubber-degrading bacterium Gordonia westfalica strain Kb1 to related bacteria and its modification. *Appl Microbiol Biotechnol*, **77,** 1317-27.

Casewit, C.J.; Goddard, III, W.A. Energetics and mechanisms for reactions involving nitrosamide, hydroxydiazenes, and diimide *N*-oxides. *J. Am. Chem. Soc*. **1982**, *104*, 3280-3287.

Cassada, D.A.; Monson, S.J.; Snow, D.D.; Spalding, R.F. Sensitive determination of RDX, nitroso-RDX metabolites, and other munitions in ground water by solid-phase extraction and isotope dilution liquid chromatography-atmospheric pressure chemical ionization mass spectrometry. *J. Chromatogr.* A **1999**, *844*, 87-95.

Cohen, S., Hachler, H. & Levy, S. 1993. Genetic and functional-analysis of the multiple antibiotic-resistance (mar) locus in *Escherichia coli*. *Journal of Bacteriology*, **175,** 1484-1492.

Coleman, N. V., Nelson, D. R. & Duxbury, T. 1998. Aerobic biodegradation of hexahydro-1,3,5-trinitro-1,3,5-triazine (RDX) as a nitrogen source by a *Rhodococcus* sp., strain DN22. *Soil Biology and Biochemistry*, **30,** 1159-1167.

Drew, D. E., von Heijne, G., Nordlund, P. & de Gier, J. W. 2001. Green fluorescent protein as an indicator to monitor membrane protein overexpression in *Escherichia coli*. *FEBS Lett*, **507,** 220-4.

EPA Method 350.1 Determination of ammonia nitrogen by semi-automated colorimetry. U.S. Environmental Protection Agency, Cincinnati, Ohio, 1993.

Fernandes, P. J., Powell, J. A. & Archer, J. A. 2001. Construction of Rhodococcus random mutagenesis libraries using Tn5 transposition complexes. *Microbiology*, **147,** 2529-36.

Fiorentino, G., Ronca, R., Cannio, R., Rossi, M. & Bartolucci, S. 2007. MarR-like transcriptional regulator involved in detoxification of aromatic compounds in *Sulfolobus solfataricus*. *Journal of Bacteriology*, **189,** 7351-7360.

Fournier, D.; Halasz, A.; Spain, J.; Fiurasek, P.; Hawari, J. Determination of key metabolites during biodegradation of hexahydro-1,3,5-trinitro-1,3,5-triazine (RDX) with *Rhodococcus* sp. strain DN22. *Appl. Environ. Microbiol.* **2002**, *68*, 166-172.

Fournier, D.; Halasz, A.; Spain, J.C.; Spanggord, R.J.; Bottaro, J.C.; Hawari, J. Biodegradation of hexahydro-1,3,5-trinitro-1,3,5-trazine ring cleavage product 4-nitro-2,4-diazabutanal by *Phanerochaete chrysosporium*. *Appl. Environ. Microbiol.* **2004**, *70*, 1123-1128.

Fournier, D.; Trott, S.; Spain, J.; Hawari, J. Metabolism of the aliphatic nitramine 4-nitro-2,4-diazabutanal by *Methylobacterium* sp. strain JS178. *App. Environ. Microbiol.* **2005**, *71*, 4199-4202.

Fuller, M.K.; Hawari, J.; Perreault, N. Extreme microaerophillic degradation of hexahydro-1,3,5-trinitro-1,3,5-triazine (RDX) by three *Rhodococcus* strains. *Lett. Appl. Microbiol*. **2010**, *51*, 313-318.

García-González, V., Govantes, F., Shaw, L. J., Burns, R. G. & Santero, E. 2003. Nitrogen control of atrazine utilization in *Pseudomonas* sp. strain ADP. *Appl Environ Microbiol,* **69,** 6987-93.

Gardner, P.R.; Gardner, A.M.; Brashear, W.T.; Suzuki, T.; Hvitved, A.N.; Setchell, K.D.R.; Olson, J.S. Hemoglobins dioxygenate nitric oxide with high fidelity. *J. Inorg. Biochem.* **2006**, *100*, 542-550.

Goldstein, S.; Czapski, G. Kinetics of nitric oxide autoxidation in aqueous solution in the absence and presence of various reductants. The nature of the oxidizing intermediates. *J. Am. Chem. Soc.* **1995**, *117*, 12078-12084.

Govantes, F., Garcia-Gonzalez, V., Porrua, O., Platero, A., Jimenez-Fernandez, A. & Santero, E. 2010. Regulation of the atrazine-degradative genes in *Pseudomonas* sp strain ADP. *Fems Microbiology Letters,* **310,** 1-8.

Green, L. C., D. A. Wagner, et al. (1982). "Analysis of nitrate, nitrite, and N-15 -labeled nitrate in biological-fluids." Analytical Biochemistry 126(1): 131-138.

Gregory, K.B.; Larese-Casanova, P.; Parkin, G.F.; Scherer, M.M. Abiotic transformation of hexahydro-1,3,5-trinitro-1,3,5-triazine by Fe^{II} bound to magnetite. *Environ. Sci. Technol*. **2004**, *38*, 1408-1414.

Guengerich, F.P. Common and uncommon cytochrome P450 reactions related to metabolism and chemical toxicity. *Chem. Res. Toxicol.* **2001**, *14*, 611-650.

Halasz, A.; Spain, J.; Paquet, L.; Beaulieu, C.; Hawari, J. Insights into the formation and degradation mechanisms of methylenedinitramine during the incubation of RDX with anaerobic sludge. *Environ. Sci. Technol.* **2002**, *36*, 633-638.

Halasz, A.; Hawari, J. Degradation routes of RDX in various redox systems. In *Aquatic Redox Chemistry*; ACS Symposium Series, Eds. P. Tratnyek, T.J. Grundl, and S. Haderlein, **2011**, Vol. 1071, pp 441-462.

Halasz, A.; Manno, D.; Strand, S.E.; Bruce, N.C.; Hawari, J. Biodegradation of RDX and MNX with *Rhodococcus* sp. strain DN22: New insight into the degradation pathway. *Environ. Sci. Technol*. **2010**, *44*, 9330-9336.

Hawari, J.; Halasz, A.; Groom, C.; Deschamps, S.; Paquet, L.; Beaulieu, C.; Corriveau, A. Photodegradation of RDX in aqueous solution: A mechanistic probe for biodegradation with *Rhodococcus* sp. *Environ. Sci. Technol*. **2002**, *36*, 5117-5123.

Hervas, A., Canosa, I. & Santero, E. 2008. Transcriptome analysis of *Pseudomonas putida* in response to nitrogen availability. *Journal of Bacteriology,* **190,** 416-420.

Hoang, T. T., A. J. Kutchma, et al. (2000). "Integration-proficient plasmids for Pseudomonas aeruginosa: Site-specific integration and use for engineering of reporter and expression strains." Plasmid 43: 59-72.

Hoffsommer, J.C.; Kubose, D.A.; Glover, D.J. Kinetic isotope effects and intermediate for aqueous alkaline homogeneous hydrolysis of 1,3,5-triaza-1,3,5-trinitrocyclohexane (RDX). *J. Phys. Chem.* **1977**, *81*, 380-385.

Ignarro, L.J.; Fukuto, J.M.; Griscavage, J.M.; Rogers, N.E.; Byrns, R.E. Oxidation of nitric oxide in aqueous solution to nitrite but not nitrate: Comparison with enzymatically formed nitric oxide from L-arginine. *Proc. Natl. Acad. Sci. USA* **1993**, *90*, 8103-8107.

Indest, K.J.; Crocker, F.H.; Athow, R. A TaqMan polymerase chain reaction method for monitoring RDX-degrading bacteria based on the *XplA* functional gene. *J. Microbiol. Methods* **2007**, *68*, 267-274.

Indest, K., Jung, C., Chen, H., Hancock, D., Florizone, C., Eltis, L. & Crocker, F. 2010. Functional characterization of pGKT2, a 182 kb plasmid containing the xplAB genes involved in the degradation of RDX by *Gordonia* sp. KTR9. *Appl Environ Microbiol*.

Jackson, R. G., Rylott, E. L., Fournier, D., Hawari, J. & Bruce, N. C. 2007. Exploring the biochemical properties and remediation applications of the unusual explosive-degrading P450 system XplA/B. *Proc.Natl.Acad.Sci.U.S.A,* **104,** 16822-16827.

Jenkins, T.F.; Hewitt, A.D.; Grant, C.L.; Thiboutot, S.; Ampleman, G.; Walsh, M.E.; Ranney, T.A.; Ramsey, C.A.; Palazzo, A.J.; Pennington, J.P. Identity and distribution of residues of energetic compounds at army live-fire training ranges. *Chemosphere* **2006**, *63*, 1280-1290.

Jourd'heuil, D.; Kang, D.; Grisham, M.B. Interactions between superoxide and nitric oxide: Implications in DNA damage and mutagenesis. *Front. Bioscie.* **1997**, *2*, d189-196.

Jung, C. M., Crocker, F. H., Eberly, J. O. & Indest, K. J. 2011. Horizontal gene transfer (HGT) as a mechanism of disseminating RDX-degrading activity among Actinomycete bacteria. *Journal of Applied Microbiology*, **110,** 1449-1459.

Kim, D.; Strathmann, T.J. Role of organically complexed iron(II) species in the reductive transformation of RDX in anoxic environments. *Environ. Sci. Technol.* **2007**, *41*, 1257-1264.

Kwon, M.J.; Finneran, K.T. Biotransformation products and mineralization potential for hexahydro-1,3,5-trinitro-1,3,5-triazine (RDX) in abiotic versus biological degradation pathways with anthraquinone-2,6-disulfonate (AQDS) and *Geobacter metallireducens*. *Biodegradation* **2008**, *19*, 705-715.

Kwon, M.J.; Finneran, K.T. Hexahydro-1,3,5-trinitro-1,3,5-triazine (RDX) reduction is currently mediated by direct electron transfer from hydroquinones and resulting biogenic Fe(II) formed during electron shuttle-amended biodegradation. *Environ. Engineer. Sci*. **2009**, *26*, 961-971.

Kwon, M.J.; Finneran, K.T. Electron shuttle-stimulated RDX mineralization and biological production of 4-nitro-2,4-diazabutanal (NDAB) in RDX-contaminated aquifer material. *Biodegradation* **2010**, DOI 10.1007/s10532-010-9352-1.

Lachance, B.; Robidoux, P.Y.; Hawari, J.; Ampleman, G.; Thiboutot, S.; Sunahara, G.I. Cytotoxic and genotoxic effects of energetic compounds on bacterial and mammalian cells in vitro. *Mutation Res.* **1999**, *444*, 25-39.

Lamberton, A.H. Some aspects of the chemistry of nitramines. *Q. Rev. Chem. Soc.* **1951**, *5*, 75-98.

Leelakriangsak, M., Huyen, N., Towe, S., van Duy, N., Becher, D., Hecker, M., Antelmann, H. & Zuber, P. 2008. Regulation of quinone detoxification by the thiol stress sensing

DUF24/MarR-like repressor, YodB in Bacillus subtilis. *Molecular Microbiology,* **67,** 1108-1124.

Lloyd, A., Marshall, B. & Mee, B. 2005. Identifying cloned Helicobacter pylori promoters by primer extension using a FAM-labelled primer and GeneScan((R)) analysis. *Journal of Microbiological Methods,* **60,** 291-298.

McCormick, N.G.; Cornell, J.H.; Kaplan, A.M. Biodegradation of hexahydro-1,3,5-trinitro-1,3,5-triazine. *Appl. Environ. Microbiol*. **1981**, *42*, 817-823.

McHugh, C.J.; Smith, W.E.; Lacey, R.; Graham, D. The first controlled reduction of the high explosive RDX. *Chem. Commun.* **2002**, *21*, 2514-2515.

McLeod, M. P., Warren, R. L., Hsiao, W. W., Araki, N., Myhre, M., Fernandes, C., Miyazawa, D., Wong, W., Lillquist, A. L., Wang, D., Dosanjh, M., Hara, H., Petrescu, A., Morin, R. D., Yang, G., Stott, J. M., *et al.* 2006. The complete genome of *Rhodococcus* sp. RHA1 provides insights into a catabolic powerhouse. *Proc Natl Acad Sci U S A,* **103,** 15582-7.

Miller, M.J.S.; Grisham, M.B. Nitric oxide as a mediator of inflammation? – You had better believe it. *Mediat. Inflammation* **1995**, *4*, 387-396.

Naja, G.; Halasz, A.; Thiboutot, S.; Ampleman, G.; Hawari, J. RDX degradation using zero-valent iron nanoparticles. *Environ. Sci. Technol*. **2008**, *42*, 4364-4370.

Nejidat, A., Kafka, L., Tekoah, Y. & Ronen, Z. 2008. Effect of organic and inorganic nitrogenous compounds on RDX degradation and cytochrome P-450 expression in *Rhodococcus* strain YH1. *Biodegradation,* **19,** 313-320.

Nelson, K. E., c. Weinel, et al. (2002). "Complete genome sequence and comparative analysis of the metabolically versatile Pseudomonas putida KT2440." Environ. Microbiol. 4: 799-808.

Newman, J. R. and C. Fuqua (1999). "Broad-host-range expression vectors that carry the l-arabinose-inducible Escherichia coli araBAD promoter and the araC regulator." Gene 227: 197-203.

Oh, B.-T.; Just, C.L.; Alvarez, P.J.J. Hexahydro-1,3,5-trinitro-1,3,5-triazine mineralization by zerovalent iron and mixed anaerobic cultures. *Environ. Sci. Technol.* **2001**, *35*, 4341-4346.

Paquet, L.; Monteil-Rivera, F.; Hatzinger, P. B.; Fuller, M. E.; Hawari, J. Analysis of the key intermediates of RDX (hexahydro-1,3,5-trinitro-1,3,5-triazine) in groundwater: occurrence, stability and preservation. *J. Environ. Monitor*. **2011**, *13*, 2304-2311.

Pietraforte, D.; Salzano, A.M.; Scorza, G.; Minetti, M. Scavenging of reactive nitrogen species by oxygenated hemoglobin: Globin radicals and nitrotyrosines distinguish nitrite from nitric oxide reaction. *Free Rad. Biol. Medic*. **2004**, *37*, 1244-1255.

Roh, H.; Yu, C.-P.; Fuller, M.E.; Chu, K.H. Identification of hexahydro-1,3,5-trinitro-1,3,5-triazine-degrading microorganisms via ^{15}N-stable isotope probing. *Environ. Sci. Technol.* **2009**, *43*, 2502-2511.

Rylott, E., Jackson, R., Edwards, J., Womack, G., Seth-Smith, H., Rathbone, D., Strand, S. & Bruce, N. 2006a. An explosive-degrading cytochrome P450 activity and its targeted application for the phytoremediation of RDX. *Nature Biotechnology,* **24,** 216-219.

Rylott, E. L., Jackson, R. G., Edwards, J., Womack, G. L., Seth-Smith, H. M., Rathbone, D. A., Strand, S. E. & Bruce, N. C. 2006b. An explosive-degrading cytochrome P450 activity and its targeted application for the phytoremediation of RDX. *Nat.Biotechnol.*

Sabbadin, F. Engineering cytochromes P450 for biocatalysis and bioremediation, Ph.D. Thesis, University of York, UK, October 2010.

Sabbadin, F., Jackson, R., Haider, K., Tampi, G., Turkenburg, J. P., Hart, S., Bruce, N. C. & Grogan, G. 2009. The 1.5-A structure of XplA-heme, an unusual cytochrome P450 heme domain that catalyzes reductive biotransformation of royal demolition explosive. *J.Biol.Chem.,* **284,** 28467-28475.

Sagi-Ben Moshe, S.; Ronen, Z.; Dahan, O.; Bernstein, A.; Weisbrod, N.; Gelman, F.; Adar, E. Isotopic evidence and quantification assessment of in situ RDX biodegradation in deep unsaturated zone. *Soil. Biol. Biochem*. **2010**, *42*, 1253-1262.

Scheideler, L. and H. Ninnemann (1986). "Nitrate reductase-activity test - phenazine methosulfate-ferricyanide stop reagent replaces post-assay treatment." Analytical Biochemistry 154(1): 29-33.

Schmidt, T.C.; Zwank, L.; Elsner, M.; Berg, M.; Meckenstock, R.U.; Haderlein, S.B. Compound-specific stable isotope analysis of organic contaminants in natural environments: a critical review of the state of the art, prospects, and future challenges. *Anal. Bioanal. Chem.* **2004**, *378*, 283-300.

Schopfer, M.P.; Wang, J.; Karlin, K.D. Bioinspired heme, heme/nonheme diiron, heme/copper, and inorganic NOx chemistry: $\bullet NO_{(g)}$ oxidation, peroxynitrite-metal chemistry, and $\bullet NO_{(g)}$ reductive coupling. *Inorg. Chem*. **2010**, *49*, 6267-6282.

Seth-Smith, H. M., Rosser, S. J., Basran, A., Travis, E. R., Dabbs, E. R., Nicklin, S. & Bruce, N. C. 2002a. Cloning, sequencing, and characterization of the hexahydro-1,3,5-trinitro-1,3,5-triazine degradation gene cluster from *Rhodococcus rhodochrous*. *Appl.Environ.Microbiol.,* **68,** 4764-4771.

Seth-Smith, H. M. B. 2002. Microbial Degradation of RDX. University of Cambridge, Institue of Biotechnology. Ref Type: Thesis/Dissertation.

Seth-Smith, H.M.B.; Edwards, J.; Rosser, S.J.; Rathbone, D.A.; Bruce, N.C. The explosive-degrading Cytochrome P450 system is highly conserved among strains of *Rhodococcus* spp. Appl. Environ. Microbiol. **2007**, *74*, 4550-4552.

Shen, C.F.; Hawari, J.; Ampleman, G.; Thiboutot, S.; Guiot, S.R. Enhanced biodegradation and fate of hexahydro-1,3,5-trinitro-1,3,5-triazine (RDX) and octahydro-1,3,5,7-tetranitro-1,3,5,7-tetrazocine (HMX) in anaerobic soil slurry bioprocess. *Bioremed. J.* **2000**, *4*, 27-39.

Sheremata, T.W.; Hawari, J. Mineralization of RDX by the white rot fungus *Phanerochaete chrysosporium* to carbon dioxide and nitrous oxide. *Environ. Sci. Technol.* **2000**, *34*, 3384-3388.

Simon, R., U. Priefer, et al. (1983). "A broad host range mobilization system for in vivo genetic-engineering - transposon mutagenesis in gram-negative bacteria." Bio-Technology 1(784-791).

Strobel, H. W.; Coon, M.J. Effect of superoxide generation and dismutation on hydroxylation reactions catalyzed by liver microsomal cytochome P-450. *J. Biol. Chem*. **1971**, *246*, 7826-7829.

Thompson, K. T., Crocker, F. H. & Fredrickson, H. L. 2005. Mineralization of the cyclic nitramine explosive hexahydro-1,3,5-trinitro-1,3,5-triazine by *Gordonia* and *Williamsia* spp. *Applied and Environmental Microbiology,* **71,** 8265-8272.

Tropel, D. & van der Meer, J. 2004. Bacterial transcriptional regulators for degradation pathways of aromatic compounds. *Microbiology and Molecular Biology Reviews,* **68,** 474-+.

Wawrik, B., Kerkhof, L., Kukor, J. & Zylstra, G. 2005. Effect of different carbon sources on community composition of bacterial enrichments from soil. *Appl Environ Microbiol,* **71,** 6776-83.

Williams, A.G.B.; Gregory, K.B.; Parkin, G.F.; Scherer, M.M. Hexahydro-1,3,5-trinitro-1,3,5-triazine transformation by biologically reduced ferrihydrite: Evolution of Fe mineralogy, surface area, and reaction rates. *Environ. Sci. Technol*. **2005**, *39*, 5183-5189.

Zhang, B.; Cox, S.B.; McMurry, S.T.; Jackson, W.A.; Cobb, G.P.; Anderson, T.A. Effect of two major *N*-nitroso hexahydro-1,3,5-trinitro-1,3,5-triazine (RDX) metabolites on earthworm reproductive success. *Environ. Poll*. **2008**, *153*, 658-667.

Zhao J.-S.; Manno, D.; Hawari, J. Regulation of hexahydro-1,3,5-trinitro-1,3,5-triazine (RDX) metabolism in *Shewanella halifaxensis* HAW-EB4 by terminal electron acceptors and involvement of c-type cytochrome. *Soc. Gen. Microbiol.* **2008**, *154*, 1026–1037.

Zhao, J.-S.; Paquet, L.; Halasz, A.; Hawari, J. Metabolism of hexahydro-1,3,5-trinitro-1,3,5-triazine through initial reduction to hexahydro-1-nitroso-3,5-dinitro-1,3,5-triazine followed by denitration in *Clostridium bifermentans* HAW-1. *Appl. Microbiol. Biotech*. **2003**, *63*, 187-193.

Zhao, J.-S.; Halasz, A.; Paquet, L.; Beaulieu, C.; Hawari, J. Biodegradation of hexahydro-1,3,5-trinitro-1,3,5-triazine and its mononitroso derivative hexahydro-1-nitroso-3,5-dinitro-1,3,5-triazine by *Klebsiella pneumoniae* strain SCZ-1 isolated from an anaerobic sludge. *Appl. Environ. Microbiol*. **2002**, *68*, 5336-5341.

Zweier, J.L.; Samouilov, A.; Kuppusamy, P. Non-enzymatic nitric oxide synthesis in biological systems. *Biochim. Biophys. Acta* **1999**, *1411*, 250-262.

Appendix A

Supporting Data

Table 1. Origin and accession numbers of bacteria used in this study

Bacterial strains	Country of isolation	Reference	NCBI acc. No.
Rhodococcus sp. 1	Belgium	This study	-
Rhodococcus sp. DS1	Belgium	This study	-
Rhodococcus sp. 3	UK	This study	-
Rhodococcus sp. 5U	Ukraine	This study	-
Rhodococcus rhodococcus 11Y	UK	(Seth-Smith et al., 2002b)	AF439261.1
Rhodococcus sp.YH1	Israel	Unpublished	AF103733.1
Rhodococcus sp. DN22	Australia	(Coleman et al., 1998)	X89240.1
Microbacterium sp MA1	US	(Andeer et al., 2009)	FJ357539
Rhodococcus sp. EG2	US	(Andeer et al., 2013)	KF571869
Gordonia sp KTR9	US	(Thompson et al., 2005)	DQ068383
Williamsia sp EG1	US	(Andeer et al., 2009)	

List of Scientific/Technical Publications

1. Halasz, A.; Manno, D.; Strand, S.; Bruce, N.; Hawari, J. (2010) Biodegradation of RDX and MNX with Rhodococcus sp. strain DN22: new insights into the degradation pathway. Environmental Science and Technology 44: 9330-9336
2. Halasz, A., D. Manno1, N. N. Perreault, F. Sabbadin, N. C. Bruce and J. Hawari (2012) Biodegradation of RDX nitroso products MNX and TNX by cytochrome P450 XplA. Environmental Science and Technology
3. Halasz, A., and J. Hawari (2011) Degradation routes of RDX in various redox systems; "Aquatic Redox Chemistry"ACS Symposium Series. Vol 1071 Ed P Tratneyk, Timothy J. Grundl , and Stefan Haderlein, Chapter 20: 441-462
4. Annamaria, H., et al. (2010). "Biodegradation of RDX and MNX with Rhodococcus sp. Strain DN22: New Insights into the Degradation Pathway." Environmental Science & Technology 44(24): 9330-9336.
5. Chong, C. S., et al. (2014). "Analysis of the xplAB-Containing Gene Cluster Involved in the Bacterial Degradation of the Explosive Hexahydro-1,3,5-Trinitro-1,3,5-Triazine." Applied and Environmental Microbiology 80(21): 6601-6610.
6. Lorenz, A., et al. (2013). "Towards engineering degradation of the explosive pollutant hexahydro-1,3,5-trinitro-1,3,5-triazine in the rhizosphere." Fems Microbiology Letters 340(1): 49-54.
7. Rylott, E. L., et al. (2011). "The explosive-degrading cytochrome P450 XplA: Biochemistry, structural features and prospects for bioremediation." Biochimica Et Biophysica Acta-Proteins and Proteomics 1814(1): 230-236.

Other Supporting Materials

None